DEPLETED MANTLE DERIVED MAGMAS AND LAURENTIAN DETRITUS IN THE SUPRACRUSTAL LIGHTHOUSE GNEISS ASSOCIATION, GRENVILLE PROVINCE, ONTARIO

by

Mark Raistrick

Submitted in partial fulfillment of the requirements
for the degree of Master of Science

at

Dalhousie University
Halifax, Nova Scotia
April 2003

DALHOUSIE UNIVERSITY

DEPARTMENT OF EARTH SCIENCES

The undersigned hereby certify that they have read and recommend to the Faculty of Graduate Studies for acceptance a thesis entitled "Depleted Mantle Derived Magmas and Laurentian Detritus in the Supracrustal Lighthouse Gneiss Association, Genville Province, Ontario" by Mark Raistrick in partial fulfillment of the requirements for the degree of Master of Science.

Dated: 7/4/2003

ExternalExaminer:_

Supervisor: _

Examining Committee: _

—

—

DALHOUSIE UNIVERSITY

DATE: 07 APRIL 2003
AUTHOR: MARK RAISTRICK
TITLE: DEPLETED MANTLE DERIVED MAGMAS AND LAURENTIAN DETRITUS IN THE SUPRACRUSTAL LIGHTHOUSE GNEISS ASSOCIATION, GRENVILLE PROVINCE, ONTARIO
DEPARTMENT OR SCHOOL: EARTH SCIENCE
DEGREE: MSc CONVOCATION: MAY YEAR: 2003

TABLE OF CONTENTS

LIST OF FIGURES

Chapter 5

Appendix A

Appendix B

Appendix C

LIST OF TABLES

Appendix B

Appendix C

ABSTRACT

The juvenile supracrustal rocks of the Lighthouse gneiss association are part of the Shawanaga domain of the Central Gneiss Belt, southwestern Grenville Province, Ontario. The Shawanaga domain is overlain by the lithologically distinctive, thrust-emplaced Parry Sound domain to the southeast, and underlain by the Britt domain of the Laurentian continental margin to the northwest. The Britt domain has experienced both Grenvillian (ca. 1120-980 Ma), and older (ca. 1450 Ma) metamorphism, whereas the Parry Sound, and Shawanaga domains only record Grenvillian events.

The upper and lower units of the Lighthouse gneiss association, separated by a narrow anorthosite body, consist of interlayered feldspathic metasediments and tholeiitic amphibolite. The Lighthouse gneiss association was highly deformed and metamorphosed to upper amphibolite facies during the Grenville orogenic cycle (ca. 1050 Ma). The protoliths of the Lighthouse gneiss association were likely to have been supercrustal rocks formed in a marginal volcanic basin(s).

U-Pb geochronology of detrital zircons from a lower unit metasediment revealed only single age 1380 Ma zircons, similar in age to the subjacent Sand Bay gneiss association. Amphibolites accompanying the lower unit metasediments have ε_{Nd} values (mean: +5.4 at 1370 Ma) similar to the DM (depleted mantle) at their time of formation, suggesting little or no contamination by older felsic crustal material. Trace element data suggests subduction modification of the DM source. The volcanic and sedimentary protoliths of the lower unit appear to have been formed soon after 1380 Ma, adjacent to the Laurentian Sand Bay gneiss association, and the contemporaneous southern mid-continent granite-rhyolite province, on juvenile Laurentian continental crust. The lower unit may represent the later stages of rifting of a continental back-arc basin, with the Sand Bay bimodal metavolcanics and siliciclastic metasediments as earlier products of the same process.

The upper unit amphibolites, like the lower unit, have ε_{Nd} values within error of the DM at 1320 Ma (mean: +5.7), suggesting that magmas did not interact in any significant way with older crustal rocks. Upper unit amphibolite trace element distribution suggests a MORB-like DM source. Metasediment detrital zircon age ranges from the upper unit vary from 1880 – 1330 Ma, and resemble ages found both on the Laurentian margin and in allochthonous rocks probably formed on the most distal part of the Laurentian margin, in particular the Parry Sound domain and parts of the Frontenac-Adirondack Belt. It is probable that the upper unit formed in a more distal, outboard setting with respect to the lower unit and Sand Bay gneiss association, and while the basin in which the upper unit was deposited continued to receive continental detritus, magmas were not appreciably contaminated by older material, or altered by subduction-zone processes.

This study supports models that treat the Mesoproterozoic history of the southwestern Laurentian margin as a series of oceanward-younging juvenile continental arcs.

Combined U-Pb detrital geochronological and Nd-isotope petrogenetic studies, along with lithological, field, geochemical and correlative data allow identification of environments of origin, where individual interpretations of the U-Pb and Nd isotopic systems can be ambiguous.

ACKNOWLEDGEMENTS

Nicholas Culshaw is thanked for his continuous support and inspiration.

MR thanks Em Lamond for her understanding and enthusiasm. MR acknowledges NSERC Operating Grant (Culshaw), and a Dalhousie science faculty scholarship. Jaroslav Dostal and Rebecca Jamieson are thanked for timely guidance. Thanks also to John Ketchum and the staff at the Jack Satterly laboratory of the Royal Ontario Museum for assistance with U-Pb analyses, and Alain Potrel and Paul Sylvester at the Atlantic Universities Regional Isotope Facility at Memorial University Newfoundland, and the GEOPTOP laboratory at the University of Quebec for Sm-Nd analyses and isotopic preparation. David Slauenthwaite did the XRF, and Robert McKay assisted with microprobe analyses. Gordon Brown is thanked for thin section preparation.

Chapter 1

Introduction

1.1 BACKGROUND

Studies of the Mesoproterozoic history of the Laurentian continent suggest that a long-lived active margin of Pacific Rim scale preceded the ca. 1.0 Ga Grenville orogeny (Kay et al. 1989, Gower and Tucker 1994, Culshaw et al. 1997, 2000, Rivers and Corrigan 2000, Carr et al. 2000, Slagstad et al. *in press*). The collisional Grenville orogeny began around 1120 Ma and continued until 980 Ma, with metamorphism and deformation migrating northwestwards over time (Culshaw et al. 1997, Ketchum and Davidson 2000, Carr et al. 2000). The resulting Grenville Province is the deeply eroded (ca. 20-30 km depth) remnant of a Himalayan-scale orogen, and is characterized by highly deformed medium to high grade gneisses stretching in a 500 km wide belt from the Baltic states to the southwestern USA (Fig. 1.1). In its southwestern outcrop in Ontario and New York, the Grenville Province is divided into three laterally continuous tectonic belts: the Central Gneiss Belt, Composite Arc Belt and Frontenac-Adirondack Belt referred to herein as the CGB, CAB, and FAB respectively (Wynne-Edwards 1972, Rivers et al. 1989, Carr et al. 2000). Davidson (1984) subdivided the CGB into lithotectonic domains that he interpreted as thrust sheets. More recently, the lithotectonic domains and the larger scale belts have been interpreted as a collage of parts of the reworked continental margin, continental juvenile arc complexes, and offshore terranes, that were amalgamated by the closure of a mid-Proterozoic ocean and subsequently telescoped by Grenvillian tectonism (e.g. Carr et al. 2000).

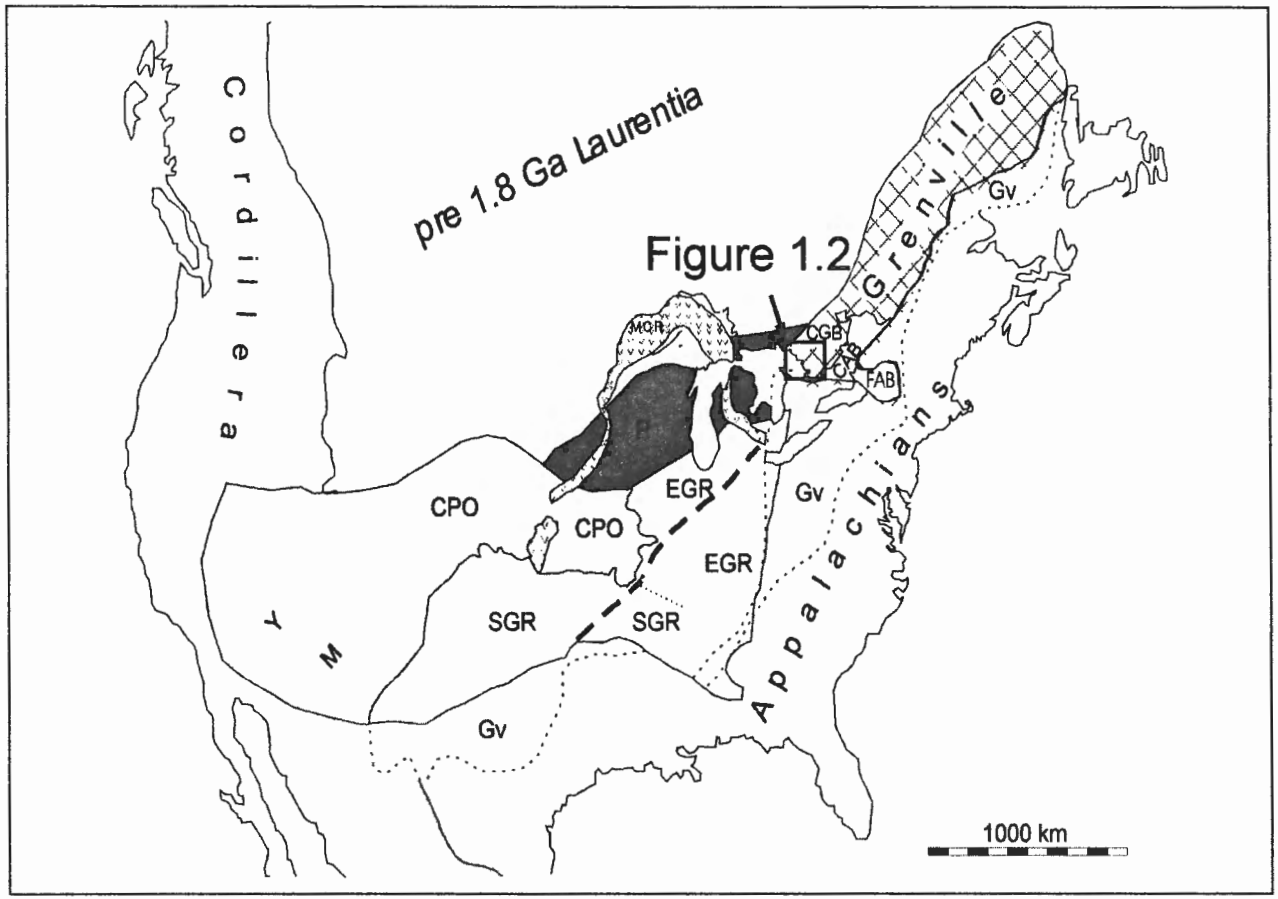

Figure 1.1. The Grenville Province in North America (Culshaw and Dostal 2002). The Georgian Bay section of the Central Gneiss Belt is outlined in bold; FAB - Frontenac Adirondack Belts and CAB - Composite Arc Belts are also indicated. Proterozoic juvenile tectonic elements include: (1.85 1.6 Ga) Y - Yavapai, M - , Mazatzal, and P - Penokean orogens, EGR and SGR eastern and southern granite rhyolite provinces (ca. 1.47 Ga and ca. 1.37 Ga). MCR - 1.1 Ga mid-continent rift, Gv - Grenville Province subcrop. Heavy dashed line is U-Pb age boundary between pre 1.45 Ga eastern and post 1.45 Ga southern granite-rhyolite provinces of Van Schmus et al. (1996).

Palaeomagnetic polar wander data (Piper 1982, Wiel et al. 1998), structural studies linking truncated Mesoproterozoic mobile belts and rifts (Moores 1991, Dalziel 1991, Fitzsimons 2000), and shared 1.0 Ga deformation and metamorphism (Dalziel 1992) lead to the conclusion that the Baltic, Laurentian, Amazonian, East Antarctic, and East Gondwanan cratons were part of a Meso-Neoproterozoic supercontinent called Rodinia (Meert and Powell 2001). The Grenville orogen was central to the construction of the Rodinian supercontinent, joining Amazonia and East Gondwana to Baltica and Laurentia (Dalziel 1992). The Baltic and Laurentian (including North Atlantic and Nain) cratons were probably already joined by the early Mesoproterozoic (Buchan et al. 2000). Grenville orogen correlatives include the Sveconorwegian orogen in southern Norway and Sweden, and the Rondonian-Sunsas Province, a Grenville age mobile belt on the western margin of the Amazonian craton (Gaàl and Gorbatschev 1986, Sadowski and Bettencourt 1997, Tassinari et al. 2000). Åhäll and Connely (1998), Benin et al. (2001) and Brewer et al. (2002) suggest that the 1.65 - 1.15 Ga pre-Sveconorwegian margin of Baltica was of Andean-type and its evolution involved continental arc and inboard magmatism, continental back arc rifting, volcanism and sedimentation, with subduction beneath the craton. In the western part of the Amazonian craton, Mesoproterozoic events included granitoid intrusion from 1.8 – 1.55 Ga, along with ca. 1.7 Ga and 1.6 – 1.57 Ga metamorphic events (Tassinari et al. 2000). The western Amazonian Rondonian-Sunsas Province has similar metamorphic ages (1.2-1.0 Ga) and structural style to the Grenville Province, including laterally extensive metamorphic belts (Sadowski and Bettencourt 1996, Tassinari et al. 2000). Recognition of a genetic link between Mesoproterozoic parts of the Laurentian margin that are now within the Grenville Province, and the mid-

continent area of the United States, has been made by numerous workers (e.g. Easton 1986a, van Breemen and Davidson 1988; Culshaw and Dostal 1997, 2002) and is considered in detail in the following section.

1.2 REGIONAL GEOLOGY

The CGB is situated immediately above and southeast, in the hanging-wall of the orogen-bounding GFTZ (Grenville Front Tectonic Zone), a southeast-dipping crustal-scale thrust zone (Fig. 1.2). The CGB has the strongest Laurentian affinities of the three Grenville tectonic belts in Ontario and New York, with reworked Archean and Palaeoproterozoic material and evidence of multiple pre-Grenville tectonothermal events. Southeast of the CGB, the CAB and FAB are volcanic arc and supracrustal sequences interpreted to have been assembled between 1300 - 1250 Ma and thrust northwestwards onto Laurentia during the early stages of the Grenville orogeny (Culshaw et al. 1997, Carr et al. 2000, Corriveau and van Breemen 2000).

Thrust- or normal- sense curviplanar shear zones, characterized by myolinitic gneisses, divide the CGB into sub-100 km scale monocyclic and polycyclic domains (Fig. 1.2); these domains comprise lithologically and metamorphically discrete packages of medium- to high-grade gneiss (Davidson 1984). Polycyclic domains have metamorphism, mineral assemblages, and plutonism related to Grenvillian and older tectonothermal events (Rivers et al. 1989, Ketchum and Davidson 2000). Monocyclic domains have only Grenville age (1120 – 980 Ma) deformation and metamorphism (Rivers et al. 1989, Ketchum and Davidson 2000). The Britt and Lower Go Home domains are polycyclic and are probably reworked parts of the Laurentian continental margin (Culshaw et al.

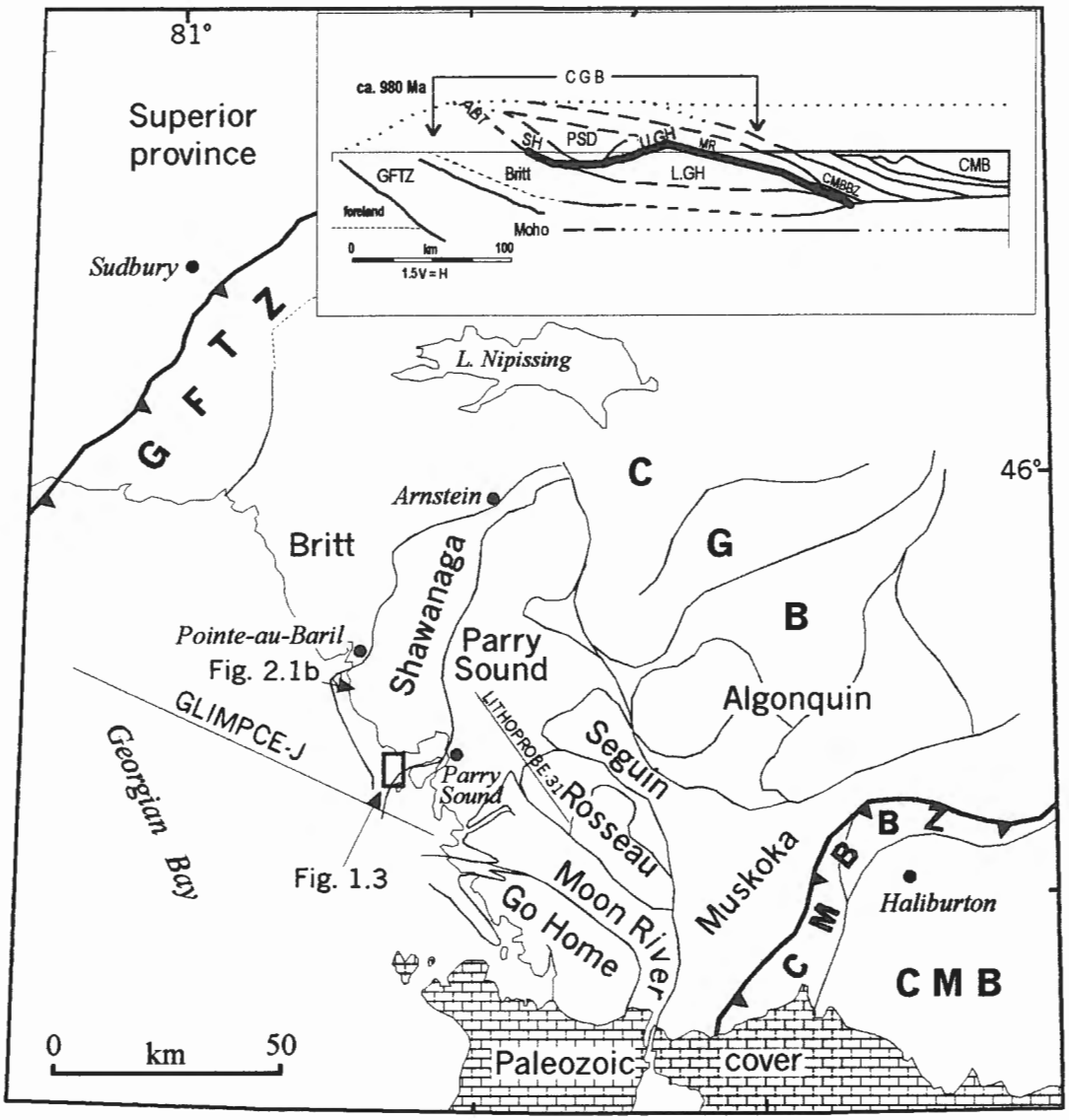

Figure 1.2. The Central Gneiss Belt of the Grenville Province along Georgian Bay, Ontario (after Culshaw et al. 1997). Approximate position of seismic traverse GLIMPCE J and Lithoprobe seismic line 31 shown. Seguin, Rosseau, and Moon River domains are commonly included with the Muskoka domain (Slagstad et al. *in press*) Inset; cross-section after Grenville orogenesis at 980 Ma, based on GLIMPCE -J profile and Lithoprobe seismic line 31, geochronological and geological data (after Culshaw et al. 1997, White et al. 1994). Key for both: GFTZ Grenville Front Tectonic Zone CGB Central Gneiss Belt, CMB Central Metasedimentary Belt (Composite Arc Belt), SH Shawanaga domain, PSD Parry Sound Domain, UGH Upper Go Home domain, MR Moon River domain (Muskoka domain), LGH Lower Go Home domain. ABT Allochthon Boundary Thrust (Shawananga Shear Zone), CMBBZ Central MetasedimentaryBelt Boundary Zone. Position of figure 1.3 and 2.1b shown.

1997, Ketchum and Davidson 2000). The Shawanaga, Muskoka (including Moon River and Seguin domains), Parry Sound, Twelve Mile Bay, and Upper Go Home domains are monocyclic and probably formed as juvenile additions to the Laurentian margin or offshore in a pre-Grenvillian ocean (Wodicka et al. 1996, Culshaw et al. 1997, Carr et al. 2000).

The Shawanaga domain (Figs. 1.2, 1.3), the focus of this study, is tectonically bounded by the structurally overlying, monocyclic Parry Sound domain on its southeast side, and underlain by the Laurentian, polycyclic Britt domain on its northwest side (Wodicka et al. 1996, Culshaw et al. 1997, Culshaw and Dostal 1997, 2002). Of all the domains of uncertain affinity, the monocyclic Shawanaga domain is closest to Laurentia. The boundary between the Shawanaga domain and the underlying Britt domain is defined by the Shawanaga shear zone, the westernmost extension of the ABT (allochthon boundary thrust). The ABT is a laterally extensive detachment, active during Grenville orogenesis, that is thought to mark the contact between the parautochthonous polycyclic (Laurentian) parts of the Grenville province and monocyclic juvenile allochthons (Rivers et al. 1989, Dickin and McNutt 1989, 1990, White et al. 1994, 2000, Culshaw et al. 1994, Ketchum and Davidson 2000). Wodicka (1994) and Culshaw and Dostal (2002) defined the boundary between the Shawanaga domain and the structurally overlying Parry Sound Domain as an unnamed extensional shear zone that disrupts the lower part of an older thrust-sense shear zone (Figs 1.2, 1.3).

The Parry Sound domain has experienced polyphase Grenvillian metamorphism including widespread granulite facies metamorphism. Although the Parry Sound domain contains migmatitic supracrustal rocks including quartzite, pelite, semipelite,

quartzofeldspathic gneiss, calc silicate, and marble, orthogneiss is the most abundant component. Orthogneiss lithologies include tonalitic, granitic and granodioritic gneiss, anorthosite and gabbro, all of which are cut by pre-metamorphic mafic dykes (Culshaw et al. 1989; Wodicka et al. 1996). Along Georgian Bay, three thrust-separated, lithologically distinctive sub-units with different protolith ages comprise the Parry Sound Domain: the ca. 1400 – 1330 Ma basal Parry Sound assemblage, the ca. 1315 Ma interior Parry Sound assemblage, and the post ca. 1130 Ma Twelve Mile Bay assemblage (Culshaw et al.1989; Culshaw et al. 1994, Wodicka et al. 1996). The Parry Sound domain is thought to have formed between 1436 ±17 Ma (the youngest detrital zircon in the basal Parry Sound quartzite) and earliest metamorphism at 1160 Ma. The Parry Sound domain has similar detrital ages to parts of the CAB and Adirondack Highlands (part of the FAB), and is probably the dissected remnant of an oceanic- or outboard continental arc (Wodicka et al. 1996). The Parry Sound domain records an early episode of granulite facies Grenvillian metamorphism and deformation at 1160-1120 Ma, at least 30 My before the beginning of any other Grenvillian metamorphism in the CGB (Culshaw et al. 1997, Slagstad et al. *in press*).

The Britt domain, with 2680 Ma trondhjemitic gneiss, ca. 2475 Ma gabbro and anorthosite (Chen et al. 1995), and ca. 1800 – 1600 Ma granitic orthogneiss cut by 1460-1430 Ma megacrystic granitoids, has strong Laurentian affinities (Culshaw et al. 1994, Carr et al. 2000). The polycyclic nature of the Britt domain is clearly shown by dykes that cut ca. 1450 Ma leucosomes, all of which were subsequently deformed and metamorphosed during the Grenville orogenic cycle (Ketchum et al. 1994, Ketchum and Davidson 2000). The dykes in the Britt domain have close geochemical affinities to the

ca.1235 Ma northwest-striking Sudbury dyke swarm on the Laurentian foreland (Krogh et al. 1987, Dudas et al. 1994). The Britt domain is probably part of an Andean-type arc complex that formed at the southeastern Laurentian continental margin in two distinct stages of crustal growth, at 1.8-1.6 Ga and 1.46-1.43 Ga (Carr et al. 2000, Slagstad et al. *in press*).

Crust-formation events in the component domains of the CGB coincided with periods of crust-formation in the mid-continent area of the USA, and to the east on the Laurentian margin of Labrador. For example, the 1750-1600 Ma arc-generation event recorded in the Britt domain is equivalent to the ca. 1.8-1.6 Ga Yavapai-Mazatzal (Central Plains) orogen, and it has been proposed that the two are genetically linked (Easton 1986a, Davidson 1986, van Breemen and Davidson, 1988). The Makkovik Province in Labrador includes evidence of generation and coeval deformation of juvenile crust in a continental arc system between 1.9-1.7 Ga (Culshaw et al. 2000). Generation of the ca. 1.38 Ga southern granite-rhyolite province was likely close in time with Shawanaga domain bimodal volcanism, and this led Culshaw and Dostal (1997, 2002) to conclude that the Shawanaga domain and younger granite - rhyolite provinces may have been contiguous before the Grenville Orogeny.

1.3 TECTONOSTRATIGRAPHY OF THE SHAWANAGA DOMAIN

The Shawanaga domain along Georgian Bay is divided into the Ojibway, Sand Bay and Lighthouse gneiss associations (Culshaw et al. 1989). The Sand Bay and Lighthouse gneiss associations (Fig. 1.3) are predominantly metasupracrustal rocks, and along with the metaplutonic Ojibway gneiss, the entire domain has been metamorphosed

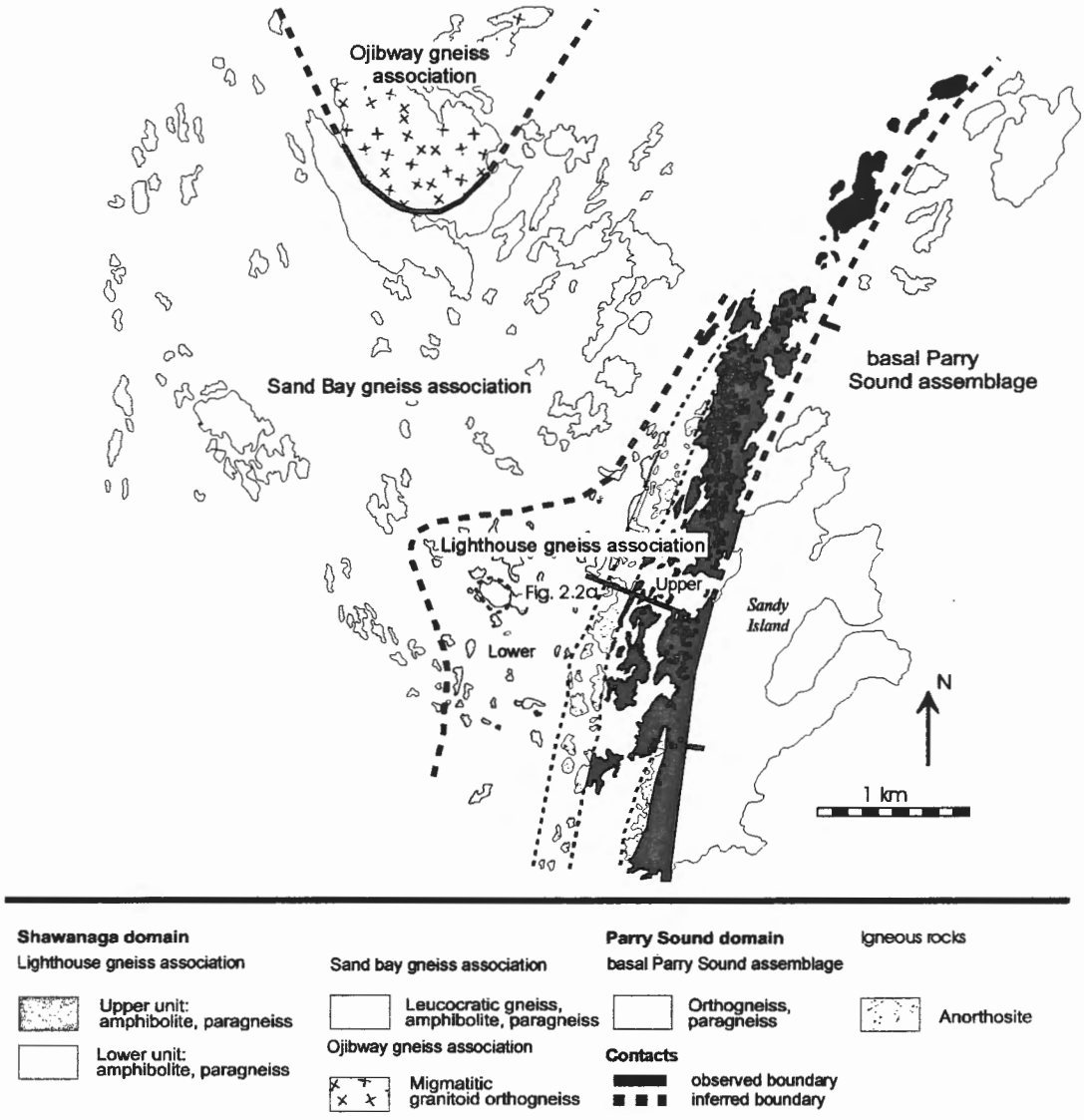

Figure 1.3. The Shawanaga and basal Parry Sound domains in the vicinity of Sandy Island, near Parry Island, Georgian Bay after Culshaw and Dostal (2002). Extensional shear zone separating Shawanaga and basal Parry Sound domain has tick on hanging wall. Position of section 2.2a shown. For sample locations see figure 2.1a.

to upper amphibolite facies, at >700°C and 10-12 kbar (Wodicka et al. 2000). Deformation and high-grade polyphase metamorphism took place between ca. 1090 and 1050 Ma and probably resulted from overthrusting of parts of the CGB and the CAB over the Shawanaga and underlying Britt domains (Culshaw et al. 1997, Wodicka et al. 2000, Slagstad et al. *in press*).

The Shawanaga shear zone, the northern boundary of the Shawanaga domain (Fig. 1.2), is the westernmost extension of the province-wide ABT. The ABT on Georgian Bay coincides with a distinct seismic reflector (White et al. 1994, 2000). Initial thrust-sense movement along the Shawanaga shear zone is inferred from hangingwall - footwall relationships, e.g. high-pressure rocks restricted to the hanging-wall, and rare thrust-sense kinematic indicators found inland from Georgian Bay (Ketchum et al. 1998, Culshaw et al. 1989, 1994, 1997). Kinematic, metamorphic, and geochronological evidence from tectonites in the Shawanaga shear zone suggests top-to-the-southeast, extensional shearing at ca. 1020 Ma (Culshaw et al. 1989, Ketchum et al. 1993, 1998 Ketchum 1995). The boundary between the basal Parry Sound assemblage and the Shawanaga domain is marked by a 1020-970 Ma high-temperature extensional shear zone that reworks an older thrust-sense shear zone in the immediate vicinity of the study area (age constraints provided by contrasting Ar-closure ages; Reynolds et al. 1995), and by the appearance in the Parry Sound domain of a suite of pre-Grenvillian cross-cutting mafic dykes (Wodicka 1994, Culshaw et al. 1997, Wodicka et al. 2000). Ductile deformation, including late orogenic extension focused on detachments such as the Shawanaga shear zone (Fig. 1.2), led to the formation of the sub-horizontal fabrics that are typical of the CGB (Culshaw et al. 1997). In the Shawanaga domain, extensional

deformation developed upright folds with hinge lines parallel to the regional stretching lineation, and affected both the sub-horizontal fabrics, and coeval, recumbent nappe-like folds (Culshaw et al. 1994).

Unlike the Britt domain, no basic dykes of Sudbury affinity are recorded from the Shawanaga domain (Culshaw and Dostal 1997). Retrogressed mafic eclogites of uncertain age, and 1170-1150 Ma podiform coronitic metagabbros (van Breemen and Davidson 1990, Ketchum and Krogh 1997, 1998, Ketchum and Davidson 2000) are found within the Shawanaga, Moon River (Muskoka), and Go Home domains.

The Ojibway gneiss association and Shawanaga pluton

The Ojibway gneiss association is a 1466 ±11 Ma orthogneiss body of granodioritic-tonalitic composition with arc-granitoid geochemistry (Slagstad et al. *in press*). Found at the base of the Shawanaga shear zone, the Shawanaga pluton is a ca. 1460 Ma body of megacrystic garnet-amphibole bearing granodiorite-granite (Culshaw et al. 1994, Ketchum 1994, Krogh pers. comm., Slagstad et al. *in press*). Compositional and age similarities between the Shawanaga pluton, Ojibway gneiss, and grey calc-alkaline gneisses from the Muskoka domain to the south (McMullen et al. 1999), led Slagstad et al. (*in press*) to suggest that the Shawanaga pluton formed with the Ojibway and Muskoka gneiss protoliths in a postulated ca. 1450 Ma Ojibway – Muskoka arc. According to Slagstad et al. (*in press*), the Ojibway – Muskoka arc formed outboard of the Laurentian Britt domain, while the latter underwent 1450 - 1430 Ma granulite facies metamorphism (Tuccillo et al. 1992, Ketchum et al. 1994). The 1450 - 1430 Ma tectonothermal event is not well understood but may have resulted from within–plate

melting and associated metamorphism of juvenile crust in a continental back-arc extensional setting (Ketchum and Davidson 2000, Carr et al. 2000).

Nd T_{DM} model ages from the Ojibway orthogneiss are somewhat older than crystallization ages, at ca.1640 Ma (Dickin and McNutt 1990). Slagstad et al. (*in press*) have interpreted the model age of the Ojibway orthogneiss to indicate minor contamination by older continental crust, though more significant contamination by younger (i.e. Mesoproterozoic) continental material cannot be ruled out.

Sand Bay gneiss association

The layered rocks of the Sand Bay gneiss association (Culshaw and Dostal 1997), interfolded with and commonly tectonically overlying the Ojibway gneiss association, include felsic orthogneiss, amphibolite and metasediments. Sand Bay metasediments include quartzites, calc-silicates and semipelites. The Sand Bay gneiss association quartzites are common and their sedimentological maturity is moderate; quartz is accompanied by feldspar, mica, titanite, epidote, ilmenite, allanite and apatite, typical thicknesses are a few metres (Culshaw and Dostal 1997). Early Palaeoproterozoic to ca.1400 Ma ages have been recorded from detrital zircons in a Sand Bay gneiss association quartzite (Krogh pers. comm.). A semipelite marker horizon, the laterally extensive Dillon schist, has yielded zircon grains ranging from 1900 ±23 Ma to 1362 ±35 Ma, giving a maximum depositional age for the Sand Bay gneiss association protoliths of ca. 1360 Ma (Culshaw and Dostal 1997). The plagioclase-biotite-quartz Dillon schist includes epidote, allanite, and magnetite in its matrix, and titanite, carbonate, tourmaline, ilmenite, and garnet in segregations (Culshaw and Dostal 1997). A sedimentary package

of subordinate quartzite interbedded with dominant semipelitic schist could be produced by alternating domination of continental siliciclastic and juvenile volcaniclastic sources, represented by the detrital zircon as semblages in the quartzite and Dillon schist respectively. From comparisons of detrital zircon ages, T. Krogh (pers. comm.) suggested that the Sand Bay metasediments received detritus from a Laurentian source, implying proximity to the Laurentian continental margin. Compared to marginal volcanic basin facies models, inferred Sand Bay sedimentary facies, in particular the alternating continental siliciclastic and juvenile volcaniclastic sources, resemble shallow-water, continental arc-proximal basin deposits, of intra-arc or back-arc type (e.g. Winn 1978, Marsaglia 1995, Petford and Atherton 1995).

A geochemical study of the Sand Bay amphibolites and felsic orthogneisses suggested their protoliths were bimodal volcanics (Culshaw and Dostal 1997). The major and trace element geochemistry of the Sand Bay amphibolites resembles modern continental tholeiites, showing no significant metamorphic disruption of diagnostic high field strength trace elements (Culshaw and Dostal 1997). The Sand Bay amphibolites have a prominent negative Nb anomaly suggesting involvement of subduction-modified mantle in their genesis. High Th/La compared to MORB indicate the possibility of minor crustal contamination. Sand Bay felsic orthogneisses have negative Eu, Ti and Nb anomalies compatible with a continental crustal or arc origin. The bimodal nature of the Sand Bay orthogneisses and their trace element geochemistry suggest formation of the igneous protoliths in a continental environment undergoing active extension, perhaps a continental rift, back-arc or intra-arc rift setting (Culshaw and Dostal 1997). Bimodal volcanic sequences are not always produced in continental environments, but can also be

produced in oceanic arc or rift settings e.g. the Izu – Bonin arc (Nishimura et al. 1992). However most authors place the Sand Bay gneiss association in an ensialic setting (Culshaw and Dostal 1997, Rivers and Corrigan 2000, Slagstad et al. *in press*).

Lighthouse gneiss association

Culshaw and Dostal (2002) showed that the layered metamorphic rocks of the Lighthouse gneiss association, like the adjacent Sand Bay gneiss association, are of volcano-sedimentary origin. The Lighthouse gneiss association lacks the distinctive felsic igneous rocks and quartzites of the Sand Bay gneiss association, and is dominated by amphibolites and feldspathic metasediments (Fig. 1.3) (Culshaw and Dostal 2002). The Lighthouse gneiss association is divided into geochemically and lithologically distinctive upper and lower units by a prominent anorthosite. Psammite-pelite pairs, common in the upper unit of the Lighthouse gneiss association, may be turbiditic greywacke-shale couplets. Quartzofeldspathic semipelites found in both the upper and lower units are interpreted as compositionally immature epiclastic sediments (Culshaw and Dostal 2002). Layered and laminated amphibolite-metasediment and amphibolite schists in the lower unit are probably reworked tuffaceous rocks (Culshaw and Dostal 2002). Culshaw and Dostal (2002) interpreted the interlayered immature clastic metasediments and meta–volcaniclastics to represent locally derived volcaniclastic rocks.

The lower unit amphibolite has a mafic tholeiite major element composition and a trace element signature resembling oceanic tholeiite with a minor subduction zone- or subduction-modified mantle influence, similar to Sand Bay amphibolite geochemistry (Culshaw and Dostal 2002). However, without other evidence (e.g. Nd isotopes) it is

difficult to discriminate between minor contributions from mantle directly above a subduction zone, or older subduction-modified continental sources (Culshaw and Dostal 2002). The amphibolites of the upper unit have no negative Nb anomaly and have trace element ratios similar to MORB (mid-ocean ridge basalt); they are therefore likely to have formed from the depleted mantle (Culshaw and Dostal 2002).

Sediments dominated by volcaniclastic rocks of turbiditic affinity, and subduction influenced basaltic lavas that grade into MORB-like basalts, are common in oceanic back-arc basins, e.g. Scotia Sea, Mariana Basin, but could also be produced by high rates of extension in marine-influenced continental back-arc basins, e.g. Sea of Japan or Tierra del Fuego - South Georgia basins (Winn 1978, Nohda and Wasserburg 1981, Cas and Wright 1987, Wilson 1989, Gamble et al. 1995, Marsaglia 1995). If the Sand Bay and Lighthouse gneiss associations are genetically linked, the progression from the bimodal-volcanic siliciclastic Sand Bay gneiss association to the volcaniclastic-turbidite, and basalt-dominated Lighthouse gneiss association might reflect progressive rifting of a continental arc terrane and growth of a back-arc basin, perhaps behind the hypothetical Muskoka - Ojibway arc (Slagstad et al. *in press*). Alternatively the Lighthouse gneiss association protoliths could have formed outboard in a marine setting, separate from the Sand Bay gneiss association protoliths in space and time. Using a combined U-Pb detrital zircon and Sm-Nd isotopic study of Lighthouse metasediments and metavolcanics respectively, it should be possible to test alternative hypotheses. Table 1.1 summarises a range of alternative interpretations of detrital zircon U-Pb age ranges and metavolcanic Sm-Nd isotopic data. Further constraints on the origin of the Lighthouse gneiss

association will be provided by comparisons of U-Pb and Sm-Nd results with geochronological and geochemical data from other CGB and Grenville Province rocks.

Detrital zircon age range► **Metavolcanic ε_{Nd} values (ca. 1.35 Ga) ▼**	**Juvenile; ca. 1.4-1.3 Ga ages**	**Wide range of ages 1.3 Ga – 3.5Ga**
High: island arc, back arc or MORB values (i.e.> +5)	a) offshore basin or b) continental basin with no magmatic contamination or older detritus	a) offshore basin near to continental margin or b) continental basin with continental detritus and no magmatic contamination
Low: continental lithosphere or enriched asthenosphere values (< +5 to - 30)	a) continental basin with juvenile detrital sources and contamination by older low ε_{Nd} material or b) offshore basin with large volume of subducted continental sediment leading to contamination by low ε_{Nd} material	a) continental basin with continental detritus and contamination by older low ε_{Nd} material or b) offshore basin with large volume of subducted continental sediment leading to contamination by low ε_{Nd} material.

Table 1.1 Alternative interpretations of a range of U-Pb and Sm-Nd results. Depleted mantle at 1.35 Ga = +5.5 - De Paolo (1981).

Chapter 2

Petrology

2.1 INTRODUCTION

High-grade metamorphism and ductile deformation have obliterated most of the primary sedimentary and igneous characteristics of the Shawanaga domain supracrustal gneisses. Studies by Culshaw and Dostal (1997, 2002) have shown that despite penetrative ductile deformation and metamorphism, the Lighthouse gneiss association and subjacent Sand Bay gneiss association metasediments preserve supracrustal successions without tectonic repetition, and that the metavolcanic rocks preserve primary igneous geochemical characteristics. Culshaw and Dostal (1997, 2002) interpreted the Lighthouse and Sand Bay gneiss associations as supracrustal rocks deposited in arc-marginal volcanic rift basins.

A mineralogical examination of selected samples (petrographic and microprobe) was undertaken in order to characterize the Lighthouse gneiss association metasediments and metavolcanics; in particular those sampled for U-Pb detrital zircon geochronology and Sm-Nd isotopic analysis. Citing geochemical and lithological evidence, Culshaw and Dostal (2002) have suggested that genetic relationships, in terms of tectonosedimentary environment and magma sources, exist between the Lighthouse and subjacent Sand Bay gneiss associations. To evaluate this hypothesis the predominant metasedimentary lithology in the Sand Bay gneiss association, the Dillon schist, and selected Sand Bay amphibolites, are described and included for comparison with the Lighthouse gneiss association lithologies. The chapter concludes with an interpretation of the metasediments and amphibolites in terms of the origin of their protoliths, and a

comparison of the geochemical characteristics of the Dillon schist and Lighthouse gneiss association metasediments. Lithological data for the Shawanaga domain is from Culshaw and Dostal (1997, 2002), Wodicka (1994), Wodicka et al. (2000), and this study (Appendix A). Up, and down-section refers to the present tectonostratigraphy and attitudes (southeast and northwest respectively), not necessarily to original younging direction which is unknown.

2.2 ANALYTICAL TECHNIQUES

Normal thin and polished C-coated sections were prepared for optical microscopy and electron microprobe analysis. The electron microprobe at Dalhousie University is a JEOL JXA-8200 with five wavelength dispersive spectrometers (WDS). The WDS are capable of analyzing elements from B to U. Operating conditions were 15Kv at 20na, with 20s counting times in WDS mode, using all 5 spectrometers. Major and trace element analysis was undertaken by X-Ray Fluorescence (XRF) at the Regional Geochemical Centre at Saint Mary's University, Halifax. See Dostal et al. (1994) for XRF analytical details.

2.3 LITHOSTRATIGRAPHY

Lighthouse gneiss association

An elongate anorthosite body divides the Lighthouse gneiss association into an upper and lower unit, each with distinctive lithological characteristics (Wodicka 1994, Culshaw and Dostal 2002). Figure 2.1a shows a measured section taken from the thickest part of the Lighthouse gneiss association in the vicinity of Sandy Island (for section location see Fig 1.3). The lack of repetition in the column suggests that it represents an

original sequence without duplication, though as a result of extensional deformation significant reduction in thickness, perhaps by as much of an order of magnitude, may have taken place (Culshaw and Dostal 2002). Positions of the samples taken for U-Pb geochronology, geochemistry, and petrological analysis are marked on fig. 2.1a. Immediately adjacent to the Sand Bay gneiss association (Fig. 1.3, 2.1a), the ca. 370m thick lower unit is dominated by amphibolite, with metasediments forming only about 10 % of the section. Quartzofeldspathic semipelite, found in a few 1-2 m thick packages with amphibolite, is the only metasedimentary lithology (Culshaw and Dostal 2002). A single semipelite from the lower unit was sampled for U-Pb detrital zircon geochronology. Lower unit amphibolites normally comprise massive granoblastic layers up to several metres thick. (Culshaw and Dostal 2002). Five amphibolites were selected for petrological and Sm-Nd isotopic analysis from the suite of samples collected by Culshaw and Dostal (2002).

Outcropping immediately beneath the extensional shear zone at the base of the Parry Sound domain (Fig. 1.3, 2.1a), the upper unit of the Lighthouse gneiss association is lithologically more diverse than the lower unit, and includes abundant amphibolite, semipelite and psammite-pelite pairs along with subordinate felsic gneiss. Semipelite and psammite-pelite are second only to amphibolite in abundance, forming about one third of the upper unit (Culshaw and Dostal 2002). The psammite-pelites comprise alternating leucosome-bearing pelitic and psammitic layers, commonly on a 10-100 cm scale. The semipelites form metre-thick uniform layers, with rare calcareous schists (Culshaw and Dostal 2002). A semipelite and a psammite from the upper unit were sampled for U-Pb detrital zircon geochronology and petrology.

Amphibolite thickness in the upper unit varies from 30m to 10cm. Variations in garnet and amphibole abundance may represent protolith compositional variability or variable metamorphism (Culshaw and Dostal 2002). From the upper unit sample suite collected by Culshaw and Dostal (2002) a subset of five amphibolites was selected.

Sand Bay gneiss association

Figure 2.1b is a representative stratigraphic column of the Sand Bay gneiss association, measured from a section traverse along Shawanaga Bay (Fig. 1.2). The succession closely resembles the Sand Bay gneisses that directly underlie the Lighthouse gneiss association in the study area. All the metasedimentary lithologies are interlayered with leucocratic quartzofeldspathic gneisses and amphibolites that together represent bimodal volcanic rocks (Culshaw et al. 1989, Culshaw and Dostal 1997). By an order of magnitude, the Dillon schist is the most extensive metasedimentary lithology in the Sand Bay gneiss association, outcropping for 30 km along strike and attaining a thickness of 350 m near Shawanaga Bay (Culshaw and Dostal 1997). A detrital zircon geochronological study of the Dillon schist revealed a combination of juvenile, and older, probably Laurentian, sources (T. Krogh pers. comm.). In the lower part of the measured section, the Sand Bay gneiss association contains more varied metasediments, including migmatitic grey gneisses, and thin calc-silicates interbedded with amphibolite. Sedimentologically immature quartzites are common throughout the section (Culshaw and Dostal 1997).

Most Sand Bay gneiss association amphibolites are migmatitic and granoblastic, lacking relict igneous textures, with layering defined by variations in amphibole,

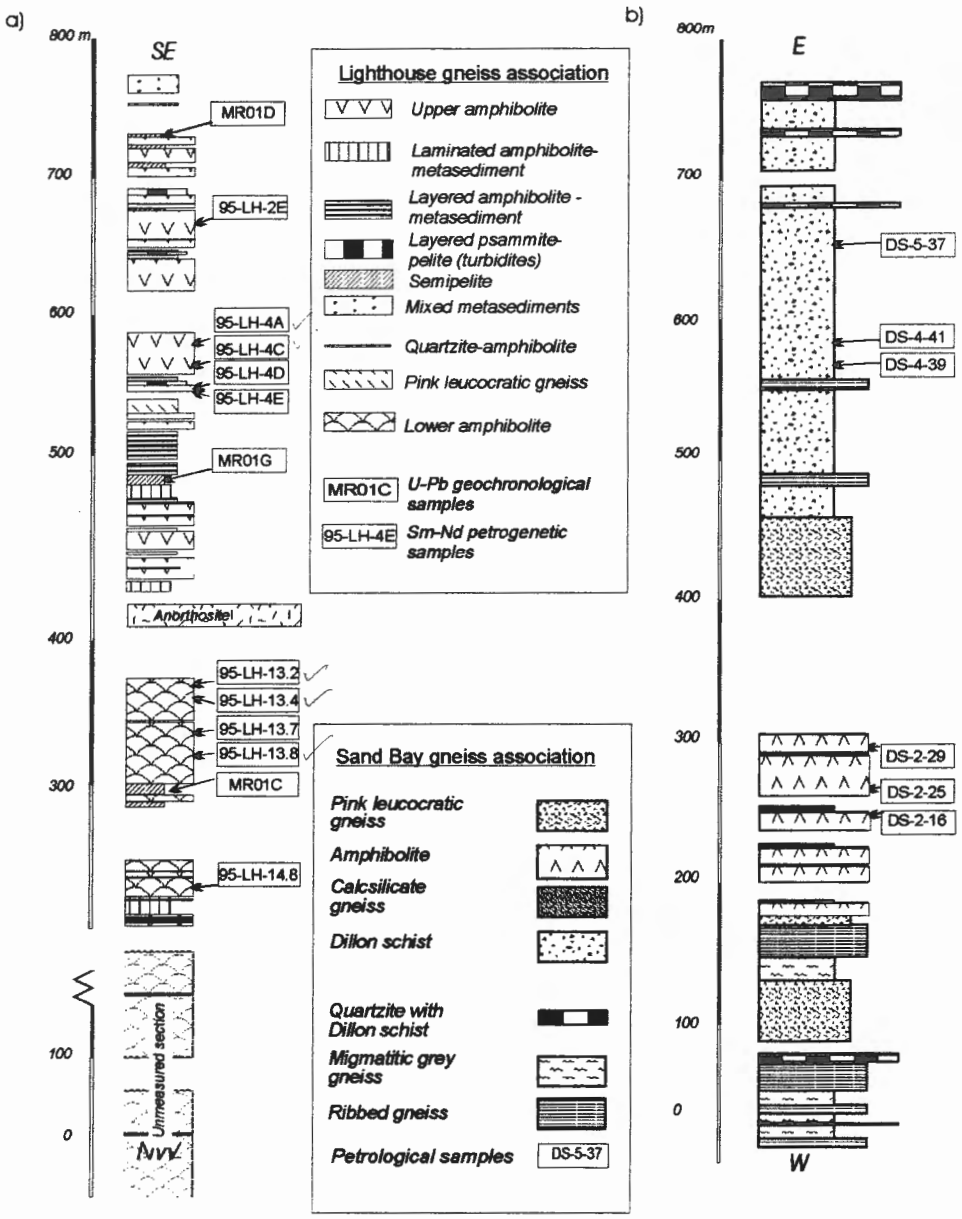

Figure 2.1. a) Measured section of the Lighthouse gneiss association, after Culshaw and Dostal (2002), U-Pb geochronology and Sm-Nd petrogenetic samples are marked. For section location see Figure 1.3. b) Measured section of the Sand Bay gneiss association, after Culshaw and Dostal (1997), petrology samples are marked DS-. For section location see Figure 1.2a.

biotite and plagioclase. From the samples collected by Culshaw and Dostal (1997), a subset of four amphibolites and three samples of the Dillon schist were selected, to allow lithological comparisons to be made between the Sand Bay and Lighthouse gneiss associations.

Metasediments

Lighthouse gneiss association - lower unit semipelite (MR01C)

Sample MR01C is from a 4m-thick semipelite in the upper part of the lower unit (Fig. 2.1a). MR01C is coarse grained and equigranular, with platy green biotite defining a metamorphic foliation. Coarse-grained alkali feldspar together with medium-grained, plagioclase, form 50% of the sample. Quartz, comprising 15% of the sample along with the two feldspar phases, defines a granoblastic texture with common 120° triple junctions. Medium-coarse grained idioblastic laths of biotite, with green-brown pleochroism, constitute about 30% of the sample. Opaque phases form the remaining 5% of the sample.

Lighthouse gneiss association - upper unit semipelite (MR01G)

MR01G is a coarse grained semipelite from a 1 metre-thick yellow-weathering layer in the middle part of the upper unit (Fig. 2.1a). Plagioclase comprises 66% of the sample forming a mosaic texture of coarse-grained crystals. Greenish biotite is found as fine – medium grained idioblastic laths forming 10% of the sample. The remainder is made up of fine-grained quartz, titanite and epidote. Titanite forms fine-grained,

diamond-shaped, highly birefringent crystals, whereas epidote is found as high relief, fine-grained, ovoid crystals.

Lighthouse gneiss association - upper unit psammite (MR01D)

Sample MR01D is an equigranular brown-grey, mediumgrained quartzofeldspathic psammite taken from a 1.5m thick garnetiferous, leucosome-free layer in the uppermost 100m of the upper unit (Fig. 2.1a). The sample is from a psammitic layer in a package of psammite-semipelite. Plagioclase feldspar, as medium grained crystals forming a granoblastic matrix, is the dominant phase comprising about 60% of the sample. Aligned greenish biotite laths comprise about 25% of the sample. Garnet porphyroblasts, forming about 10% of the sample, are coarse-grained, and their rims appear to be breaking down into fine-grained plagioclase. Minor quantities of apatite and very fine-grained zircon are also found.

Table 2.1 summarises the mineralogy of the three Lighthouse gneiss association metasediment samples.

	plagioclase feldspar	alkali feldspar	biotite	quartz	accessories (see Table 2.2)
MR01C-lower unit	40	10	30	15	5
MR01G-upper unit	65	/	20	/	15
MR01D-upper unit	60	/	25	/	15

Table 2.1. Summary of mineralogy of Lighthouse gneiss association metasediments (modal%).

Microprobe data

Feldspar analyses from metasediment samples MR01C, MR01D and MR01G and the Dillon schist are plotted on Fig. 2.2a and are tabulated in Appendix A. The lower unit

sample (MR01C) includes both alkali and plagioclase feldspar. Alkali feldspars from MR01C have compositions between Or_{50}-Or_{92}. The plagioclase feldspars in MR01C average ca. An_{20}, and are oligoclase. Feldspars from the upper unit samples (MR01G, MR01D) are more calcic than the lower unit, and alkali feldspar is absent. Andesine (An_{33}) from MR01G is the most calcic plagioclase in the Lighthouse gneiss association. The uppermost sample MR01D has the least diverse feldspar compositions with all analyses overlapping in the oligoclase field, averaging An_{20}.

Biotite Fe/(Fe+Mg) values vary from 0.54-0.63 in samples from the Lighthouse gneiss association. Fe/(Fe+Mg) values increase up-section, with the highest values found in the uppermost sample, MR01D.

	MR01C	MR01G	MR01D	Dillon schist
apatite	X	X	X	O
titanite	O	x	O	O
garnet	O	O	X	O
zircon	X	x	X	X
amphibole	O	x	O	X
epidote	O	X	O	X
magnetite	O	O	X	X
ilmenite	O	x	O	X

Table 2.2 Summary of metasediment accessory phases from the upper and lower units, Lighthouse gneiss association, and segregation-free samples of Dillon schist. X = abundant (1-5modal%), x=present (<1modal%), 0=not found.

Compositions of accessory phases in the Lighthouse gneiss association metasediments are shown in Table 2.2, and further details are presented in Appendix A.

Garnet (Alm_{69-71} Sps_{47-15} Prp_9 Grs_{4-6}) only occurs in MR01D, the sample from the uppermost part of the upper unit. Zircon and apatite are rare submicroscopic grains in all the samples. Sample MR01G has the greatest variety of accessory minerals including titanite, amphibole, epidote, and ilmenite, as well as zircon and apatite.

The Sand Bay gneiss association - Dillon schist

Petrography

The petrography of three leucosome-free Dillon schist samples is summarized in Table 2.3. Samples are equigranular and coarse-grained, with quartz and feldspar typically forming a granoblastic matrix. The stratigraphic positions of the three samples are shown on fig. 2.1a.

	plagioclase feldspar	biotite	quartz	accessories (see table 2.2)
DS-4-39	55	25	10	10
DS-4-41	50	30	10	10
DS-5-37	65	25	5	5

Table 2.3. Summary of mineralogy of selected Dillon schist samples (%).

Microprobe data

Feldspar compositions from the Dillon schist samples are plotted on fig. 2.2a, and listed in Appendix A. All 21 analyses are low-CaO oligoclase feldspar averaging An_{12}.

Biotite compositions vary from moderately phlogopitic to more anninitic types. Highest Fe/(Fe+Mg) is found in the stratigraphically lowest samples, with DS-4-39 having Fe/(Fe+Mg) of 0.37. Fe/(Fe+Mg) decreases up section to more phlogopitic

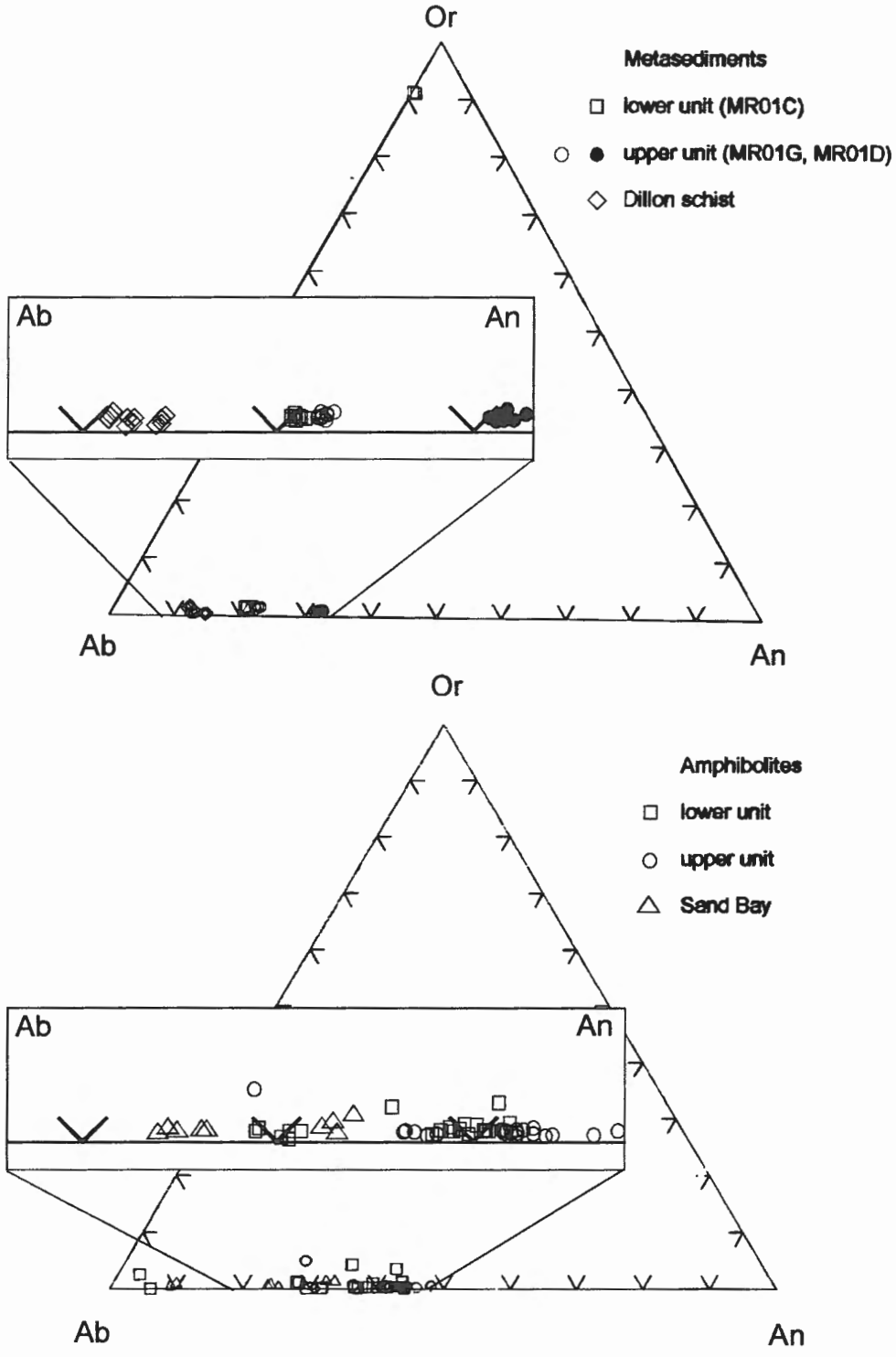

Figure 2.2 Metasediment and amphibolite feldspar compositions from the Lighthouse gneiss association and Dillon schist.

compositions, reaching about 0.31 in sample DS-5-37.

The most abundant accessory phases in leucosome free samples of the Dillon schist are magnetite and ilmenite, together forming up to 10% of some samples (Table 2.2, Appendix A).

Metavolcanics

Lighthouse gneiss association amphibolites-lower unit

The lower unit amphibolites are petrographically uniform, being dominated by granoblastic coarse-grained idioblastic amphibole, and yellowish plagioclase. Accessory phases include fine-grained apatite, ilmenite, and quartz.

Lighthouse gneiss association amphibolites-upper unit

Upper unit amphibolites are dominated by coarse-grained pleochroic green idioblastic amphibole, with subordinate yellow-grey plagioclase, accessory ilmenite, titanite, apatite, quartz, and rare skeletal garnet (Alm_{53} Sps_7 Prp_9 Grs_{31} – Appendix A).

Sand Bay gneiss association amphibolites

Coarse-grained idioblastic amphibole, the dominant phase in the amphibolites from the Sand Bay gneiss association, is accompanied by plagioclase, biotite, and rare clinopyroxene, with accessory magnetite, ilmenite, apatite, and quartz.

Microprobe data

Lighthouse gneiss association upper unit samples have a restricted range of compositions between An_{29} to An_{48} (Fig. 2.2b). Lower unit plagioclase compositions from An_4 to An_{43}, with low An samples overlapping with Sand Bay amphibolite

plagioclase compositions (Fig. 2.2b). Plagioclase compositions from two Sand Bay amphibolites have a wide range from An_9 to An_{35} (Fig. 2.3, Appendix A-Table A1). The range of plagioclase compositions within individual samples is typically narrow e.g. An_{26-28} (95-LH-14.2). Plagioclase is typically unzoned with compositions similar in the center and margins of the crystals.

Table 2.4 summarizes amphibolite accessory phases found in the upper and lower unit samples, and the Sand Bay gneiss association.

Amphibole compositional variability is limited both within and between amphibolite samples from the upper unit, lower unit, and the Sand Bay gneiss association. All amphiboles are hornblende, with total variations in mol % Fe, Ca, and Mg less than ±4% (Appendix A).

	upper unit	lower unit	Sand Bay gneiss association
apatite	X	X	X
titanite	X	X	X
quartz	X	x	X
biotite	O	O	X
ilmenite	X	X	X
garnet	X	O	O

Table 2.4 Summary of amphibolite accessory phases from the upper and lower units, Lighthouse gneiss association, and Sand Bay amphibolites. X = abundant (1-5modal%), x=present (<1modal%), 0=not found.

2.4 DISCUSSION

The upper and lower units in the Lighthouse gneiss association are lithologically similar, both being composed of interlayered feldspathic metasediments and amphibolite. The Sand Bay gneiss association also includes feldspathic metasediments and amphibolite, along with felsic orthogneiss and more silicic metasediments.

Metasediments

As Culshaw and Dostal (2002) have pointed out, Lighthouse gneiss association metasediment compositions vary between the upper and lower units. Variation in plagioclase feldspar composition of An_{20}-An_{32} within the upper unit is greater than variation between the upper and lower units (means of An_{26} and An_{21} respectively). Plagioclase compositions from the lower unit (MR01C; mean An_{22}) and upper unit (MR01D; An_{22-24}) overlap. Upper unit sample MR01G is distinguished by uniformly higher An compositions (mean An_{31}). MR01D is distinguished from the other samples by the presence of garnet. The lower unit sample MR01C is the only sample analysed that contains alkali feldspar. Apart from ubiquitous zircon and apatite, no strong similarities in the range of accessory minerals unite any of the metasedimentary samples. MR01G has the greatest accessory mineral diversity in the Lighthouse gneiss association metasediments, with titanite, amphibole, and epidote accompanying zircon and apatite. In summary, a wider range of mineralogical variation is found within the upper unit than within the lower unit, and samples from both units overlap. With the exception of alkali feldspar in MR01C, and garnet in MR01D no significant petrological differences distinguish the upper and lower units.

Wodicka et al. (2000), in a detailed metamorphic study of the Lighthouse gneiss association and adjacent supracrustal gneisses reported similar mineral assemblages to those described here. Peak metamorphic assemblages in a semipelite from the upper unit of the Lighthouse gneiss association, in addition to the minerals already mentioned, include kyanite and rutile in a semipelite; characterizing early upper amphibolite peak metamorphism, and muscovite formed during retrogression (Wodicka et al. 2000). Wodicka et al. (2000) also record abundant leucosome, indicating partial melting Peak metamorphic pressure and temperature estimates locally exceed 10 kbar and 750°C, and may have been synchronous with thrust-related deformation (Wodicka et al. 2000).

Culshaw and Dostal (2002) have suggested that the Lighthouse gneiss association metasedimentary protoliths were sedimentologically immature volcaniclastic turbidites. The mineralogical data presented here are compatible with sedimentary protoliths derived from mafic volcanic rocks. The abundance of biotite and scarcity of quartz suggest low-SiO_2 mafic sedimentary protoliths, emphasising the compositional immaturity of the Lighthouse gneiss association metasediment protoliths, and supporting the conclusions of Culshaw and Dostal (2002).

The Dillon schist samples, as might be expected from a uniform, thick metasedimentary unit, have homogenous mineral assemblages and mineral compositions. Feldspars cluster tightly about low-Ca oligoclase, and biotites have a more restricted range of compositions than the Lighthouse gneiss association metasediments. In the leucosome-free samples, accessory minerals are limited to Fe-oxides, epidote, zircon, and amphibole, although Culshaw and Dostal (1997) also report the presence of local

muscovite and scapolite, and in veins and segregations diverse accessory minerals including chlorite, amphibole, tourmaline, and garnet.

The Lighthouse gneiss association metasediments are similar to the Dillon schist in gross mineralogy, being dominated by plagioclase and biotite, however the microprobe study reveals subtle compositional differences between the two. Dillon schist plagioclases are significantly less calcic than any Lighthouse metasediment plagioclases (An_{14} versus An_{23}), and alkali feldspar was not found in the Dillon schist samples, though N. Culshaw (pers. comm.) has recorded alkali feldspar from other Dillon schist samples. Biotite from the Dillon schist is typically more magnesian than biotite from the Lighthouse gneiss association metasediments, and the absence of Fe-oxides as accessory phases in the Lighthouse gneiss association metasediments further distinguishes the two. The microprobe study has not indicated a strong mineralogical link between the Dillon schist and metasediments from either unit of the Lighthouse gneiss association. Metasediment mineralogical variation within the Lighthouse gneiss association is as great as the variation between the Lighthouse gneiss association and the Dillon schist. The mineralogical differences between the Dillon schist and Lighthouse metasediments, and mineralogical variation within the Lighthouse gneiss association, probably reflect variations in protolith composition. A wide variation in mineralogical composition is not unexpected in sediments generated during continental back-arc rifting, as a wide variety of possible sediment sources are available in such an environment. Further investigation of sedimentological linkages between the Lighthouse gneiss association metasediments and the Dillon schist could be accomplished by a detrital zircon geochronological, isotopic, and geochemical study.

Metavolcanics (amphibolites)

From petrography, geochemistry, and field relations Culshaw and Dostal (2002) concluded that the amphibolites of the Lighthouse gneiss association originated as fine-grained basaltic volcanic rocks. In terms of plagioclase compositions, there is much compositional overlap between the Sand Bay amphibolites and the lower unit of the Lighthouse gneiss association. Overlap between feldspars from the upper and lower unit, like Sand Bay –lower unit feldspar compositional overlap, probably reflects the bulk compositional similarities of these tholeiitic basaltic rocks, with feldspar compositional scatter perhaps reflecting metamorphic disruption (Culshaw and Dostal 1997, 2002).

Wodicka et al. (2000), in a detailed metamorphic study of samples taken from a shear zone immediately beneath the Parry Sound domain, report a similar assemblage to that described here along with more abundant garnet, accessory biotite, scapolite, and rare clinopyroxene, typical of mafic rocks at upper amphibolite facies.

Origin of the Dillon schist and Lighthouse gneiss association metasediments; trace element constraints.

Culshaw and Dostal (2002), citing geochemical and lithological evidence, suggested that the Lighthouse gneiss association and the Sand Bay gneiss association protoliths were genetically related. Diagnostic trace elements are used in the following section to investigate possible correlation between the metasedimentary protoliths of the Sand Bay, and upper and lower Lighthouse gneiss associations, and to identify likely depositional environments.

By almost an order of magnitude, the Dillon schist is the thickest metasedimentary unit in the entire Shawanaga domain (Fig. 2.1). Interleaving of the pelitic Dillon schist with bimodal metavolcanics and siliciclastic metasediments, along with its complement of two thirds juvenile (i.e. 6 grains ca. 1380 Ma) and one third older (3 grains ca. 1.7 – 1.8 Ga) detrital zircons suggests older continental and juvenile-volcanic sedimentary components were available to the basin in which the Dillon schist protolith was deposited (T. Krogh pers. comm., Culshaw and Dostal 1997). Possible shared sediment sources might include mafic and felsic volcaniclastics, continental sediments, and detritus derived from the erosion of Laurentian margin magmatic arcs (Culshaw and Dostal 1997, Rivers and Corrigan 2000, Slagstad et al. *in press*). With respect to the Lighthouse gneiss association, Culshaw and Dostal (2002) have suggested that the upper unit metasediment protoliths included high-energy facies of turbiditic affinity, and the rarer lower unit metasediments originated as immature epiclastic rocks. The detrital zircon geochronological characteristics of the upper and lower units of the Lighthouse gneiss association are investigated in the following chapter.

Processes from diagenesis to high-grade metamorphism are expected to have affected the geochemical composition of the Shawanaga domain supracrustals, and the widespread segregations enclosed within them suggest that a significant volume of the rocks was mobile in a fluid or melt phase. Studies of segregation-free interlayered metavolcanic gneisses (Culshaw and Dostal 1997) have shown that, in terms of the high field-strength elements (HFSE), these rocks retain their original volcanic compositions, preserving typical magmatic evolutionary trends. In a detailed study of Shawanaga domain gneisses Slagstad et al. (*in press*) have demonstrated that metamorphism in the

presence of fluid or melt has mobilized many elements, especially the large-ion lithophile elements (LILE), and also SiO_2, but that the HFSE are generally immobile. Studies of the mobility of elements during metamorphism (e.g. Fralick and Kronberg 1997, Rollinson 1996, Taylor and McLennan 1985) agree with the conclusions of Slagstad et al. (*in press)* and Culshaw and Dostal (1997) and it seems reasonable to assume that the HFSE (Ti, P, Zr, Hf, Y, Nb) will preserve sedimentary source characteristics.

Figure 2.3 shows Zr/Y and Nb/Y data from Shawanaga domain gneisses and CGB plutonic orthogneisses. Used as a tectonomagmatic discriminant diagram (Fitton et al. 1997, Brewer et al. 2002), the log Zr/Y and log Nb/Y plot distinguishes rocks derived from the depleted mantle (i.e. mid-ocean ridge basalts -MORB), mantle plumes (OIB), the sub-continental mantle, and a variety of crustal sources, it is therefore a useful tool for investigating the origin of volcaniclastic rocks. Basaltic volcanics from both back-arc basins and active juvenile continental arcs have compositions close to the MORB field (Wilson 1989). Continental flood basalts plot between MORB, OIB, SCLM, and crustal compositions

Metasediments from the upper and lower units of the Lighthouse gneiss association plot on a trend between the MORB field, the Lighthouse and Sand Bay amphibolites, and average upper crustal compositions, compatible with a sediment contribution from both the basaltic protoliths of the Shawanaga domain amphibolites (and/or MORB-like material) and continental crust (Fig. 2.3). Metasediments from the upper unit of the Lighthouse gneiss association have higher Nb/Y than the metasediment sample from the lower unit, suggesting Nb enrichment, perhaps as a result of minor

contributions from an enriched mantle component (OIB). No OIB-like material has yet been identified in the southwestern Grenville Province.

In log Zr/Y and log Nb/Y terms, samples of the Dillon schist (Fig. 2.3) are different from either of the Lighthouse metasedimentary samples, plotting on a high Zr/Y trend between MORB and samples of Laurentian arc rocks; CGB plutonic orthogneisses, and 1.9-1.7 Ga Laurentian arc granitoids. The Sand Bay felsic orthogneisses, which have compositions similar to the CGB plutonic orthogneisses, are another possible source of sediment for the Dillon schist protoliths. The Dillon schist Nb-Zr-Y data and the detrital zircon geochronological data (T.Krogh pers. comm.) together suggest that the protolith formed from a combination of ca. 1.38 Ga MORB-like and 1.9-1.7 Ga arc-granitoid sources, probably in a continental rift setting.

Metasediments from both the upper and lower units of the Lighthouse gneiss association have compositions between continental crustal rocks and Shawanaga domain amphibolites, suggesting both units formed from a similar combination of sources (Fig. 2.3). The upper and lower units probably formed in similar tectonic environments, i.e. back-arc basins dominated by volcaniclastic detritus and with some continental sedimentary input. The Lighthouse gneiss association metasediments and the Dillon schist probably shared a low Zr/Y, low Nb/Y MORB -like sediment source, perhaps the younger ca. 1.38 Ga detrital zircon source in the Dillon schist, though contributions from two different high Nb/Y, high Zr/Y sources, resembling average upper crust and Laurentian arc granitoids, distinguish the two. The Nb-Zr-Y differences between the

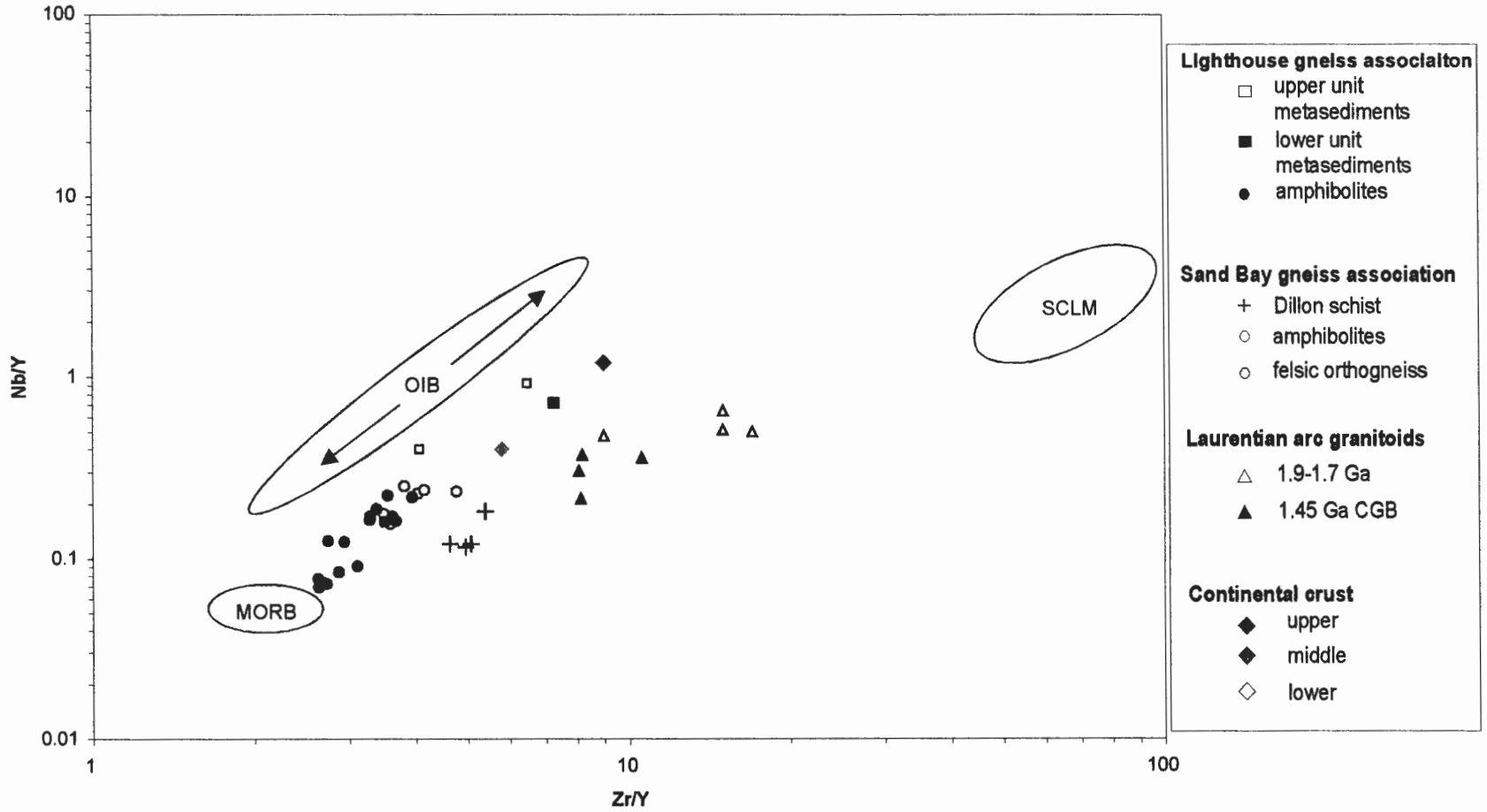

Figure 2.3. Log Zr/Y v log Nb/Y plot for Lighthouse and Sand Bay gneiss association supracrustal rocks. Sources: 1.45 Ga Laurentian arc granitoids - T.Slagstad pers. comm., 1.9-1.7 Ga Laurentian arc granitoids - Barr et al.(2001), Van Schmus et al. (1993), Crustal data - Rudnick and Fountain (1995), Shawanaga domain Culshaw and Dostal (1997, 2002) and this study, MORB (mid-ocean ridge basalt), OIB (ocean island basalt), and SCLM (sub-continental lithospheric mantle) - Wilson 1989.

Dillon schist and the Lighthouse metasediments suggest that they did not form in the same tectonosedimentary environment, and if they are related, a change in sedimentary sources from CGB plutonic orthogneiss-like to average crustal compositions is required. Arc granitoids have higher Zr/Y, and lower Nb/Y than average continental crust as a result of preferential retention of Nb in the downgoing slab and consequent Nb deficiency in the overlying mantle and crust.

The Nb-Zr-Y and detrital zircon data could be explained by initial arc rifting producing the Dillon schist protolith from erosion of arc (or arc-derived) rocks, possibly of 1.9-1.7 Ga age, and 1.38 Ga juvenile volcanics, followed by a change to a more open rift where average continental detritus replaced the arc detritus, producing the protoliths of the Lighthouse gneiss association metasediments. A detrital zircon study would resolve whether the 1.38 Ga juvenile source in the Dillon schist is found in either unit of the Lighthouse gneiss association, and identify any continental sources that contributed zircons.

In summary, although the Dillon schist and Lighthouse gneiss association metasediments share a low Nb/Y, low Zr/Y source, they are distinguished by two contrasting high Nb/Y and Zr/Y sources, suggesting different, but not necessarily unrelated, tectonsedimentrary environments. The two units of the Lighthouse gneiss association have metasediment Nb-Zr-Y compositions compatible with their formation in the same tectonosedimentary environment.

Chapter 3

U-Pb results

3.1 INTRODUCTION

Detrital zircon geochronological studies interpret single grain U-Pb ages in terms of sediment source rock zircon crystallization ages. The spectrum of detrital zircon ages from a sedimentary rock reflects the age diversity of the zircons in its source area. Zircon is durable from sedimentary to high-grade metamorphic conditions and retains U and Pb to high temperatures (>800 °C; Faure 1986). Pb loss as a result of metamorphic fluid transfer, or diffusion can lead to discordance between the ^{235}U-^{207}Pb and ^{238}U-^{206}Pb systems. Concordia plots allow the evaluation and interpretation of discordant data. The thermal and mechanical robustness of zircon, along with high precision analytical techniques, make U-Pb zircon dating a reliable method for provenance studies of ancient sediments at high metamorphic grade.

3.2 ANALYTICAL TECHNIQUES

U-Pb analyses were carried out by thermal ionization mass spectrometry (TIMS) at the Jack Satterley Geochronology Laboratory of the Royal Ontario Museum, Toronto. Three samples between 15 and 25 kg were pulverized by jaw crusher and disc mill into ca. 0.25mm fragments. The heavy mineral fraction was concentrated from the crushed powder using a Wilfey table. Further concentration of the heavy mineral fraction was accomplished by bromoform and methylene iodide heavy liquid separation. Zircon was separated from the remaining heavy minerals using a Frantz isodynamic magnetic separator. Grains were selected on the basis of optical quality from the non-magnetic and

least magnetic fractions, commonly at the 0°, 1°, and 2° side-tilt positions. Approximately 75 grains from each sample were hand picked in alcohol under a binocular microscope, and then air abraded following the procedures of Krogh (1982). Abrasion times varied from 15-50 hours, depending on the mechanical resistance of the grains. From the abraded fraction, morphologically diverse grains representing the range of grain morphologies were selected for analysis. From photographic images grain weights were estimated by measuring grain dimensions and applying a spreadsheet calculation.

Due to small grain weight (<0.004mg), conventional column chemistry techniques for Pb and U extraction are unnecessary. Individual grains were cleaned in acetone and $HN0_3$ and then loaded into Teflon bombs with HF and a calibrated spike of $^{205}Pb/^{235}U$ (Krogh and Davis 1975). The sealed Teflon bombs were heated at 195°C for 4-5 days. Dissolved zircons were loaded with phosphoric acid and silica gel onto outgassed Re filaments, and analysed at temperatures between 1400 °C and 1650 °C on a VG354 mass spectrometer in single collector mode using a Daly detector system. U and Pb isotopic data were corrected for isotopic fractionation, spike, blank, and initial common Pb. U decay constants used are from Jaffey et al. (1971). U-Pb age calculations used the ROM in-house software ROMAGE. Quoted errors are at the 95% confidence level, and are reported in Table 3.1 and shown as ellipses on Figs. 3.2 - 3.5. Regression lines (discordia) follow the maximum likelihood function and error expansion routine of Davis (1982) Further information on regression lines, and error calculations can be found in Appendix B.

3.3 RESULTS

MR01C - Lighthouse gneiss association lower unit semipelite

Sample MR01C, from the central part of the lower unit of the Lighthouse gneiss association in the Sandy Island area (Fig. 1.3, 2.1a), is part of a homogenous three-metre thick alkali feldspar-biotite-quartz semipelite sandwiched between amphibolite layers. Leucosomes present elsewhere in the lower unit are absent from the vicinity of the sample. The 0° non-magnetic, 0°magnetic, and 1°magnetic Frantz fractions yielded a variety of zircon sizes and morphologies including smaller, equant, inclusion-free crystals, and larger elongate prisms with and without opaque inclusions. Nine colourless grains representing the full range of size, morphology and internal features were selected for single-grain analysis (Fig. 3.1a).

The analyses vary from concordant to slightly discordant (Fig. 3.2, Table 3.1) and despite their morphological diversity (Fig. 3.1), these zircons yield a narrow range of ages between 1384 ±3.7 Ma and 1342 ±6.4 Ma. Although Grain Z5, the most discordant analysis, has the highest U (423 ppm), no correlation of U with discordance is found, as concordant grain Z9 also has high U (355 ppm). The average U content of 300 ppm and Th/U ratio of 0.45 collectively suggest that the detrital zircons are of igneous, not metamorphic, origin (Table 3.1).

The best age estimate of the source comes from two overlapping concordant analyses, Z8 and Z9, with a weighted mean of 1383.0 ± 3.9 Ma. Three discordant grains (Z2, Z6, Z7), and the two concordant analyses (Z8, Z9) lie on a discordia with a lower intercept of 1053 +120/-126 Ma and upper intercept of 1387 +21/-11 Ma (Fig. 3.2). The

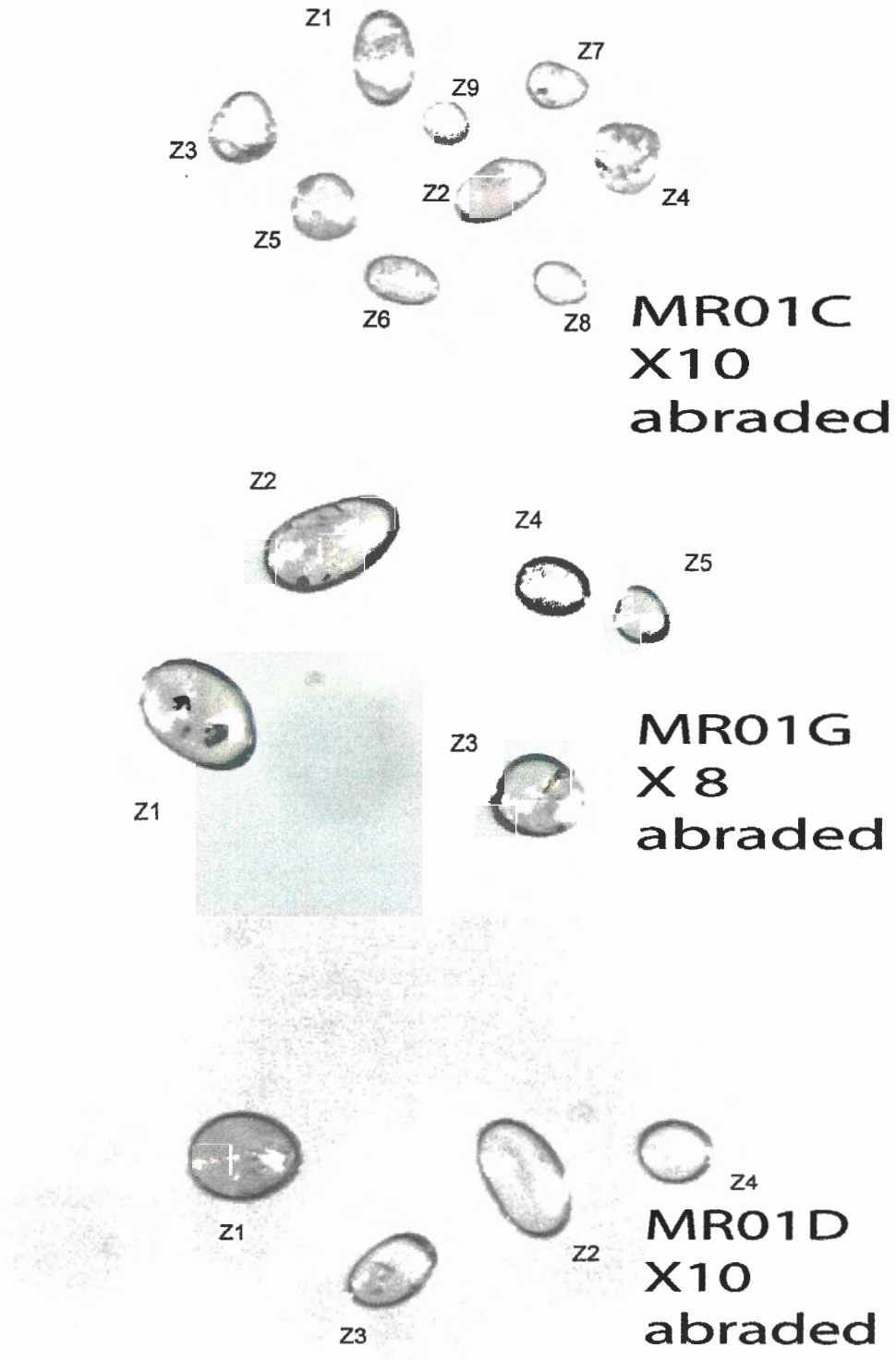

Figure 3.1 Photographs of abraded zircons: samples MR01C, MR01G, and MR01D, field of view approximately 10 mm.

Sample	Fraction	Weight (mg)	U (ppm)	Th/U	common Pb (pg)	207Pb/204Pb	206Pb/238U	2 sigma	207Pb/235U	2 sigma	207Pb/206Pb (Ma)	2 sigma	discord. (%)
Lower Unit													
MR01C semipelite													
jk9p10	Z1 2:1 trs cr pr	0.0014	231	0.49	5.18	98.8	0.2363	0.0007	2.863	0.024	1379.1	13.1	0.9
jk9p11	Z2 2:1 trs pr	0.0009	180	0.62	0.76	290.8	0.2322	0.0008	2.787	0.011	1361.6	5.2	1.3
jk9p12	Z3 trs cr pr	0.0011	333	0.45	1.29	393.9	0.2365	0.0008	2.868	0.011	1381.5	4.9	1.1
jk9p13	Z4 eq trs incl	0.0011	280	0.48	0.75	560.9	0.2361	0.0009	2.867	0.012	1384.2	3.7	1.4
jk9p14	Z5 eq trs pr	0.0006	423	0.44	0.59	577.1	0.232	0.0009	2.811	0.011	1379.6	3.1	2.8
jk9p15	Z6 2:1 trs pr incl	0.0006	187	0.5	0.6	258.4	0.2324	0.0009	2.784	0.013	1357.8	5.6	0.9
jk9p16	Z7 eq trs pr incl	0.0006	167	0.41	0.65	209.8	0.2287	0.0006	2.718	0.012	1342.5	6.4	1.2
jk9p17	Z8 eq trs pr	0.0003	387	0.49	0.58	286.1	0.2389	0.0008	2.901	0.012	1383.3	4.9	0.2
jk9p18	Z9 eq trs pr	0.0002	355	0.45	0.56	185.6	0.2392	0.0007	2.903	0.014	1382.5	7	0
Upper Unit													
MR01D garnet psammite													
jk9p6	Z1 eq trs pr	0.0023	323	0.85	0.95	1845.9	0.323	0.0013	5.029	0.02	1847	2.4	2.6
jk9p7	Z2 3:1 trs pr incl	0.0021	2198	0.25	0.87	6496.9	0.2227	0.0007	2.626	0.009	1328	2.3	2.7
jk9p8	Z3 2:1 trs pr incl	0.0017	59	0.41	0.82	192.8	0.2492	0.0011	3.108	0.018	1435.1	7	0.1
jk9p9	Z4 eq trs pr	0.0012	685	0.36	0.63	1657.2	0.2295	0.0006	2.721	0.008	1337.8	1.8	0.5
MR01G semipelite													
jk9p1	Z1 2:1 trs pr incl	0.0039	92	0.35	0.81	670	0.2523	0.0011	3.185	0.013	1458	4.2	0.6
jk9p2	Z2 3:1 trs pr incl	0.0028	109	0.36	0.67	605.1	0.2319	0.0011	2.772	0.013	1354.1	3.1	0.8
jk9p3	Z3 eq trs pr incl	0.002	97	0.55	0.77	330.4	0.2274	0.0008	2.678	0.012	1325.1	4.4	0.3
jk9p4	Z4 2:1 trs pr	0.0009	73	0.8	0.73	128.9	0.2292	0.0008	2.708	0.018	1331.3	10	0.1
jk9p5	Z5 eq trs pr	0.0007	32	0.66	1.02	43.3	0.2293	0.0015	2.705	0.066	1327.7	41.8	0.3

Footnotes
- Z - zircon; eq - equant; pr - prism; trs - transparent; op - opaque incl - inclusions; 2:1, 3:1, etc. - length:breadth ratio.
- common Pb - Total common Pb, blank isotopic composition: 206/204 - 18.221, 207/204 - 15.612, 208/204 - 39.36
- Th/U calculated from radiogenic 208Pb/206Pb ratio and 207Pb/206Pb age.
- discord. - per cent discordance for the given 207Pb/206Pb age
- decay constants are from Jaffey et al. (1971).

Table 3.1. U-Pb isotopic data, upper and lower units, Lighthouse gneiss association.

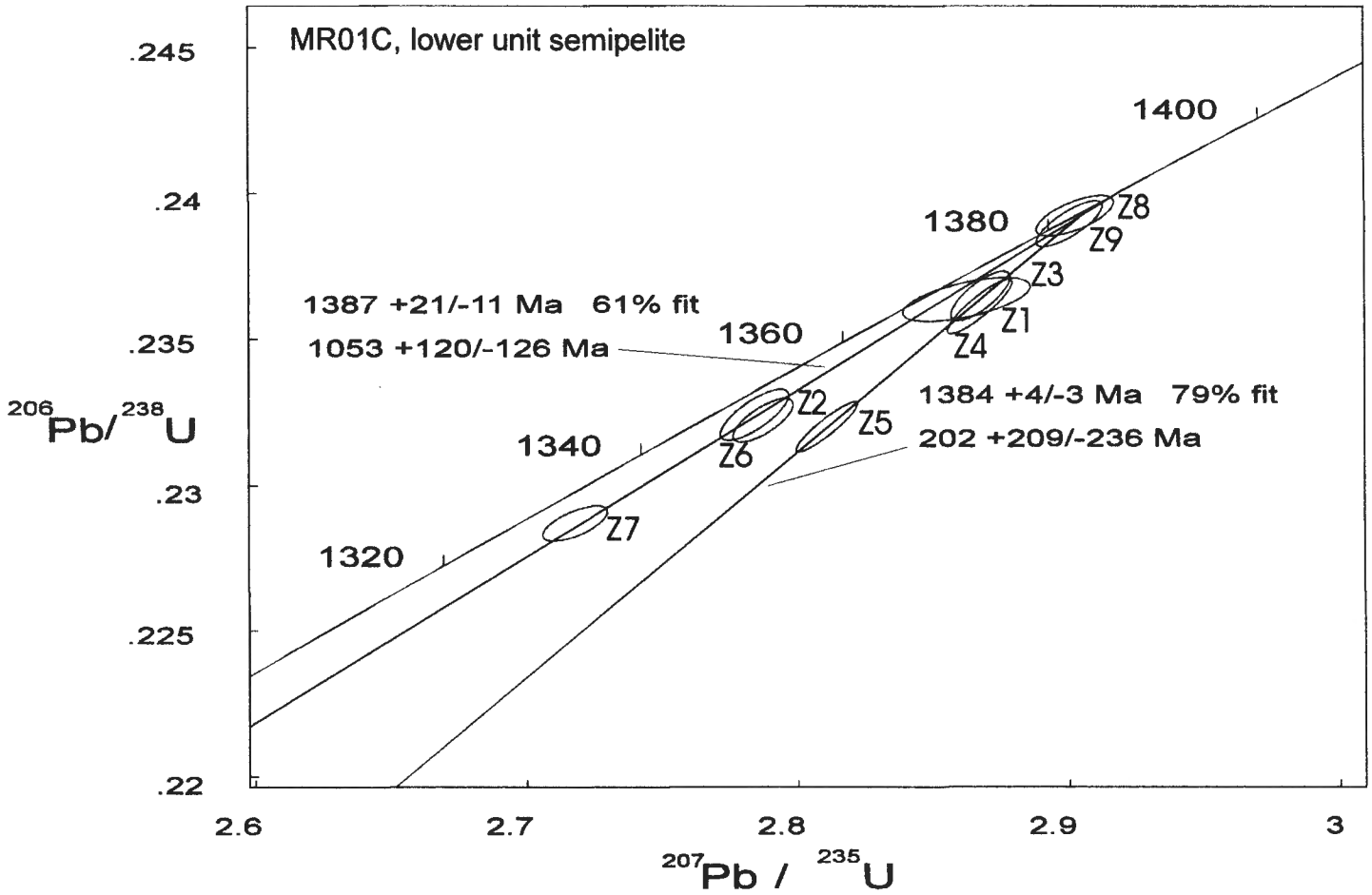

Figure 3.2. U-Pb isotopic data for metasedimentary rock MR01C, lower unit Lighthouse gneiss association. See text for additional details.

lower intercept could reflect Pb-loss during regional amphibolite facies metamorphism at ca. 1050 Ma (Tuccillo et al. 1992, Bussy et al. 1995, Krogh 1997, Timmerman et al. 1997, Wodicka et al. 2000). Four grains (Z1, Z3, Z4, and Z5) appear to have suffered more recent Pb loss and, with Z8 and Z9, lie on a discordia between 1384 +4/-3 Ma and 202 +209/-236 Ma, possibly resulting from gradual diffusive Pb-loss. The grains that experienced ca. 1050 Ma Pb-loss may have reacted more vigorously with fluids mobile during metamorphism than the grains that experienced only diffusive Pb-loss. A discordia produced from all the discordant grains in MR01C would have a similar upper intercept of ca. 1380 Ma, along with a lower intercept ca. 700 Ma, of no obvious geological meaning.

The lower unit metasediments were deposited after 1380 Ma, and it is likely that a single juvenile source contributed all nine grains. There are no detrital zircon ages that might be expected if sediment came from the Laurentian craton or the polycyclic parts of the Central Gneiss Belt. It is possible, although unlikely, that further single grain analyses could reveal non-juvenile sources. A sedimentary package dominated by single-age zircons is likely to have a volcanic source, reinforcing the interpretation of Culshaw and Dostal (2002) that the Lighthouse gneiss association lower unit protoliths were immature volcaniclastic rocks.

MR01G-Lighthouse gneiss association upper unit semipelite

Sample MR01G was collected from the lower part of the upper unit, adjacent to an elongate body of anorthosite (Fig. 1.3, 2.1a). Outcropping as a 0.5 m thick, yellowish, leucosome-free homogenous layer, MR01G is dominated by plagioclase feldspar and

biotite (Culshaw and Dostal 2002). Five high-quality zircon grains were analysed, chosen from the 0° magnetic and 0° non-magnetic fractions, to reflect morphological variability, size, and variations in internal appearance (Fig. 3.1b).

The ages range from a slightly discordant grain at 1458 ±4.2 Ma (Z1) to three concordant to slightly discordant grains (Z3, Z4, Z5) that cluster around 1330 Ma (Table 3.1, Fig. 3.3). Of all the new analyses reported in this study, the MR01G zircon fractions have the lowest U contents (mean U = 82.6 ppm), and average discordance is lowest of the three samples, at 0.4 %. Although the oldest grain is the biggest, there is no strong correlation between grain size and age (Table 3.1). Grain Z1 at 1458 ±4.2 Ma and Z2 at 1354 ±3.1 Ma have similar weights and morphologies despite ca. 100 My age difference (Fig 3.1b). Grains Z4 and Z5 have a weighted mean of 1329.5 ±12.5 Ma which likely represents a maximum depositional age for the protolith of MR01G. Z2 at 1354 ±3.1 Ma may be a discordant grain of ca. 1385 Ma vintage as it falls on the 1385 – 1050 Ma discordia line generated for sample MR01C (Figs. 3.3, 3.5).

MR01D-Lighthouse gneiss association upper unit garnet psammite

This garnetiferous quartzofeldspathic psammite is sampled from interlayered psammite-semipelite from the uppermost part of the Lighthouse gneiss association (Fig. 1.3). The layer sampled is less than 1.5m thick and is sandwiched between massive, rusty-weathering amphibolite layers. As it is a compositionally immature feldspar-biotite-quartz semipelite, this layer, like the other Lighthouse gneiss association metasedimentary rocks, was probably derived from a local source. The four single high-quality grains extracted from MR01D broadly represent the range of zircon

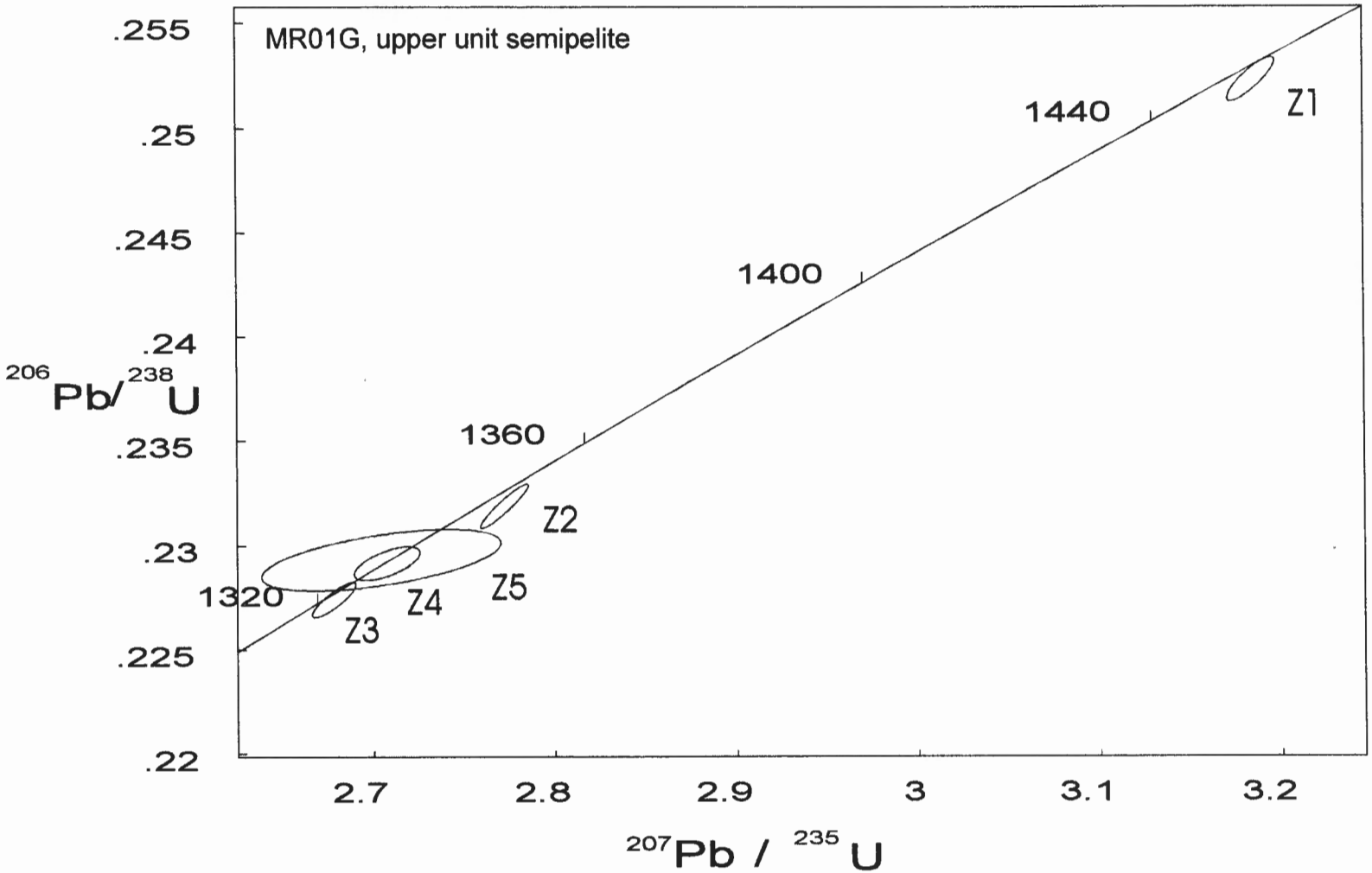

Figure 3.3. U-Pb isotopic data for metasedimentary rock MR01G, upper unit Lighthouse gneiss association. See text for additional details.

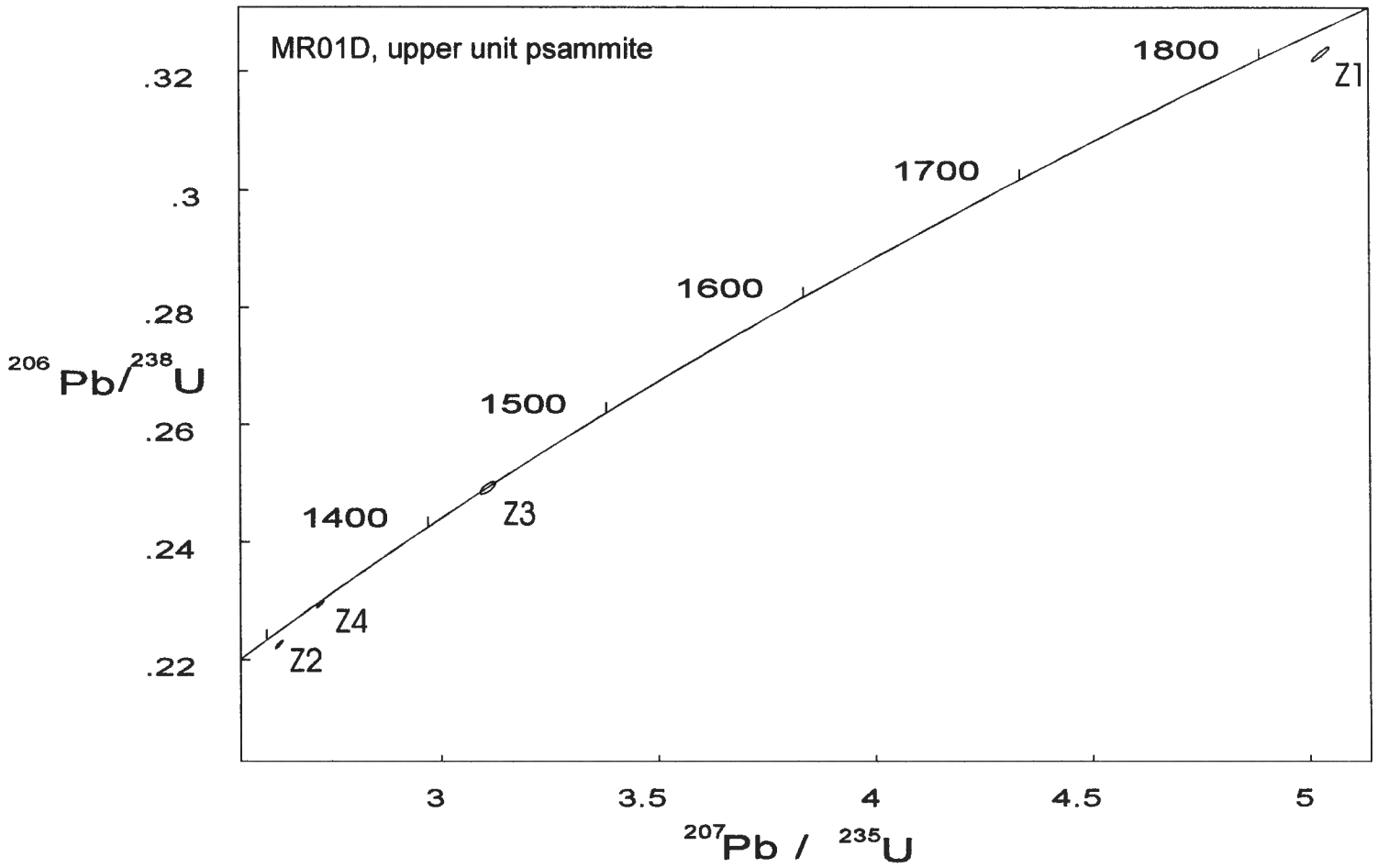

Figure 3.4. U-Pb isotopic data for metasedimentary rock MR01D, upper unit Lighthouse gneiss association. See text for additional details.

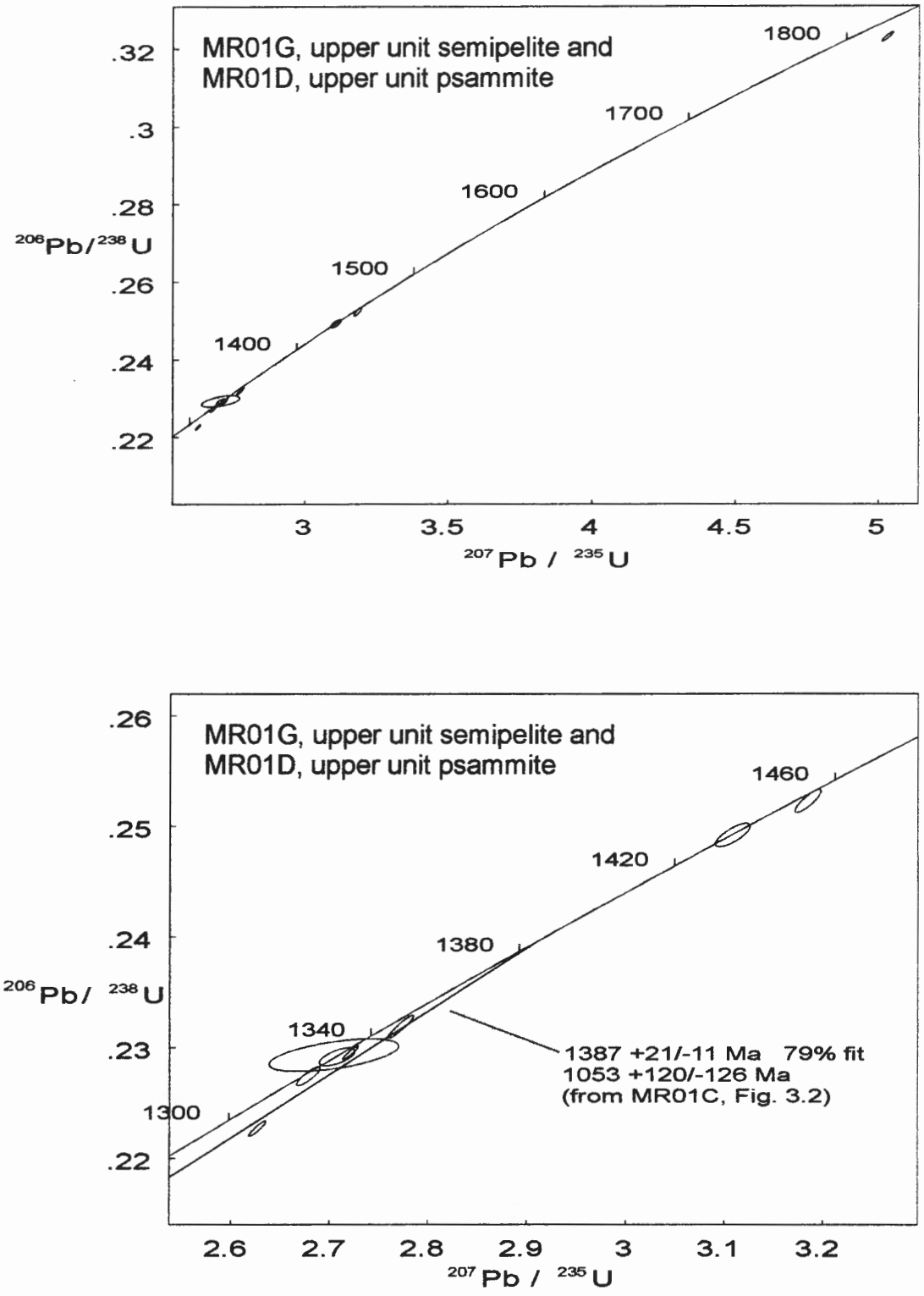

Figure 3.5. U-Pb isotopic data for metasedimentary rocks MR01D and MR01G, upper unit Lighthouse gneiss association. See text for additional details.

morphologies, sizes, and internal features found in the non-magnetic 0°, and magnetic 0°, 1°, and 3° fractions (Fig. 3.1c).

The four analysed grains vary from mildly discordant to concordant (Fig. 3.4, Table 3.1) and from 1847 ±2.4 Ma (Z1) to 1328 ±2.3 Ma (Z2). In the sample there is no correlation between U content and discordance, U content and age, or age and grain size (Table 3.1). A 1435 ±7 Ma grain with small inclusions (Z3) is concordant and represents a contribution from a source of this age. The oldest zircon, a smoky ovoid grain (Z1) dated at 1847 ±2.4 Ma is 2.6% discordant and may have formed at 1882 Ma if ca. 1050 Ma Pb-loss is assumed. The near-concordant analysis Z4 (0.5%) provides a maximum depositional age of ca. 1338 Ma (Table 3.1).

3.4 DISCUSSION

Provenance of the lower unit metasediments - MR01C

Circa. 1380 Ma single grain detrital zircon ages (1394 ±16Ma, 1383 ±48 Ma, 1368 ±36 Ma, and 1362 ±35Ma) are reported from the Dillon Schist member of the subjacent Sand Bay gneiss association (T. Krogh pers. comm.). Four detrital zircons from the Dillon schist and nine from the lower unit are within error of 1380 Ma (Fig. 3.6). Similarity in detrital ages, field relationships and lithologies between the lower unit metasediments and the Dillon schist suggests a genetic link between the two. Culshaw and Dostal (2002) proposed that the Sand Bay gneiss association igneous protoliths were produced during ca. 1370 Ma rifting on the southeastern margin of Laurentia, coincident with the production of the southern granite-rhyolite province (Van Schmus et al. 1996). It is possible that the basin in which the lower unit metasediments were deposited received

detritus from similar sources to those that produced the Sand Bay gneiss association metasediments; and that the ubiquitous ca. 1380 Ma zircons in MR01C and the Dillon schist were created by mid-continent magmatism. The presence of Palaeoproterozoic zircons in the mineralogically immature Dillon Schist and the Sand Bay quartzites (Fig. 3.6) contrasts with the absence of such ages in the zircons analysed from the lower unit semipelite, perhaps reflecting a hiatus in the supply of older sediment during deposition of the lower unit. The absence of older sediment might be explained by uplift at the basin margins changing sediment transfer patterns, exhaustion of the older sediment source, or overabundance of juvenile material.

As no pre-1380 Ma grains have been recorded from MR01C, the lower unit could have formed in a juvenile oceanic setting, perhaps adjacent to the Parry Sound domain. The La Bostonnais tonalite – granodiorite arc complex in the Central Gneiss Terrane of Quebec includes ages between 1400 and 1370 Ma (Nadeau and Van Breemen 1994, Corrigan and Van Breemen 1997). The igneous protolith of the Isabella Island granitic gneiss in the basal Parry Sound domain has been dated at 1383 ±14 Ma (Wodicka et al. 1996), and megacrystic granodiorite and tonalitic gneiss from the basal Parry Sound domain, have 1394-1364 Ma and 1383-1332 Ma igneous age brackets respectively (Wodicka et al. 1996). The Parry Sound domain rocks are a possible source of lower unit detritus. Alternatively the lower unit could have formed in a continental basin isolated from older sources and receiving only juvenile detritus, perhaps a continental back-arc basin formed behind the ca. 1450 Ma Muskoka-Ojibway arc, synchronous, and perhaps contiguous with, the mid-continental magmatism that produced the southern granite-

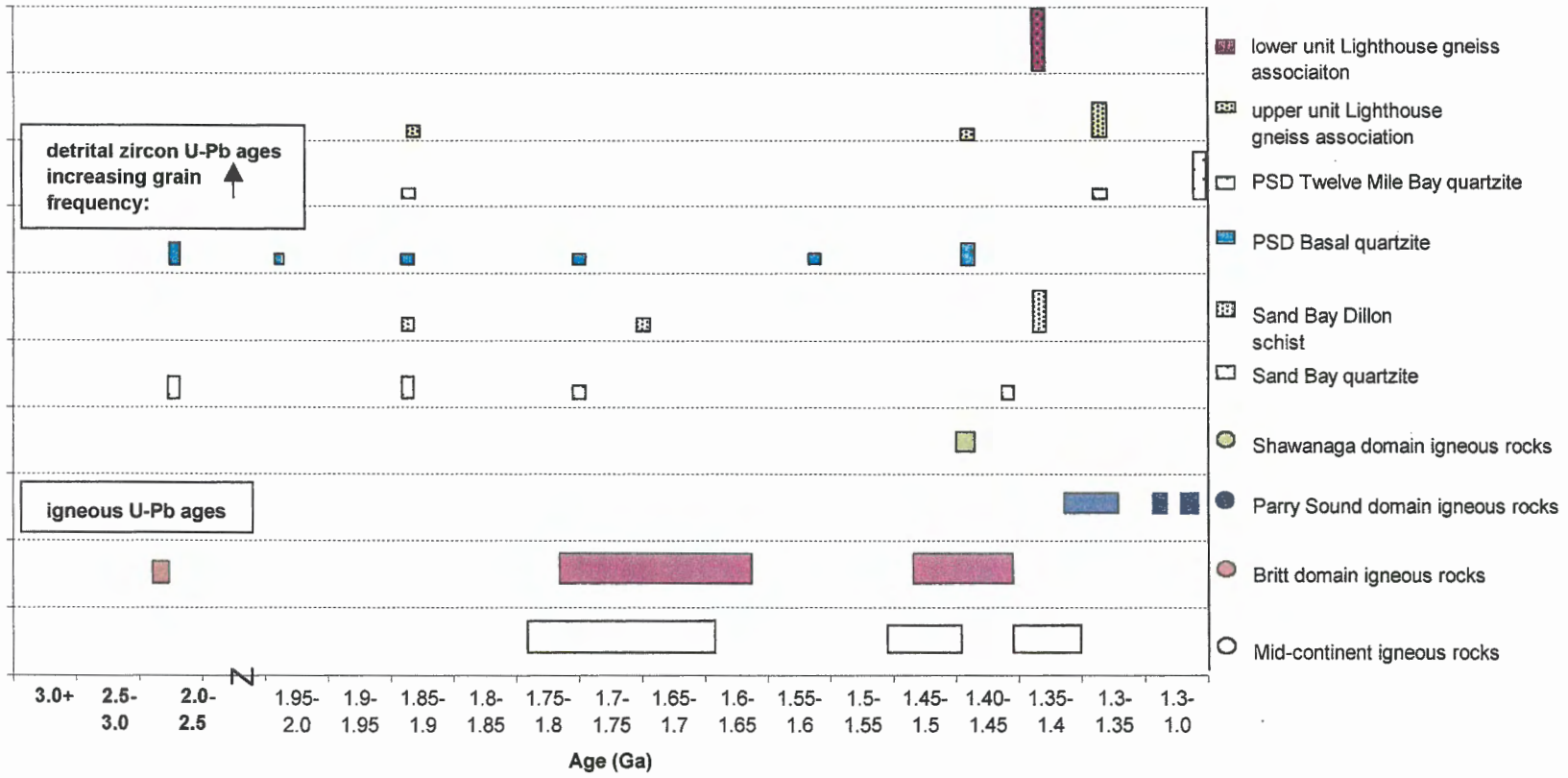

Figure 3.6. Age distribution of selected CGB supracrustal and (meta)igneous rocks. For data sources see text and Appendix B.

rhyolite province. Making the distinction between continental and oceanic tectonic environments for the lower unit should be possible using Nd isotopes.

Provenance of the upper unit metasediments - MR01D and MR01G

Four analyses from the upper unit (Z3, Z4, Z5 from MR01G, and Z2 from MR01D) have $^{207}Pb/^{206}Pb$ ages of ca. 1330 Ma (Table 3.1, Fig. 3.5). The upper unit probably has a major contribution from a ca. 1330 Ma source, along with subordinate ca. 1460 and ca. 1880 Ma sources, and was deposited after 1330 Ma. From sample MR01G, Z2 at 1354 ±3.1 Ma may be a discordant grain of ca. 1385 Ma vintage as it falls on the 1385 – 1050 Ma discordia line generated for lower unit sample MR01C (Figs. 3.3, 3.5).

Figure 3.6 shows detrital and igneous age ranges from the Shawanaga, Parry Sound and Britt domains, along with mid-continent igneous ages. Circa 1455 Ma ages are common in the monocyclic Shawanaga and Muskoka domains in plutonic orthogneiss (e.g. Ojibway, Shawanaga, and Muskoka plutons) and metasedimentary rocks (Sand Bay quartzite) (Culshaw and Dostal 1997, 2002, Ketchum and Davidson 2000). Continental granitoids with ca. 1450 Ma ages are common in the Laurentian parts of the Central Gneiss Belt, e.g. Bell Lake, Chief Lake and Mann Island plutons (Corrigan et al. 1994, Rivers 1997, Ketchum and Davidson 2000, Slagstad et al *in press*). Wodicka et al. (1996) reported 1436 ± 17 Ma, 1439 ± 22 Ma and 1867 ±4 Ma detrital ages from the nearby basal Parry Sound quartzite (Fig. 3.6). Apart from the ca 1880 Ma grain found in the upper unit, ca. 1880 Ma U-Pb ages in the Central Gneiss Belt are only known from a detrital grain in the basal Parry Sound quartzite (Wodicka et al. 1996), and a single detrital grain from an impure quartzite from the Sand Bay gneiss association (T.Krogh

pers. comm.). Ca. 1335 Ma and 1880 Ma grains are reported from the Flinton Group of the Elzevir Terrane of the Central Metasedimentary belt (c.f. Composite Arc Belt), and from the Frontenac quartzite of the Frontenac Adirondack Belt (McLelland and Chiarenzelli 1990, Sager-Kinsman and Parrish 1993). Considering the volume of Laurentian juvenile crust thought to have been produced between 1900-1750 Ma (Nelson and DePaolo 1985, Patchett and Arndt 1986, Simms 1993) it is perhaps surprising that igneous rocks and detritus in this age range are not more common in the Central Gneiss Belt.

Interior Parry Sound domain igneous rocks, the Whitestone anorthosite, and a tonalitic-granodioritic gneiss, have yielded ca.1350 ±50 Ma and 1314 +12/-9 Ma crystallization ages respectively (Van Breemen et al. 1986, Wodicka et al. 1996). Igneous ages of 1340 –1330 Ma are also found to the south in the Frontenac-Adirondack Belt (McLelland and Chiarenzelli 1990). A single ca. 1330 Ma U-Pb igneous age is reported from the Laurentian southern granite-rhyolite province (Van Schmus et al. 1996). As the upper unit samples share ca. 1450 Ma and ca. 1880 Ma detrital ages with basal quartzite of the Parry Sound domain, and ca. 1330 Ma igneous ages with the interior Parry Sound domain, the Parry Sound domain and upper unit are probably linked, although the prominence of the ca. 1330 Ma source distinguishes the lower unit from the basal quartzite. Wodicka et al. (1996) suggested that the Parry Sound domain might have formed offshore, adjacent to the Frontenac –Adirondack Belt. As the latter is a possible source for the ca. 1330 Ma upper unit detritus, and shares ca. 1880 Ma detrital ages with the upper unit and the Basal Parry Sound quartzite, a link between the Parry Sound domain, upper Lighthouse gneiss association, Frontenac-Adirondack belt, and possibly

the Elzevir terrane of the Composite arc belt is possible. The ca. 1330 Ma, ca 1450 Ma and ca. 1880 Ma grains probably represent sediment derived from the Laurentian margin.

As an alternative to the Parry Sound domain – Frontenac-Adirondack Belt linkage, if the upper unit was part of the evolving Sand Bay- Lighthouse rift it could represent a change in the depositional regime when older, continental material (e.g. ca. 1455 Ma detritus, perhaps from the Laurentian Britt domain, and ca. 1880 Ma detritus, from juvenile crust added to the Laurentian margin ca. 1900 Ma), again entered the basin. Few detrital links join the upper unit and the lower unit and Sand Bay metasediments, apart from the two ca. 1450 Ma and two ca. 1880 Ma Laurentian grains in the upper unit and the Sand Bay quartzite. The upper unit data indicate that continental source rocks supplied ca 1.88-1.33 Ga detritus; however the presence of continental basement during deposition of the upper unit is less certain and the basin may have had oceanic characteristics.

The contrast between the upper unit and lower units of the Lighthouse gneiss association is striking; they appear to share only one detrital age, the discordant grain Z2 from MR01G, which potentially has the same ca. 1385 Ma age as the detrital grains in sample MR01C. The differences between the upper and lower units probably reflect separation in space and/or time. Culshaw and Dostal (2002) suggested, on geochemical grounds, that the upper and lower unit volcanics formed from different mantle sources. Differing mantle sources may have resulted from formation in separate locations, or evolution of the mantle source. The detrital zircon study presented here further highlights the differences between the two parts of the Lighthouse gneiss association. Correlation of the upper and lower units with rock packages that have different pre-Grenvillian tectonic

evolution would support the proposal that the two units formed in different places and at different times. A scenario that might link the upper and lower units would involve the generation of the two units from progressively older rocks, as their source terrane eroded. Initial erosion of the uppermost, youngest, e.g. 1.33 Ga, source rocks (accompanied by far-traveled older Laurentian detritus) could have produced the upper unit with its component of 1.33 Ga grains. Continued erosion could reveal a source of older ca. 1.38 Ga detritus, eroded to form the lower unit.

The limited number of grains analysed from the upper and lower units (18 in total) do not make statistical analysis of grain populations worthwhile. In addition, also as a result of the size of the study, it is possible that sources contributing zircons to the upper and lower unit sedimentary protoliths have not been sampled.

Chapter 4

Sm-Nd results

4.1 INTRODUCTION

Sm-Nd isotopic studies interpret $^{143}Nd/^{144}Nd$ of modern and ancient igneous rocks in terms of mantle sources and magmatic evolution. Sm and Nd are light rare earth elements (LREE). Nd has two geologically important isotopes: radiogenic ^{143}Nd and stable ^{144}Nd. ^{143}Nd is produced by ^{147}Sm decay ($^{147}Sm \rightarrow ^{143}Nd + \alpha$; $t_{½} = 1.06 \times 10^{11}$ yr). The Sm – Nd isotope system is appropriate for analysis of mantle-derived magmas for three reasons: (1) Nd is more incompatible than Sm during partial melting, and as a result Nd is fractionated from Sm as melting proceeds; (2) $^{143}Nd/^{144}Nd$ is not fractionated by melting or crystallization; (3) the Sm- Nd system is robust with respect to post-crystallization disturbance i.e. there is no fractionation of $^{143}Nd/^{144}Nd$ by most intra-crustal processes. Thus the $^{143}Nd/^{144}Nd$ of a magmatic rock is a result of the melting history of its source. The ε_{Nd} notation, developed by DePaolo and Wasserburg (1976) has become a standard way of comparing the $^{143}Nd/^{144}Nd$ of rocks derived from different magma sources. ε_{Nd} values are calculated using the following equation:

$$\varepsilon_{Nd}(t) = ([(^{143}Nd/^{144}Nd)_{sample}^{(t)} / (^{143}Nd/^{144}Nd)_{CHUR}^{(t)}]-1) * 10^4$$

A sample's ε_{Nd} value represents the deviation of its $^{143}Nd/^{144}Nd$ from the hypothetical chondritic uniform reservoir (CHUR) $^{143}Nd/^{144}Nd$ value at time (t). The depleted mantle (DM) has experienced melt extraction events since about 4.0 Ga and as a result Sm/Nd (see 1 above), and therefore $^{143}Nd/^{144}Nd$ and ε_{Nd} have increased at a higher rate in the DM than in crustal melts extracted since that time. Present-day ε_{Nd} values

measured in magmas derived from the DM (e.g. mid-ocean ridge basalts) are between +10 and +15. Continental material, produced from low Sm/Nd melts extracted from the DM, has evolved lower $^{143}Nd/^{144}Nd$, and lower ε_{Nd} values than CHUR and the DM. Present day ε_{Nd} values for continental crust are between –5 and –30, inversely proportional to age and Sm/Nd (Zindler and Hart 1986).

The Sm-Nd tool is more robust than other isotopic systems used to study igneous petrogenesis, e.g. Rb-Sr, Th- and U-Pb, all of which are based on elements that are more mobile than Sm and Nd, and are therefore more easily disturbed by metamorphism or metasomatism (Faure 1986).

4.2 ANALYTICAL TECHNIQUES

Five amphibolite samples of basaltic tholeiite composition, from each unit of the Lighthouse gneiss association, have been analysed for $^{143}Nd/^{144}Nd$ and $^{147}Sm/^{144}Nd$ isotopic ratios. Sample preparation was done at the GEOTOP laboratory, University of Québec at Montréal. About 0.1g of sample was dissolved in HF and $HN0_3$ in screw-top Teflon bombs. A mixed $^{150}Nd/^{149}Sm$ spike was added to each sample prior to acid digestion. After five days of digestion, the solution was evaporated to dryness and then taken up in 6N HCl acid. The dried solution was taken up in 2.5N HCl and loaded into cationic exchange chromatography columns using an AG50W – X8 resin. The REE fraction was purified and Sm and Nd were isolated using a secondary column loaded with HDEHP (di2-ethyl-hexyl) treated Teflon powder. All reagents were purified by a sub-boiling process in order to ensure a low contamination level.

Analyses took place at the Atlantic Universities Regional Isotope Facility (AURIF), Memorial University, St Johns, Newfoundland. Measurements were made using a static multicollector configuration on a Finnigan MAT 262 mass spectrometer. Data are reported relative to the La Jolla Nd standard, $^{143}Nd/^{144}Nd = 0.511887 \pm 17$ (2 sigma). Using the AURIF system, and including GEOTOP sample preparation, cumulative analytical errors are less than 0.2% ($^{147}Sm/^{144}Nd$), thus calculated ε_{Nd} values have errors less than ±0.5 units. Analytical errors include uncertainty in blank and spike composition, systematic error in mass discrimination and ionization efficiency, and variation in ion beam intensity resulting from unstable sample fusion. ε_{Nd} values (De Paolo and Wasserburg 1976) are used throughout, and are calculated assuming present day $^{147}Sm/^{144}Nd_{CHUR} = 0.1967$ and $^{143}Nd/^{144}Nd_{CHUR} = 0.512638$ (Zindler and Hart 1986, Appendix C). The DM evolution model is that of De Paolo (1981). ε_{Nd} values are calculated for a crystallization age estimated from U-Pb geochronological and field data.

4.3 RESULTS

The Lighthouse gneiss association samples are all from thick, segregation-free amphibolite layers that probably represent individual flows (Culshaw and Dostal 2002). ε_{Nd} values for the amphibolites of the Lighthouse Gneiss association are calculated for an igneous crystallization age of 1.37 Ga for the lower, and 1.32 Ga for the upper unit, assuming magma eruption soon after earliest estimates for deposition of interlayered metasediment protoliths (Chapter 3, J. Ketchum pers. comm.). The ages chosen for calculating ε_{Nd} values are not critical, as the high $^{147}Sm/^{144}Nd$ ratios in the amphibolites, relative to felsic rocks or contaminated basaltic magmas, do not lead to large changes in

ε_{Nd} over time. ε_{Nd} values are within the DM range even if crystallization ages are changed by ±100 My. Trace element geochemical data are from Culshaw and Dostal (2002).

Lower unit

ε_{Nd} values for amphibolites from the lower unit of the Lighthouse gneiss association vary from +5.3 ±0.5 to +6.3 ±0.5 (Table 4.1, Fig. 4.1). Sample 95-LH-13.2 has the highest ε_{Nd} value in the lower unit at +6.3 ±0.5, and sample 95-LH-13.7 has the lowest ε_{Nd} value at +5.3 ±0.5. All the samples from the lower unit are within error of each other, and have a mean of +5.72. The lower unit values are slightly higher than the mean DM value but lie within the range of likely DM values at 1.37 Ga (Fig 4.1).

Upper unit

ε_{Nd} values from the upper unit range between +5.3 ±0.5 (95-LH-2E) and +5.8 ±0.4 (95-LH-4A), and have a mean of 5.4 (Table 4.1, Fig. 4.1). All analyses are within error of each other and are slightly above the mean DM evolution line of (DePaolo 1981), but lie within the range of likely DM values at 1.32 Ga (Fig. 4.1).

4.4 DISCUSSION

Petrogenesis

Modern magmas derived from the DM have a range of Nd isotopic compositions (Zindler and Hart 1986). DePaolo (1981) recognized the variability in DM-derived magmas and used a mean island arc Nd isotopic value to calculate a ε_{Nd} evolution line for

Sample	Rock type	Age (t-Ga)	Sm (ppm)	Nd (ppm)	measured 143Nd/144Nd	measured 147Sm/144Nd	2 sigma (147Sm/144Nd)	E Nd (t)
Lighthouse gneiss association, lower unit								
95-LH-13.2	amphibolite	1.37	3.586	11.72	0.512855	0.1850	5	**6.3**
95-LH-13.4	amphibolite	1.37	3.485	11.23	0.512839	0.1876	5	**5.5**
95-LH-13.7	amphibolite	1.37	3.617	11.56	0.512841	0.1891	5	**5.3**
95-LH-13.8	amphibolite	1.37	3.729	11.84	0.512883	0.1903	4	**5.9**
95-LH-14.8	amphibolite	1.37	3.919	12.98	0.512811	0.1826	4	**5.8**
Lighthouse gneiss association, upper unit								
95-LH-2E	amphibolite	1.32	4.464	17.04	0.512575	0.1584	5	**5.3**
95-LH-4A	amphibolite	1.32	2.205	7.643	0.512739	0.1744	4	**5.8**
95-LH-4C	amphibolite	1.32	2.649	8.938	0.512772	0.1792	4	**5.6**
95-LH-4D	amphibolite	1.32	4.603	16.38	0.512672	0.1699	5	**5.3**

Table 4.1. Sm-Nd isotopic data; Lighthouse gneiss association. See text for analytical details.
Upper unit t=1.32 Ga, lower unit t=1.37 Ga

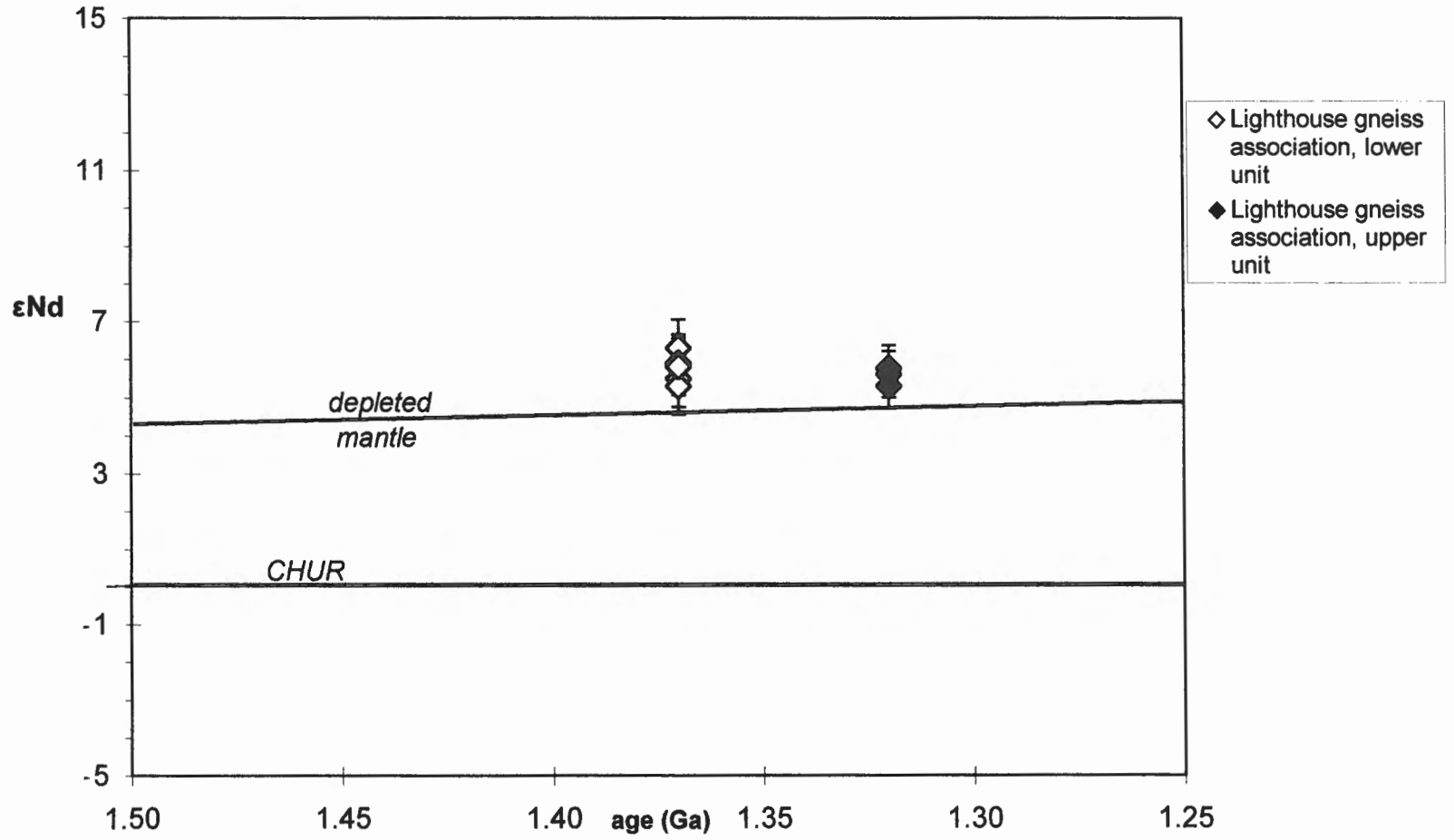

Figure 4.2. ε_{Nd} vs. time diagram for Lighthouse gneiss association amphibolites. Dotted lines are upper and lower boundaries for the DM based on DePaolo (1981). Lower unit t =1.37 Ga, upper unit t = 1.32 Ga.

the DM. The samples from the upper and lower units of the Lighthouse gneiss association have higher than average DM ε_{Nd} values at the time of their formation, but these values are within the range of DM-derived magmas if variation in DM composition was as wide at ca. 1.37 Ga and 1.32 Ga as it is in samples from the modern mantle (Fig. 4.1).

Culshaw and Dostal (2002), noting negative Nb anomalies and moderate Th/La ratios in amphibolite samples from the lower unit of the Lighthouse gneiss association, suggested that the magmatic protoliths of the lower unit could have been contaminated by subduction-modified mantle or by continental crust. The lower unit ε_{Nd} results, which are within error of the DM value at 1.37 Ga, suggest that the negative Nb anomaly and increased Th/La ratios were the result of subduction modification of the DM, and not contamination by older felsic crust with reduced ε_{Nd} values.

As DM-derived tholeiitic magmas have Nd concentrations around ca. 10% of evolved crustal rocks, small volumes of crustal contaminant can greatly alter tholeiitic magma Nd isotopic ratios. Very small volumes of older contaminant, or contamination by juvenile continental crust, are not within the analytical resolution of the ε_{Nd} system, and therefore cannot be ruled out. Two contamination scenarios that would be undetectable using the ε_{Nd} system are; (1) 1% contamination of 1.37 Ga DM-derived magma (average Nd = 8ppm, $\varepsilon_{Nd} = +4.7$) by 3.0 Ga Archean felsic crust (Nd = 25ppm, $\varepsilon_{Nd} = -18$) would produce magma with an ε_{Nd} value reduced by 0.5 ε_{Nd} units from DM values (case A, fig. 4.2). (2) Up to 11% contamination of DM-derived magmas by 1.45 Ga felsic crust would lead to a similar lowering of ε_{Nd} values in the resultant magma, and would also alter its major element characteristics (case B fig. 4.2, Appendix C). A reduction of 0.5 ε_{Nd} units

would be within analytical error, and could not be resolved. Contamination by DM-derived 1.37 Ga juvenile continental crust would of course leave ε_{Nd} values indistinguishable from the DM value at that time. Modeling details can be found in Appendix C.

Upper unit ε_{Nd} values averaging + 5.4 are within error of the DM value at 1.32 Ga, suggesting that contamination by low ε_{Nd} older crustal material did not take place. The lack of a negative Nb anomaly, along with high Ti and low Th/La in the upper unit, confirm the absence of significant contamination by continental crust (Culshaw and Dostal 2002). As with the lower unit, the upper unit may have been contaminated by older crust, but this contamination must have been limited in volume to less than a few percent, otherwise it would be within the resolution of the ε_{Nd} system and would alter the MORB-like trace element signature.

The ε_{Nd} values of the two units are indistinguishable, suggesting a DM source was present during generation of both units, however only in the case of the lower unit does the DM source appear to have been modified by subduction processes. The upper unit strongly resembles MORB, and shows no sign of contamination or subduction modification in ε_{Nd} or trace element terms.

Tectonic setting

Culshaw and Dostal (2002) have suggested that the lower unit was generated in a back-arc setting. The ε_{Nd} results indicate that significant contamination of the magmatic precursors to the lower unit amphibolites did not take place, and if the back-arc basin was situated on continental crust, this crust must have been juvenile or allowed

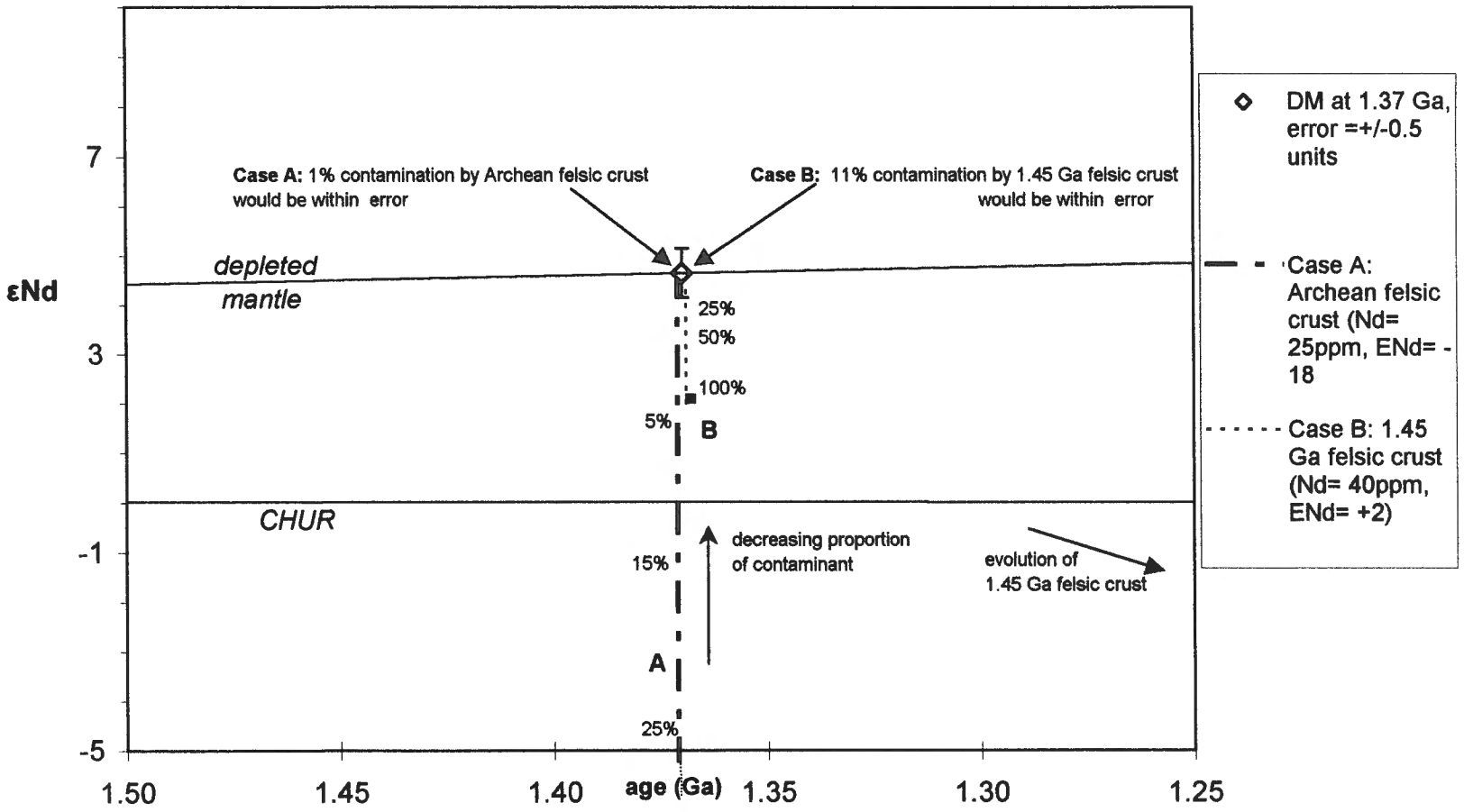

Figure 4.2. ε_{Nd} vs. time diagram showing the sensitivity of 1.37 Ga magmas to contamination by Archean (3.0 Ga), and Mesoproterozoic (1.45 Ga) felsic crust, for modeling details see Appendix C.

contamination-free magma transfer. Alternatively the back-arc basin in which the lower unit accumulated could have formed from a juvenile oceanic arc.

The upper unit shows no indication of contamination or influence of subduction-related processes. Culshaw and Dostal (2002), combining geochemical and lithological data, proposed that the upper unit may have formed in a back-arc setting. The ε_{Nd} results suggest that magmatism in this back-arc basin produced unmodified DM-derived compositions. Though minor contamination cannot be ruled out, a depleted mantle origin in a large back-arc basin is the preferred interpretation for the upper unit. Culshaw and Dostal (2002) suggested that the upper and lower units may have been genetically related with trace element geochemical differences between the units resulting from evolution of their mantle sources; the consistent ε_{Nd} data lend some support to this proposal. In the following section the two units are considered together, in both a continental and an oceanic context, and compared to nearby magmatic and supracrustal sequences.

Though an oceanic setting is plausible for the formation of the upper unit, a continental setting is considered for both units, as the ε_{Nd} data do not rule out contamination by juvenile crust or a contamination-free continental origin. In a continental setting, the lower unit could have been produced by extension of a continental back-arc basin with magma erupted via efficient contamination-free conduits from subduction-modified DM, or from DM contaminated by juvenile continental crust. The upper unit, in a continental context, may represent a later stage when a continental back-arc basin received only DM-derived magma unaltered by subduction. A continental setting suggests that the upper and lower units might be genetically related to the

subjacent Sand Bay gneiss association metavolcanics. The Sand Bay gneiss association metavolcanics have been shown by Culshaw and Dostal (1997) to be subduction-related, crustally contaminated bimodal volcanics, erupted onto the Laurentian margin after ca. 1.38 Ga. The Laurentian margin at ca. 1.38 Ga was probably dominated by juvenile crust, analogous to the precursors of the younger granite-rhyolite provinces of the mid-continental USA (Culshaw and Dostal 2002, Slagstad et al. *in press*). Extension and rifting of the Laurentian margin may have melted the juvenile continental crust, and these melts, accompanied by mantle-derived magmas, could be preserved as the bimodal Sand Bay gneiss association felsic orthogneiss and amphibolites (metarhyolites and metabasalts). Further extension may have led to the generation, from subduction-modified mantle, of the contamination-free magmatic precursors of the lower Lighthouse gneiss association amphibolites, as suggested by Culshaw and Dostal (2002). Continued high rates of extension during production of the Lighthouse gneiss association metavolcanics might have led to the change from a subduction-modified sub-continental mantle source to the unmodified, DM sources that were the precursors to the upper unit amphibolites.

Connections between the Lighthouse and the subjacent Sand Bay gneiss association metavolcanic protoliths could usefully be investigated by a detrital zircon geochronological study to compare Sand Bay and Lighthouse upper and lower unit metasediments, and a Sm-Nd isotopic investigation of the magmatic protoliths and contaminants of the Sand Bay gneiss association metavolcanics.

In an oceanic setting, extension of a back-arc basin adjacent to an island arc complex could change magma characteristics from subduction-modified mantle to

unmodified or MORB-like, a pattern reflected in upper and lower unit amphibolite trace element variation (Culshaw and Dostal 2002). The oceanic character, in lithological and ε_{Nd} terms, of the upper and lower units, and their proximity to the overlying 'exotic, far-travelled' Parry Sound domain (Wodicka 1994, Wodicka et al. 1996) suggests an alternative to the Sand Bay linkage. The upper and lower units and the Parry Sound domain may have formed in close proximity in a distal, perhaps offshore, setting. Detrital zircon correlation between the Parry Sound Domain and the Lighthouse gneiss association metasediments would favour this interpretation.

Alternatively, as Culshaw and Dostal (2002) have suggested, the upper and lower units could have formed in separate places and at different times, and been juxtaposed during the Grenvillian orogenic cycle. The lower unit could correlate with the Sand Bay gneiss association and the active Laurentian margin, and the upper unit with allochthonous distal units, perhaps the Parry Sound domain.

Chapter 5

Geological synthesis

5.1 INTRODUCTION

The following chapter contains a synthesis of the geochronological, geochemical and lithological data and interpretations. The upper and lower units of the Lighthouse gneiss association are interpreted in a petrogenetic and plate tectonic framework and their status with respect to the evolution of the region during the Mesoproterozoic is evaluated. Possible modern and ancient analogues of the evolution of the southwestern Laurentian continental margin are discussed. The conclusions suggest that the tectonic evolution of the Mesoproterozoic southwestern Laurentian margin was characterized by a series of oceanward younging juvenile continental arcs and back-arc basins. The upper and lower units are considered separately, and then the relationship between them is discussed.

5.2 GEOLOGICAL SYNTHESIS

Origin of the lower unit

ε_{Nd} values, averaging +5.7 in the lower unit amphibolites, along with other geochemical evidence including negative Nb anomalies and high Th/La (Culshaw and Dostal 2002), suggest that the lower unit magmatic protoliths were DM-derived magmas, affected by subduction zone processes, but not appreciably contaminated by older continental crust. Analytical and geological errors using the Nd isotopic system hamper contaminant identification; modeling suggests that, for example; up to 1% contamination of magma derived from the DM at 1.37 Ga by 2.5 Ga felsic crust, or up to 11%

contamination by 1.45 Ga felsic crust, will be undetectable, and therefore cannot be excluded.

Nine single-grain U-Pb analyses of detrital zircons extracted from a lower unit metasediment yielded a single age population of ca. 1.38 Ga grains. Culshaw and Dostal (2002) suggested that the lower unit metasediment protoliths were immature volcaniclastic rocks that might have been deposited in a marginal basin. A detrital source providing only single-age grains to a volcanic marginal basin is compatible with the oceanic setting implied by the magmatic compositions. However, a number of lines of evidence suggest that the juvenile detrital source was continental, and despite the absence of older continental contamination, the basin probably formed on, or immediately adjacent to, continental crust. Numerous ca. 1.38 Ga detrital zircons are found in the Dillon schist, a thick semipelitic unit from within the subjacent Sand Bay gneiss association (Culshaw and Dostal 1997, T. Krogh pers. comm.), implying a detrital link between the Sand Bay gneiss association and the lower unit of the Lighthouse gneiss association. Trace element geochemistry suggests a magmatic link between amphibolites from the lower unit and amphibolites from the Sand Bay gneiss association (Culshaw and Dostal 2002). A Laurentian continental setting is likely for the Sand Bay gneiss association protoliths: older detrital zircons from the Dillon schist and a Sand Bay quartzite have an age range that appears to represent Laurentian provenance (T. Krogh pers. comm.), and intercalated felsic orthogneisses are interpreted as Laurentian continental crustal melts (Culshaw and Dostal 1997).

Culshaw and Dostal (2002) proposed further links between the Sand Bay gneiss association and Laurentia, suggesting that the felsic orthogneisses and amphibolites are

along-strike equivalents of the 1.38 Ga mid-continent southern granite-rhyolite province (Van Schmus et al. 1996) extensively reworked during the Grenville orogenic cycle. The 1.38 Ga detrital source in the Sand Bay gneiss association metasediments, and therefore the 1.38 Ga population identified in the lower unit zircons, could be from ca. 1.38 Ga equivalents of the southern granite-rhyolite province. As a result of the extraction of the juvenile arc precursors to the mid-continent granite-rhyolite provinces and their equivalents within the Central Gneiss Belt (CGB), the mantle beneath this part of the Laurentian margin would have been modified by subduction-zone processes (Van Schmus et. al 1996, Culshaw and Dostal 2002). The trace element characteristics of the lower unit magmatic protoliths could be explained if they originated from a part of the mantle modified during the extraction of the precursor arcs of the mid-continental granite-rhyolite provinces and equivalent CGB rocks. By combining lithological and geochemical data Culshaw and Dostal (2002) suggested that the lower unit was deposited in a back-arc basin with marine characteristics. The new Sm-Nd petrogenetic and U-Pb detrital zircon geochronological data suggest that the back-arc basin formed after 1.38 Ga on or immediately adjacent to attenuated Laurentian continental crust of mid-continent granite-rhyolite province affinity. The back-arc basin included both the protoliths of the Sand Bay gneiss association and the lower unit of the Lighthouse gneiss association.

1.38 Ga igneous rocks are also found in the overlying Parry Sound domain (Wodicka 1996), it is therefore possible that the lower unit was produced adjacent to, and received detritus from, the Parry Sound domain, outboard of the mid-continent - Sand Bay part of the Laurentian margin. However, the links between the Sand Bay gneiss association and the lower unit, i.e. thirteen detrital grains ca. 1.38 Ga and similar

amphibolite trace element geochemistry, are much stronger than the links (3 igneous ages ca. 1.38 Ga) between the lower unit and the Parry Sound domain.

Possible modern analogues of the lower unit, e.g. outboard continental back-arc basins formed on attenuated continental basement and erupting subduction modified, continental contamination-free magmas, include the Aleutian basins, Campbell Plateau, and the Sea of Japan (Nohda and Wasserburg 1981, Cas and Wright 1987, Wilson 1989, Kay et al. 1990). Mesozoic examples include the Andean Tierra del Fuego - South Georgia basin (Winn 1974), and the Ross Sea and West Antarctic sectors of the Jurassic Antarctic Gondwanan margin (Storey et al. 1992), both of which record early rhyolitic magmatism, followed by turbiditic sedimentation and voluminous basaltic magmatism. Kay et al. (1989) have suggested that the history of felsic magmatism on the Gondwanan margin from the Middle Palaeozoic to the Jurassic was analogous to mid-continent magmatism on the Laurentian margin during the Mesoproterozoic. The tectonomagmatic evolution of the basin in which the Sand Bay-lower unit sequence was formed may be analogous to the tectonomagmatic evolution of the West Antarctic Gondwanan margin. Storey et al. (1992) described a bimodal back-arc magmatic sequence on the Gondwanan margin of West Antarctica; crustally contaminated early bimodal volcanics were followed by basic magmas that evolved from crustally contaminated to uncontaminated MORB types with DM-like ε_{Nd}.

Origin of the upper unit

The amphibolites of the upper unit, like those of the lower unit, have high ε_{Nd} values, averaging +5.4, within error of the DM at ca. 1.32 Ga. The upper unit ε_{Nd} data suggest that DM-derived parental magmas were not significantly contaminated by older

felsic crust. The absence of an older crustal contaminant is compatible with the conclusions of Culshaw and Dostal (2002) who proposed that the protoliths to the upper unit amphibolites, which lack a negative Nb anomaly and have low Th/La, were generated from MORB-like DM, and were not contaminated by continental crust. Although very small volumes of continental contaminant cannot be ruled out, significant contamination by juvenile continental crust is unlikely for the upper unit as it has both high ε_{Nd} along with MORB-like trace element distribution.

Culshaw and Dostal (2002) have interpreted the upper unit metasediments as high-energy turbidite deposits, a typical back-arc basin facies (e.g. Marsaglia 1995). A semipelite and a psammite from the upper unit yielded detrital zircons with a range of U-Pb ages between ca. 1.33 Ga and ca. 1.88 Ga. Of the nine grains analysed from the upper unit, six are juvenile with U-Pb ages ca. 1.33 Ga, and three have older U-Pb ages, ca. 1.45 Ga and ca. 1.88 Ga. The spectrum of detrital ages in the upper unit probably reflects a combination of older continental (Laurentian) and juvenile sources. Strong detrital links exist between the igneous and metasedimentary rocks of the Parry Sound domain and the upper unit of the Lighthouse gneiss association. The upper unit shares ca. 1.33 Ga ages with a number of Parry Sound domain igneous rocks (Wodicka et al. 1996), and igneous rocks from parts of the allochthonous Frontenac Adirondack Belt (FAB) (e.g. McLelland and Chiarenzelli 1990, McLelland et al. 1996); both are possible sources of the youngest detritus. Circa 1.45 Ga and ca. 1.88 Ga detrital ages are also found in metasediments from the Parry Sound domain and FAB (Sager-Kinsman and Parrish 1993, Wodicka et al. 1996). Both the FAB and Parry Sound domain probably originated as juvenile continental arcs outboard of the Laurentian margin (McLelland et al. 1993, McLelland et al. 1996,

Carr et al. 2000). Ca. 1.45 Ga rocks are abundant on the Laurentian margin and include the voluminous ca. 1.45 Ga magmas in the Britt, Shawanaga, and Muskoka domains of the CGB (Ketchum and Davidson 2000). When compared with their abundance in the southwestern Grenville Province, ca. 1.45 Ga rocks are not particularly common in other continents or cratons likely to have been adjacent to Laurentia during the Mesoproterozoic, for example East Antarctica (Fitzsimmons 2000), Amazonia (Tassinari et al. 2000), and Baltica (Åhäll and Connely 1998). The ca. 1.9 Ga Ketelidian-Makkovikian and Penokean orogens involved ca. 1.9 Ga generation and 1.8-1.7 Ga accretion of juvenile crust, including continental arcs and island arcs, throughout Laurentia and the adjacent North Atlantic and Baltic cratons (Patchett and Bridgewater 1984, Nelson and DePaolo 1985, Simms 1993, Culshaw et al. 2000, Ketchum et al. 2002), providing abundant sources for the ca. 1.88 Ga detritus in the FAB, Parry Sound domain, and upper unit.

The lack of significant contamination in the upper unit amphibolites suggests that the basin into which the upper amphibolite protoliths were erupted was floored by oceanic or highly attenuated juvenile continental crust. Despite the presence of Laurentian detritus of various ages, the detrital age range which correlates with allochthonous distal continental rocks such as the Parry Sound domain and FAB, together with MORB-like magmatic compositions, suggest that the back-arc basin in which the upper unit protoliths were deposited formed on the most oceanward part of the Laurentian continental margin. From the differing detrital populations it is inferred that deposition of the upper unit protoliths took place ca. 50 My after the lower unit protoliths were deposited.

Modern analogues of the upper unit i.e. outboard continental back-arc basins with MORB-like magmatism might include the Sandwich, Scotia, and Lesser Antilles back-arc basins, where MORB-like magmas (with DM-like ε_{Nd}) were emplaced into basins containing continental detritus (Hawkesworth et al. 1977, Davidson 1985, Cas and Wright 1987, Wilson 1989).

The lack of contamination by older crust in both the upper and lower units suggests that incorporation of continental material via subduction into the mantle source of their magmatic protoliths was severely limited. The presence of Laurentian detritus in the upper unit metasediments indicates that the arc did not block detritus from entering the marginal basin in which the upper unit was deposited, and therefore the basin probably formed between the arc and the continent with subduction towards the continent.

Correlation of the upper and lower units

Though indistinguishable in ε_{Nd} terms, the upper and lower units are distinct in terms of amphibolite trace element geochemistry and detrital ages. Neither unit has evidence of significant crustal contamination, and despite the fact that detrital ages link both units to the Laurentian margin, the characteristics of the links are quite different, with probable deposition ages separated by ca. 50 My. Correlation of the upper and lower units with parts of the Grenville Province having different tectonic evolution suggests significant geographical and temporal separation for their sites of origin. The two grains of ca.1.45 Ga age found in the upper unit of the Lighthouse gneiss association are not particularly strong evidence for including this unit with the Sand Bay-Lighthouse sequence (which also includes 1.45 Ga detritus), as ca. 1.45 Ga igneous rocks were

widespread on the Laurentian margin and would have been available as a detrital source over a wide area for a considerable period of time (Ketchum and Davidson 2000). Combined Zr-Nb-Y data suggest that the sedimentary protoliths of the upper and lower units both formed from a mixture of MORB-like juvenile magmatic and continental sedimentary sources, and although these data suggest similar tectonosedimentary environments for both units, they do not necessitate accumulation in the same basin. Although evidence for contamination by older crust is absent, and a DM source (or subduction-modified DM in the case of the lower unit), is prevalent in both units, their distinctive detrital zircon populations are persuasive evidence that they were probably not part of the same basin.

The two units could be linked by an eroding source area that initially yielded young detritus, producing the upper unit, and was then eroded to expose deeper level older detritus, the lower unit. However, the change in magmatic characteristics of the two units over time, from the subduction-modified lower unit, to the MORB-like upper unit, which is a pattern typical of evolving rifts (Wilson 1989), suggests that the upper unit is unlikely to represent the early stages of evolution of the tectonic environment in which the two units formed.

The most efficient way to distinguish the upper and lower units is on the basis of field appearance and lithology. The characteristic features of the upper unit are its metasediments, in particular the alternating 10-100cm thick psammite-pelite pairs, laminated composite amphibolite-metasediment, and varied metasediments including amphibole-bearing calcareous schists, and massive quartzofeldspathic semipelite (Culshaw and Dostal 2002). The field appearance of upper and lower unit amphibolites is

variable, and similar amphibolite lithologies are found in both units. The lower unit lacks the characteristic layered and laminated lithologies of the upper unit, and includes monotonous quartzofeldspathic semipelite. Along strike and inland from the high-quality outcrop of the study area, both units become more attenuated, and soil and vegetation cover increase, hampering identification of the upper and lower units.

Further discussion on the origin and evolution of the upper and lower units is considered with respect to models for the evolution of a broad spectrum of parts of the pre-Grenvillian Laurentian margin.

5.3 THE UPPER AND LOWER UNITS IN THE CONTEXT OF THE EVOLVING LAURENTIAN MARGIN

The most recent models of the evolution of the Laurentian margin during the Palaeoproterozoic and Mesoproterozoic consider the margin to be the oldest example of a Pacific–rim scale, active Andean- or western Pacific-type margin (Kay et al. 1989, Gower and Tucker 1994 Culshaw et al. 2000, Carr et al. 2000, Rivers and Corrigan 2000, Slagstad et al. *in press*). In a detailed study of the tectono-magmatic evolution of the CGB Muskoka and Shawanaga domains, Slagstad et al. *(in press)* propose a juvenile continental arc (the Muskoka-Ojibway arc) that was affected by compression and repeated arc-rifting. Slagstad et al. (*in press*) suggested that arc growth on the Laurentian margin began before 1.45 Ga, with arc-rifting at 1.45 Ga accompanied by voluminous plutonism. Magma sources for the arc-rift rocks may have been the pre-1.45 Ga continental arcs, or a basaltic underplate (Slagstad et al. *in press*). High-grade metamorphism on the continental margin between 1.45-1.43 Ga was followed by

renewed arc-extension after 1.4 Ga. Circa 1.44 Ga High-grade metamorphism may have been caused by lower crustal extension, or arc compression (Slagstad et al. *in press*). The Sand Bay gneiss association and the lower unit of the Lighthouse gneiss association could be supracrustal manifestations of the post-1.4 Ga rifting of the Muskoka–Ojibway arc. Culshaw and Dostal (2002) and Slagstad et al. (*in press*) recognized numerous links between the younger granite-rhyolite provinces and the CGB. The Sand Bay – lower Lighthouse sequence is consistent with a model of Laurentian margin rifting after 1.38 Ga, probably behind a juvenile continental arc leading to the creation of the southern granite-rhyolite province which formed from melts of juvenile continental arc rocks (Fig. 5.1a,b). The basin in which the Sand Bay-lower Lighthouse sequence accumulated probably formed in the vicinity of along-strike equivalents of the southern granite-rhyolite province, possible sources of the abundant 1.38 Ga detritus (Fig. 5.1c).

Ca. 1.45 Ga and ca. 1.88 Ga detrital ages in the upper unit are compatible with a Laurentian margin sediment source. In the Grenville Province, the ca. 1.33 Ga ages in the upper unit are found only in allochthonous rock units such as the Parry Sound domain and the FAB. Wodicka et al. (1996) suggested that the Parry Sound domain, because of its distinctive lithologies, detrital zircon age range, and tectonometamorphic history, formed as an arc on the most distal part of the Laurentian margin or just offshore, adjacent to the FAB, and outboard of the other CGB protoliths (Fig. 5.1c). The upper unit of the Lighthouse gneiss association could represent a volcanosedimentary sequence deposited in a basin adjacent to the Parry Sound arc. The basin in which the upper unit accumulated may have formed as a result of the rifting of the Parry Sound arc from the Laurentian margin (Fig. 5.1d). The FAB is likely to represent a juvenile continental arc

and associated basin rifted from Laurentia, the oldest parts of which formed at ca. 1.33 Ga (McLelland et al. 1993, Gower 1996, McLelland et al. 1996, Carr et al. 2000). The oldest FAB rocks, the ca. 1.33-1.30 tonalites and charnockites of the Adirondack Highlands and the ca. 1.35 Ga Mt Holly volcanics, may represent initial growth of the Adirondack arc (McLelland et al. 1996). Further Parry Sound arc growth ca. 1.33 Ga, represented by the basal and interior Parry Sound tonalities, took place immediately before growth of the back-arc basin in which the upper unit protoliths accumulated (Fig. 5.1d). Parry Sound arc rifting is speculative, as rift-related rocks have not been found so far in the Parry Sound domain.

The position of the upper unit protoliths, outboard of the Parry Sound arc and Sand Bay-lower unit sequence, is not reconcilable with the model of in-sequence thrusting proposed for the evolution of the Central Gneiss Belt (Culshaw et al. 1997). In-sequence thrusting would be expected to emplace the upper unit above and to the southeast of the Parry Sound domain, not in its present day situation, below and northwest of the Parry Sound domain, adjacent to the lower unit.

Alternatively, if the upper unit of the Lighthouse gneiss association formed, along with the Sand Bay- lower unit sequence as a result of Muskoka-Ojibway arc extension, following rifting ca. 1.45, and ca. 1.38 Ga, a third stage of Muskoka-Ojibway rifting after 1.33 Ga would be necessary.

A possible link between the upper and lower units is found in the 1.38 – 1.33 Ga igneous rocks in the Parry Sound domain and the possible 1.38 Ga detrital zircon in the upper unit, which correlate with similar detrital ages in the lower unit and Sand Bay

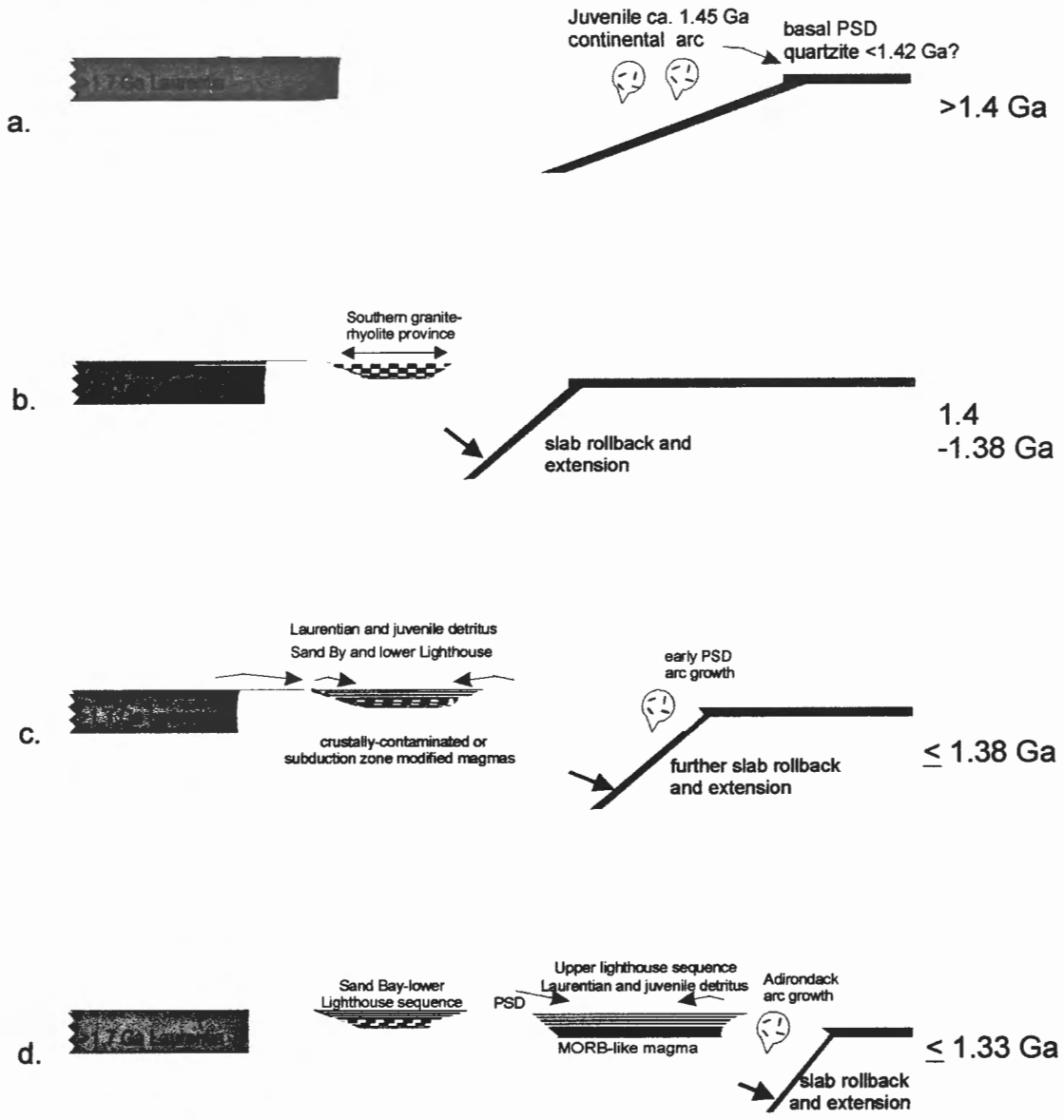

Figure 5.1. Tectonic evolution of the southwestern Laurentian margin between ca. 1.4 and 1.3 Ga. a) Repeated juvenile continental arc growth on the Laurentian margin 1.9- 1.4 Ga. Possible post-1.45 Ga back-arc magmatism, deposition of oldest Parry Sound domain (PSD) metasedimentary protoliths (Basal Parry Sound quartzite) after 1.43 Ga on fore-arc or passive margin (not shown). b) 1.40-1.38 Ga generation of equivalents of southern granite-rhyolite province from melting of juvenile arc rocks in back-arc. c) Parry Sound arc growth and generation of equivalents of the younger parts of the southern granite-rhyolite province along with the Sand Bay and lower Lighthouse gneiss association protoliths. Extension possibly driven by slab roll back. Supracrustal rocks characterized by alternation of Laurentian and juvenile detritus, and bimodal magmas with subduction-modification or crustal influence. d) Rifting of Parry Sound arc and growth of Adirondack arc outboard and creation of large back-arc basin with MOR- like magma characteristics and both juvenile and Laurentian detritus. See text for discussion of Grenvillian juxtaposition of the upper and lower units.

gneiss associations, and abundant ca.1.38 Ga U-Pb ages along with rarer ca. 1.33 Ga U-Pb ages from the southern granite-rhyolite province (Van Schmus et al. 1996). Perhaps the Parry Sound arc began forming at ca. 1.38 Ga, outboard of the lower unit-Sand Bay basin as the latter began accumulating detritus; some 50 My later the upper unit was generated in the lower unit-Sand Bay basin adjacent to the Parry Sound arc.

The two main causes of back-arc extension are thought to be trenchward arc migration as a result of slab dip steepening (slab-rollback) and, less importantly, small-scale mantle convection at the margins of the basin exerting drag on the base of the back-arc basin lithosphere (Hamilton 1995). The 50 My gap between the back-arc basin extension that led to accumulation of the upper and lower units of the Lighthouse gneiss association could also be the result of changes in the dip of the subducting slab. Steepening of slab dip could have initiated back-arc extension ca. 1.38 Ga forming the basin in which the Sand Bay-lower Lighthouse protoliths accumulated, melting older continental arcs, producing the rhyolitic protoliths of the Sand Bay felsic orthogneisses, and the younger granite-rhyolite province, and allowing mantle-derived magmas (e.g. the lower unit amphibolites) to erupt (Fig. 5.1c). As a result of slab rollback the location of arc growth may have moved outboard, perhaps forming the oldest igneous protoliths (ca. 1.38 Ga) of the Parry Sound domain. The basal Parry Sound quartzite appears to have been formed soon after 1.43 Ga, much earlier than the Parry Sound domain igneous protoliths, and is probably unrelated to the Parry Sound arc (Wodicka et al. 1996). The basal Parry Sound quartzite may have accumulated on the oceanward margin of the Muskoka-Ojibway arc system, and then have been incorporated into the growing Parry Sound arc (Fig. 5.1a). Following Parry Sound arc construction, slab dip may have again

steepened initiating, after ca. 1.33 Ga, the growth of the outboard back-arc basin in which the upper unit protoliths were deposited (Fig. 5.1d).

During the 50 My between Sand Bay – lower unit protolith accumulation (≤ ca. 1.38 Ga) and the generation of the upper unit protoliths (≤ ca. 1.33 Ga), the margin could have experienced a period of arc growth without further back-arc extension. Evidence of ca. 1.35 Ga arc-growth includes the two ca. 1.35 Ga igneous rocks from the Parry Sound domain, but unfortunately these U-Pb ages have ca. ±50 My errors and therefore they could also have formed during older or younger events (Wodicka et al. 1996). The Laurentian margin between ca. 1.38-1.33 Ga could have been dominated by transcurrent tectonics, which could explain the postulated changes in slab dip, and may explain the absence of ca. 1.45 Ga Muskoka-Ojibiway detritus in the Dillon schist and lower unit, or alternatively, an unseen back-arc sequence could have accumulated during the 50 My gap. As the detrital connections between the upper and lower units are weak, and because they correlate with different parts of the margin, the upper and lower units are unlikely to be parts of a continuous stratigraphic succession.

5.4 ANALOGUES OF THE LIGHTHOUSE GNEISS ASSOCIATION AND MESOPROTEROZOIC SOUTHWESTERN LAURENTIAN MARGIN.

Most plate reconstructions and tectonic models for the Mesoproterozoic evolution of Laurentia include Baltica to the northeast (present coordinates), and many treat the Baltica-Laurentian margin as a laterally continuous long-lived active margin, perhaps the earliest well-documented Pacific-scale margin in earth history (Buchan et al. 2000, Culshaw et al. 2000, Karlstrom et al. 2001, Horte and Torsvik 2002). It is sensible to look

to other parts of this margin, and also to more recent geological events for analogues of the patterns of juvenile continental arc growth, rifting, and sedimentation recorded in the Lighthouse gneiss association and southwestern Grenville Province.

Baltica

The evolution of Mesoproterozoic Baltica was characterised by crustal growth, including juvenile continental arc generation, arc accretion, sedimentation and volcanism (Åhäll et al. 2000, Åhäll and Connely 1998, Brewer et al. 2002). The Transscandinavian igneous belt includes ca. 1.9 Ga and ca. 1.75-1.55 Ga juvenile continental crust reworked before ca. 1.5 Ga, a similar pattern to that recorded in the southwest Grenville Province, and in Labrador to the northeast (Gower 1996, Culshaw et al. 2000, Carr et al. 2000). Post 1.7 Ga tectonic activity on the Baltic margin, preceding the ca. 1.05 Ga Sveconorwegian orogeny, involved repeated arc growth, rifting, sedimentation, volcanism, and inboard plutonism, on the Baltic continental margin, again a similar pattern to that proposed for the tectonic evolution of the southwestern Grenville Province (Åhäll and Connely 1998, Bingen et al. 2001, Brewer et al. 2002). Inboard plutonism at ca. 1.68-1.65 Ga, 1.62-1.58 Ga, and 1.56-1.55 Ga, possibly as a result of extension in a large arc - back-arc system, led to the emplacement of series of rapakivi-type igneous suites, sub-parallel to and probably ca. 500 km inboard of the active margin (Åhäll and Connelly 1998).

Post-1.55 Ga Baltic active margin activity included the generation of the Bandak and Dal Groups, dissected volcanosedimentary sequences found in the Rogaland-Hardangervidda and Telemark-Bamble terranes respectively. The Bandak and Dal groups both accumulated on a basement of attenuated 1.7-1.5 Ga juvenile crust (Brewer at al.

2002). Characterised by thick bimodal volcanics, and accompanied by volcaniclastic turbiditic sediments and siliciclastic sediments including slates and arkoses, the Bandak and Dal Groups are interpreted as thick back-arc basin deposits deposited between 1.2 – 1.16 Ga behind a juvenile continental arc (Brewer et al. 2002). ε_{Nd} values of +1 to –3 (t = ca. 1.175) for the Bandak and Dal volcanics suggest interaction between DM-derived magmas (ε_{Nd} = +4) and older continental crustal basement (e.g. ε_{Nd} = -15) (Brewer et al. 2002). Though they are good analogues, sharing many lithotectonic and geochemical features with the Lighthouse and Sand Bay gneiss associations, the Bandak and Dal groups are an order of magnitude thicker. However the Lighthouse and Sand Bay gneiss associations experienced intense attenuation during the Grenville orogenic cycle, and their protoliths may have been as thick as the Bandak and Dal groups were prior to Sveconorwegian orogenesis (Culshaw and Dostal 1997, Brewer et al. 2002).

Due to the pervasive ductile deformation and orogenic telescoping affecting the CGB domains, sedimentary thickness, back-arc basin dimensions, and arc longevity are difficult to estimate. However, age relations of domains in the CGB, CAB, and FAB suggest that the southwestern Grenville Province includes the remnants of multiple small oceanward-younging juvenile continental arcs and back-arc basins. The Baltic margin appears to preserve longer-lived back-arc basins, with limited juvenile Mesoproterozoic crust (e.g. Menuge and Brewer 1996), perhaps reflecting a more stable tectonic regime during arc formation on the Baltic margin than on the southwestern Laurentian margin. A pattern of stable subduction and gradual slab-rollback in the Baltic area could have produced two inboard long-lived back-arc basins at 1.6-1.5 Ga and 1.16-1.12 Ga. In southwestern Laurentia the site of back-arc extension moved oceanwards repeatedly

between 1.5 – 1.2 Ga, producing a western Pacific-type laterally-extensive juvenile margin and numerous back-arc basins. The oceanward growth of the southwestern Laurentian active margin may have been in response to oceanward movement of the site of steepest slab dip. Movement of the site of steepest slab dip may have resulted from strike-slip activity or changes in the density of the oceanic crust. The Lighthouse gneiss association amphibolites have no evidence of interaction with older crust, and may differ from the contaminated Baltic back-arc basin amphibolites (Brewer et al. 2002) as a result of magma being generated in the vicinity of juvenile Mesoproterozoic rather than Palaeoproterozoic or older continental crust, implied by Nd isotopes of the Baltic metavolcanics.

Eastern and Southern Laurentia

Between Baltica and the southwestern Laurentian margin there were probably a few thousand kilometers of Mesoproterozoic active margin (e.g. Karlstrom et al. 2001), remnants of which are found throughout the Grenville Province, in Ontario, Quebec, and Labrador.

Like the southwestern Grenville Province and the Sveconorwegian Province, the Makkovik Province, the Pinware terrane, and rocks formed in the Labradorian orogen of Labrador represent southern outboard extensions of the Mesoproterozoic continental margin formed by the growth of continental arcs, back-arc basins, and accretion of island arc terranes (Gower 1996, Ketchum et al. 2002). In Labrador, to the south of the Palaeoproterozoic Makkovik Province, the calc-alkaline plutonic rocks, mafic, anorthositic and metasedimentary gneiss of the 1.69-1.6 Ga Labradorian orogen probably represent an accreted arc terrane (Gower and Tucker 1994, Gower 1996, Gower et al.

2002). Construction of the 1.51-1.45 Ga Pinware terrane east of the Labradorian orogen resulted from growth of a continental arc-back-arc system (Gower 1996). Extension on the Labrador margin of Laurentia is recorded in the 1.74- 1.69 Ga, and 1.45 – 1.23 Ga intervals, both of which appear to have been associated with arc rifting and magmatism (Gower 1996, Culshaw et al. 2000, Ketchum et al. 2002, Gower et al. 2002).

The Wakeham Supergroup (Martignole et al. 1994), found within the Grenville Province in eastern Quebec, is a bimodal-volcanic and siliciclastic sequence with a minor plutonic component, formed in two distinctive episodes at ca. 1.27 Ga, and 1.18 Ga. The ca. 1.27 Ga Aguanus Group, the older part of the Wakeham Supergroup, includes sedimentologically mature arenites succeeded by a bimodal volcanic sequence, intruded by gabbroic sills and granitoids. A deformational event affecting only the Aguanus Group preceded the deposition of the Davy Group with its distinctive fanglomerates (with clasts of Aguanus metasediment), siliciclastics and tholeiites. A Davy Group tholeiite yielded a ca. 1.17Ga U-Pb age interpreted to represent igneous crystallization (Martignole et al. 1994). The bimodal, alkaline volcanics of the Wakeham Supergroup have intraplate trace element distributions suggesting an intracontinental origin, and sedimentary facies resembling continental-rift types (Martignole et al. 1994). It is likely that the Wakeham Supergroup formed in an intra-continental rift basin in two stages separated by an interval of early Grenvillian compression (Corriveau and van Breemen 2000). Two-stage evolution of the basin in which the Wakeham Supergroup was deposited is compatible with the punctuated extensional tectonic regime proposed for the southwestern Laurentian margin.

The ca. 1.38 Ga La Bostonnais complex in central Quebec probably represents a continental juvenile arc, perhaps with an older reworked island arc component (Nadeau and Van Breemen 1994, Corrigan and Van Breemen 1997, Rivers and Corrigan 2000). The La Bostonnais arc complex formed contemporaneously with the older magmatic rocks of the PSD.

The BCEMS (Bancroft-Cabonga-Elzevir-Mazinaw-Sharbot Lake) terranes of the Composite Arc Belt (CAB) include pillow lavas and platformal sediments, and probably represent a back-arc basin sequence. Despite reaching an estimated width of 500km, the volcanic rocks deposited in the BCEMS basin were pervasively contaminated by continental crust (Smith et al. 1997, Rivers and Corrigan 2000). Formed after ca. 1.29 Ga, the BCEMS basin post-dates Lighthouse gneiss association protolith accumulation by at least 40 My, and though the two are probably not related, parts of the BCEMS terranes may be analogous to the protoliths of the Lighthouse and Sand Bay gneiss associations. The evolution of the La Bostonnais arc and BCEMS terranes is consistent with intermittent arc growth and rifting on the Laurentian margin.

The Apsley Formation of the Elzevir terrane

The 500m thick supracrustal Apsley Formation outcrops over 140km^2 in the Elzevir terrane, a component of the BCEMS terranes, within the Composite Arc Belt (Central Metasedimentary Belt - Fig 1.2). Though it includes similar facies to the Sand Bay and Lighthouse gneiss associations, and has metasediment trace element compositions that are very similar to the Dillon schist of the Sand Bay gneiss association (Fig. 5.2), the Apsley Formation is at least 40 My younger than the upper unit of the Lighthouse gneiss association (Shaw 1972, Easton 1986b). M. Easton (pers. comm.) has

pointed out the very similar field characteristics of the Apsley Formation to the Sand Bay and Lighthouse gneiss associations. Due to lower grade metamorphism and less pervasive deformation the Apsley gneiss yields more detailed tectonosedimentary data than the Lighthouse and Sand Bay gneiss associations, and palaoenvironmental reconstruction has been possible (Easton 1986b). The Apsley Formation may provide a well-preserved analogue of the upper Lighthouse and lower Lighthouse-Sand Bay sequences. Characteristics of the Apsley Formation, lower Lighthouse-Sand Bay gneiss association, and upper Lighthouse gneiss association are summarised in Table 5.1.

The Apsley Formation includes all the metasedimentary lithologies found in the Sand Bay gneiss association, and the upper and lower units of the Lighthouse gneiss association. Metasediments of turbiditic affinity in the upper unit of the Lighthouse gneiss association may be analogous to the volcaniclastic turbidite facies of the Apsley formation, and it is possible that the upper unit protoliths, like the Apsley Formation protoliths, formed on the flanks of a submerged volcanic centre (Easton 1986b). Easton (1986b) proposed an Aleutian island arc analogue for the Apsley Formation protoliths, contrasting with the back-arc setting proposed for the Sand Bay and Lighthouse gneiss association protoliths. Metasediment geochemistry suggests that the upper unit of the Lighthouse gneiss association formed from a mixture of MORB-like and continental sources, compatible with its detrital zircon age distribution (Fig. 5.2, Table 5.1). Like the upper unit, the lower unit of the Lighthouse gneiss association could have formed in an environment where MORB-like and continental sediment sources were available (Fig. 5.2), though older continental detrital zircons are absent from the lower unit metasediment samples.

The Sand Bay gneiss association, with which the lower unit is intimately related, has metasediment geochemistry compatible with a mixture of Laurentian margin arc granitoid (CGB plutonic orthogneisses or 1.9-1.7 Ga granitoid) detritus and MORB-like material (Fig. 5.2). Apsley Formation metasediment geochemistry closely resembles the Dillon schist of the Sand Bay gneiss association, suggesting a similar combination of MORB-like and arc granitoid material contributed sediment to the Apsley Formation protoliths (Fig. 5.2). The Apsley Formation metasediment protoliths were probably produced in a setting where arc granitoid detritus was available, suggesting the proximity of an eroded arc. If, as Easton (1986b) suggests, the Apsley Formation protoliths accumulated on the margins of a volcanic center, the volcanic centre would need to have formed close to a source of arc granitoid detritus.

Although they have similar compositions in Zr-Nb-Y space, Apsley Formation metavolcanics contrast with both the Sand Bay-lower Lighthouse gneiss association and the upper Lighthouse gneiss association metavolcanics. The calc-alkaline Apsley Formation metavolcanics probably formed from arc magmas, whereas both of the other two sequences have metavolcanic compositions that preclude formation in an arc (Table 5.1, Easton 1986b, Culshaw and Dostal 1997, 2002).

	Apsley Formation	Sand Bay-lower Lighthouse gneiss associations	upper Lighthouse gneiss association
age (Ga)	1.29-1.25	<ca. 1.38	<ca. 1.33
sedimentary facies	alternating fine-coarse-grained volcaniclastic-siliciclastic facies, tuffs and carbonates - submarine volcanic fan facies	immature quartzite, immature calcareous quartzofeldspathic sediments -continental- rift related	quartzofeldspathic greywacke-shales, -high-energy turbiditic deposits
metasediment geochemistry (Fig. 2.3)	between MORB and Laurentian margin arc-granitoid compositions	Dillon schist (Sand Bay)-between MORB and Laurentian margin arc-granitoid compositions (and felsic orthogneisses) Lower Lighthouse – between MORB and average crustal compositions	between MORB and average crustal compositions, elevated Nb/Y (perhaps a minor enriched mantle component)
detrital zircons	n/a	ca. 2.3 Ga-juvenile (1.38 Ga)	ca. 1.85 Ga-juvenile(1.33 Ga)
volcanic types	andesitic basalt, dacite, and rhyolite	rhyolite and basalt	basalt
metavolcanic geochemistry	calc-alkaline -Nb anomaly, low Ti no εNd data arc-related	tholeiitic -Nb anomaly, high Ti, high Cr DM-like εNd (lower Lighthouse) subduction-modified but not arc derived magmas, no older crustal contamination	tholeiitic low Th/La, high Ti, high Cr, no Nb anomaly DM-like εNd MORB-like
interpretation	intra-arc rift, or arc-proximal deposit, active arc nearby, continental proximity unknown	Sand Bay – early rift of inactive continental arc or arc derived rocks; Lower Lighthouse – more evolved continental back-arc rift with no direct arc influence in sediments or magmas	large back-arc basin producing MORB-like magmas, near to eroding continental margin.

Table 5.1. Summary of metavolcanic and metasediment protolith characteristics; upper Lighthouse gneiss association, lower Lighthouse and Sand Bay gneiss associations, and Apsley Formation. Sources - Shaw 1972, Easton 1986b Culshaw and Dostal 1997, 2002, and this study).

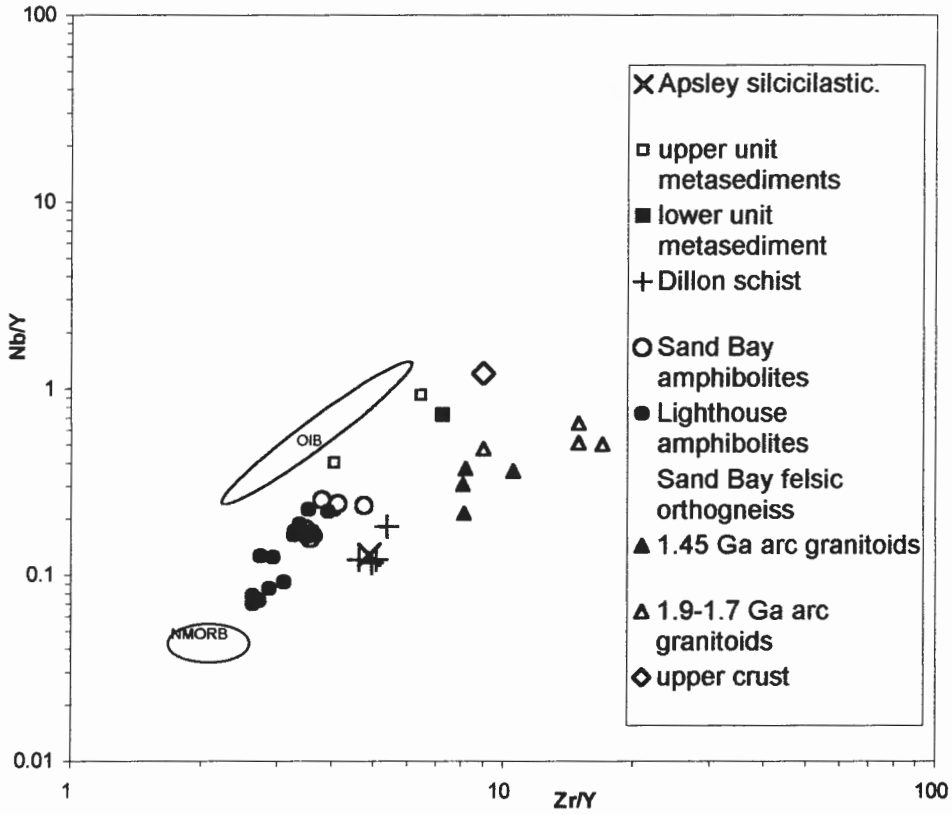

Figure 5.2. Log Zr/Y v log Nb/Y plot for Lighthouse and Sand Bay gneiss association supracrustal rocks and Apsley Formation (Easton 1986b). Other data; see Fig. 2.3.

While the detrital zircon geochronological data and regional correlation suggest that the upper unit and lower unit sequences formed at different times, they both have lithological and geochemical characteristics compatible with a back-arc origin. The Sand Bay part of the Sand Bay-lower unit sequence includes metasediments with protolith compositions similar to continental arc-rift facies, and metavolcanic geochemistry suggesting that the magmatic protoliths may have originated in a continental rift setting. Unlike the Apsley Formation, the Sand Bay gneiss association (and lower Lighthouse gneiss association) metavolcanic protoliths formed from subduction-modified but not sub-arc mantle sources. It is likely that the Apsley protoliths formed on or immediately

adjacent to an eroding active arc, whereas the Sand Bay-lower Lighthouse sequence began to form in an extensional continental rift where continental arc detritus was available, but active arc magmatism absent.

Avalonia

We learn from the Late Precambrian-Palaeozoic history of the Laurentian margin that once-.contiguous terranes and adjacent continental margins can become separated by enormous distances, and rifted continental arc terranes may end up docked against a continental margin with which they have no genetic affinity (Nance and Thompson 1996). The Avalonian terranes of Brittany, southern Britain, and eastern North America were formed on the Neoproterozoic-Early Palaozoic Iapetus margin of the Gondwanan supercontinent. As a result of Palaeozoic orogenesis and Mesozoic rifting the Avalonian terranes are now found either side of the North and South Atlantic oceans (Nance and Thompson 1996). Though extensively reworked during the Caledonian-Appalachian orogenic cycle, the Avalonian terranes preserve evidence of Neoproterozoic pre-Iapetus subduction and Palaeozoic rifting. United by their arc-character, age, and affinity with the Gondwanan margin, the Avalon terranes differ in their longevity, and in the parts of the margin with which they correlate. Though now separated by up to ca. 7000 km, the correlation of the West Avalonian terrane of northeastern North America, which is now docked against the Laurentian margin, with the Amazonian craton, has been demonstrated using a combination of Sm-Nd petrogenetic, and U-Pb detrital zircon studies (Nance and Murphy 1996). Detrital zircon age spectra from the Western Avalonian terranes correlate with age spectra from the Amazonian craton, and Sm-Nd isotopic studies of Western Avalonian volcanics suggest Amazonian Tocantins-type

basement was a magmatic contaminant (Nance and Murphy 1996). The pattern of terrane separation and distribution that dominates the Avalonian history of the Palaeozoic Laurentian margin may have resulted from the increased influence of transcurrent tectonics during arc growth.

Transcurrent tectonics is a possible cause for the juxtaposition of unrelated rock units in the Grenville province. The lower unit of the Lighthouse and the Sand Bay gneiss association correlate with rocks of the Laurentian margin in the immediate vicinity of the Central Gneiss Belt, i.e. the southern granite-rhyolite province, suggesting their protoliths formed near to their present location and experienced little or no transcurrent movement either before or during the Grenville orogenic cycle. The upper unit correlates with rocks of ca. 1.88 Ga, ca. 1.45 Ga, and ca. 1.33 Ga age. Circa 1.88 Ga rocks are common, found in Baltica, the North Atlantic craton and throughout the Laurentian margin. Circa 1.33 Ga, and especially ca. 1.45 Ga rocks are characteristic of the southwestern Grenville province (e.g. Fitzsimmons 2000) suggesting, once again, that transcurrent movement played only a minor role in the evolution of the upper unit.

Sea of Japan

The Mesozoic-Cenozoic evolution of the Japanese part of the Eurasian continental margin provides an excellent modern analogue to the Mesoproterozoic Laurentian margin. In northeastern China and the Korean peninsula, the Palaeoproterozoic and Neoproterozoic rocks of the Eurasian margin accumulated a passive margin sequence in the Early Mesozoic (Masao et al. 1965). Continental volcanic and siliciclastic rift sequences are recorded from the Lower Triassic to the Middle Jurassic (Uyeda and Miyashiro 1974, Masao et al. 1965), and may either represent extension of the continental

margin as the Pacific Ocean began to grow, or perhaps early back-arc extension. The Upper Jurassic saw the initiation of arc-related volcanism in northeastern China, with the eruption of andesitic lavas, followed thereafter by Lower Cretaceous rifting, rhyolitic volcanism, and siliciclastic sedimentation inboard of the arc (Uyeda and Miyashiro 1974). Pre-Cenozoic back-arc rifting on the Japanese Eurasian margin was restricted to small ensialic basins (Uyeda and Miyashiro 1974).

The oldest oceanic crust of the Japan Sea may have formed in the Mid-Cretaceous, though correlative dating of the crust is hampered by multiple minor spreading centers and few magnetic anomalies (Sugimura and Uyeda 1973, Uyeda and Miyashiro 1974, Jolivet et al. 1995). The interval between the Upper Cretaceous and the Oligocene appears to have been a time of relative inactivity with marine transgressions in the inboard basins, and arc-related andesitic volcanism on Japan (Jolivet et al. 1995, Uyeda and Miyashiro 1974). The Miocene saw the establishment of Japan as an island arc with vigorous calc-alkaline magmatism on Japan and inboard bimodal volcanism as extension in the region of the Japan Sea was renewed (Nohda and Wasserburg 1981, Jolivet et al. 1995). During the Miocene, high rates of extension behind the Japanese island arc led to the establishment of the 1×10^6 km^2, 3 km deep Sea of Japan, with a mid-basin spreading centre (Nohda and Wasserburg 1981). Extension that formed the Sea of Japan probably resulted from subduction of old, cold, and therefore dense oceanic lithosphere (Jolivet et al. 1995). In the Late Miocene, a 2 km thick turbiditic and acid-intermediate-basaltic volcanic sequence formed at the margins of the Sea of Japan (Uyeda and Miyashiro 1974). Some magmatic rocks from the north Japan Sea geochemically resemble MORB, with DM-like ε_{Nd} values (Pouclet et al. 1995, Nohda

and Wasserburg 1981), however, most Japan Sea magmatic rocks have lowered εNd values suggesting pervasive contamination by continental crust (Nohda and Wasserburg 1981).

Similarities exist between the evolution of the Eurasian margin–Japanese system and the Mesoproterozoic southwestern Laurentian margin. Early extension in northeastern China, characterized by continental sedimentation and continental volcanism, followed ca. 100 My later by Japan Sea rifting which produced oceanic crust with a flanking cover of volcanics and turbidites, resemble the lower Lighthouse - Sand Bay sequence, and the upper Lighthouse-Parry Sound domain sequence respectively. The Cretaceous Eurasian margin arc (Uyeda and Miyashiro 1974) may be analogous to the Muskoka-Ojibway arc, and the early and late Cenozoic history of the Japan arc to the juvenile Parry Sound and Adirondack arcs respectively. The Japanese arc includes parts of the Eurasian margin, including older metamorphic rocks and part of a continental accretionary prism (Isozaki 1996), in contrast with the Parry Sound domain and Adirondack Highlands which preserve limited evidence of older continental material, i.e. lowered ε_{Nd} values (McLelland et al. 1993, 1996, Wodicka et al. 1996). It is interesting to note that despite the large size of the Sea of Japan, most magmas are still contaminated with continental material, contrasting with the metavolcanic rocks of either unit of the Lighthouse gneiss association. The differences in magmatic ε_{Nd} are perhaps to be expected as the attenuated Eurasian margin includes thick Precambrian sedimentary sequences along with Palaeoproterozoic basement, in contrast to the juvenile Mesoproterozoic granite-rhyolite provinces of the Laurentian margin.

5.5 CONCLUSIONS

Combined U-Pb geochronological, Sm-Nd petrogenetic, geochemical and lithological data from highly deformed rocks allow the identification of tectonic environments, correlation across wide areas of metamorphic rocks, and integration with models of tectonic evolution.

The Lighthouse gneiss association comprises two supracrustal units. The lower unit, with subduction-modified DM-derived magmatic protoliths and single-age detrital zircons, correlates with juvenile rocks formed on rifted Mesoproterozoic Laurentia. The lower unit probably formed in a back-arc basin on attenuated juvenile continental crust. The upper unit of the Lighthouse gneiss association has magmatic compositions indistinguishable from DM-derived MORB. With abundant Laurentian detritus, the upper unit probably formed in a back-arc basin on the outermost edge of the Laurentian margin, a basin large enough to produce MORB-like magmas. A possible link between the upper and lower units is suggested by a single ca. 1.38 Ga discordant zircon in the upper unit. The geochronological correlation between the upper unit and more outboard terranes and terrane fragments is much stronger than the tenuous link between the upper and lower units.

An offshore origin for the lower unit is unlikely as it shares both numerous detrital ages and similar amphibolite geochemistry with the Laurentian Sand Bay gneiss association. The upper unit is a better candidate for oceanic status with MORB-like magmatic geochemistry, however it correlates with outboard juvenile continental arcs, and includes multi-age Laurentian detritus, which together emphasize continental proximity. In summary, as the detrital zircon U-Pb data suggests the deposition ages of

the two units are separated by about 50 My, and as they correlate with progressively oceanward parts of the growing Laurentian margin, a link between the two units and their respective basins is unlikely.

The Mesoproterozoic evolution of southwestern Laurentia, as represented by the Grenville Province of Ontario, involved a series of arcs and associated back-arc basins forming on the continental margin. Age relations suggest a general pattern of oceanward-younging. Extension in a continental back-arc setting, behind the Muskoka-Ojibway arc, probably produced the voluminous ca. 1.45 Ga plutonic rocks of the Britt domain (Slagstad et al. *in press*). Between ca. 1.45 Ga and 1.38 Ga the margin may have experienced relative quiescence, and the youngest zircons from the basal PSD quartzite suggest that it was deposited during this time interval. Further extension and volcanism around 1.38 Ga led to the generation of the younger southern granite-rhyolite province of the mid-continent, and the formation on the Laurentian margin of the continental back-arc basin in which the Sand Bay-lower Lighthouse gneiss association protoliths accumulated. The proposed Parry Sound arc, which includes the upper unit as an associated back-arc basin deposit, was constructed after 1.38 Ga outboard of the basin in which the Sand Bay-lower Lighthouse gneiss association protoliths accumulated. Despite the presence of Laurentian detritus, the back-arc basin formed after ca. 1.33 Ga, in which the upper unit protoliths accumulated, had MORB-like magmatic characteristics.

The Japan Sea provides a modern analogue of the Mesoproterozoic Laurentian margin as represented by the Lighthouse gneiss association and southwestern Grenville Province. The evolution of the Japanese region from the Late Mesozoic to the present day

encompasses at least two stages of back-arc rifting. Establishment of a series of continental volcanic rift basins in the Cretaceous was followed ca. 100 My afterwards by slab roll-back, and growth of the Sea of Japan, an extensive marginal basin between the rifted Japanese continental arc and the margin of the Eurasian continent. The Sea of Japan back-arc basin has oceanic magmatic and sedimentary characteristics.

The Lighthouse gneiss association is perhaps best divided into two separate units. The lower unit should be assigned to the Laurentian Sand Bay gneiss association, and the upper unit grouped with allochthonous rock packages, formed later and further oceanward, such as the Parry Sound domain and the Frontenac-Adirondack Belt.

5.6 FUTURE DIRECTIONS

The presence of mid-continental granite-rhyolite province crust as basement to the basin in which the Sand Bay-lower Lighthouse protoliths accumulated, could be tested by an ε_{Nd} -study of the felsic orthogneisses and amphibolites of the Sand Bay gneiss association. Culshaw and Dostal (2002) suggested that the felsic orthogneisses were crustal melts, perhaps derived from the protoliths to the CGB plutonic orthogneisses. ε_{Nd} values between –1 and +3 for the felsic orthogneiss would suggest a mid-continental granite-rhyolite province and CGB plutonic orthogneiss affinity (Van Schmus et al. 1996). ε_{Nd}– Nd(concentration) contaminant modeling of the Sand Bay amphibolites would provide further constraints on the identity of the local crust (e.g. Tomlinson 2000). The extent of the juvenile Laurentian margin, and the along-strike continuation of the granite-rhyolite provinces into the Grenville Province would be better constrained by a

more complete understanding of the tectonic setting of the Sand Bay metavolcanic protoliths.

The status of the Parry Sound domain, and the growth and structure of the hypothetical Parry Sound arc could be usefully resolved by an $\varepsilon_{Nd,}$ and major and trace element petrogenetic, and geochronological study of Parry Sound orthogneisses. Investigating the age and character of magmas related to arc-growth and arc-rifting, and the involvement of older crust in Parry Sound magmatic protoliths, would further constrain the timing and site of arc formation and arc rifting on this outboard part of the Mesoproterozoic Laurentian margin.

Nb-Zr-Y and lithological data suggest that the Dillon schist of the Sand Bay gneiss association and parts of the Apsley Formation of the Composite Arc Belt formed in similar environments from sedimentary sources with similar compositions. A detrital zircon geochronolgical study of selected metasediments from the Apsley Formation (especially those that resemble the Sand Bay and Lighthouse gneiss association metasediments), and an ε_{Nd} study of Apsley metavolcanics, would help resolve the status of the Apsley Formation with respect to the Laurentian margin i.e. its age, possible basement, correlative units, and affinity with the continental margin. As the Apsley Formation appears to be a well-preserved Grenvillian analogue of the Lighthouse and Sand Bay gneiss associations, a more complete understanding of the Apsley Formation would help refine the episodic back-arc rifting model for the southwestern Grenville Province.

	lower unit					
sample	LH-95-13.2	LH-95-13.4	LH-95-13.7	LH-95-13.8	LH-95-14.8	MR01C
rock type	amphibolite	amphibolite	amphibolite	amphibolite	amphibolite	semipelite
latitude	45° 16' 43"	45° 16' 47"	45° 16' 49"	45° 16' 50"	45° 16' 55"	45° 16' 55"
longitude	80° 16' 45"	80° 16' 42"	80° 16' 42"	80° 16' 42"	80° 16' 43"	80° 16' 45"

	upper unit					
sample	95-LH-2E	95-LH-4A	95-LH-4C	95-LH-4D	MR01G	MR01D
rock type	amphibolite	amphibolite	amphibolite	amphibolite	semipelite	psammite
latitude	45° 16' 24"	45° 16' 29"	45° 16' 28"	45° 16' 30"	45° 16' 50"	45° 16' 35"
longitude	80° 16' 20"	80° 16' 21"	80° 16' 23"	80° 16' 25"	80° 16' 35"	80° 16' 20"

Table A1. Sample locations; UTM coordinates

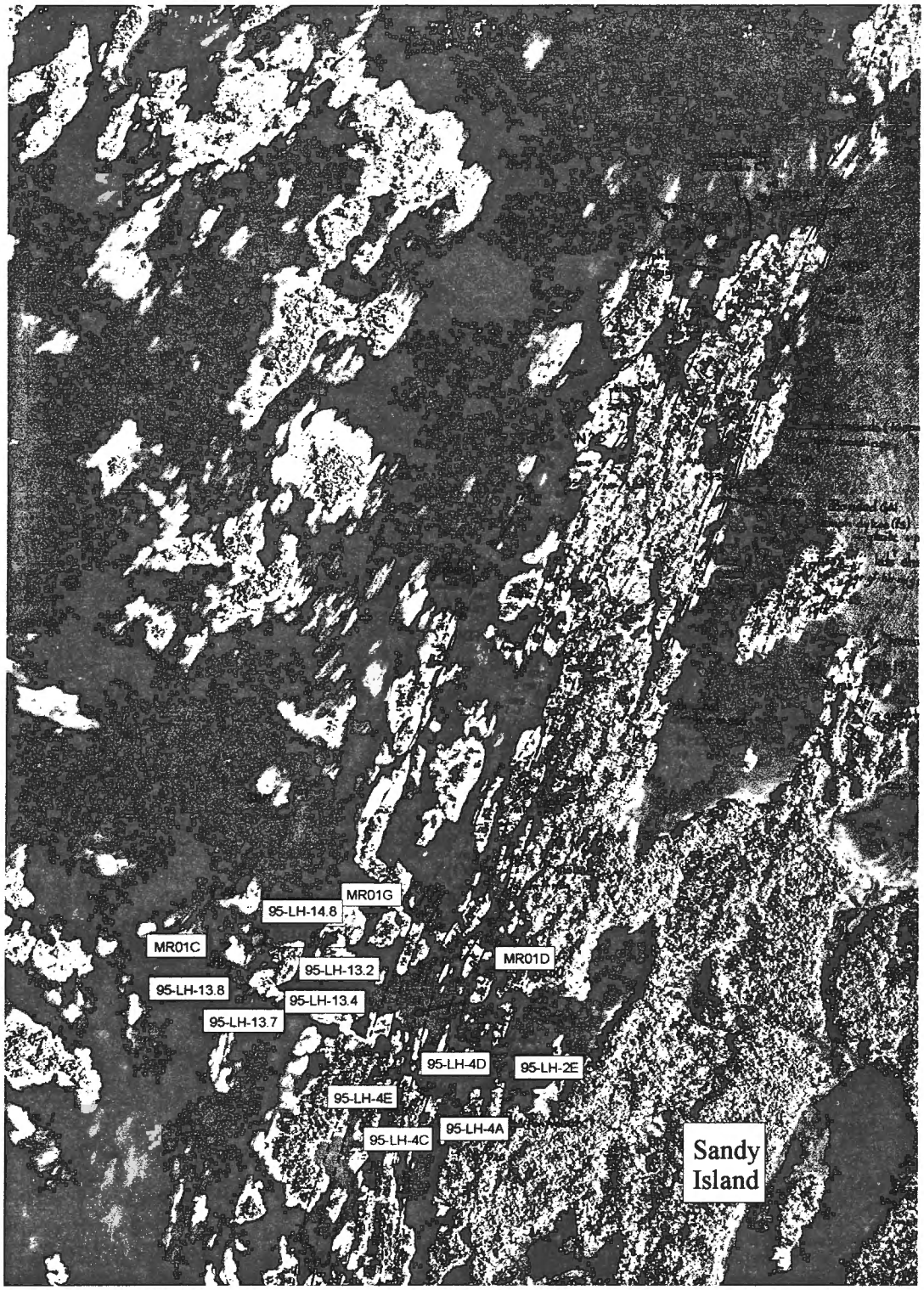

Figure A1. Air photo showing sample locations, same area as Fig. 1.3..

	MR01Cps(5)	MR01Cps(11)	MR01Cps(2)	MR01Cps(6)	MR01Gps(1)	MR01Gps(4)	MR01Gps(1)	MR01Gps(9)	MR01Dps(1)	MR01Dps(6)	MR01Dps(8)	MR01Dps(14)
SiO2	36.952	36.929	37.02	37.24	35.61	35.239	36.2	35.019	34.826	35.067	35.366	35.248
TiO2	2.803	2.939	3.1	3.156	2.936	2.948	2.93	2.972	3.908	3.982	4.072	3.905
Al2O3	15.446	15.507	15.86	15.932	15.677	15.572	16.4	15.314	16.479	16.593	16.576	16.88
Cr2O3	0.033	0.044	0.035	0.021	0.001	0	0.021	0.015	0.045	0.035	0.014	0.048
FeO	20.875	20.782	21.237	20.868	22.055	22.181	22.146	22.251	22.618	22.597	22.636	22.181
MnO	0.274	0.259	0.33	0.299	0.235	0.266	0.323	0.251	0.185	0.158	0.178	0.174
MgO	9.993	9.926	9.739	9.872	8.682	8.706	8.681	8.677	7.479	7.271	7.342	7.372
CaO	0.006	0.031	0.019	0	0	0.007	0.014	0	0	0.013	0.01	0.005
Na2O	0.068	0.084	0.083	0.074	0.045	0.075	0.047	0.053	0.052	0.049	0.047	0.055
K2O	10.386	10.213	9.861	10.203	9.872	9.791	9.529	9.928	10.461	10.15	10.281	10.233
P2O5	0	0		0.051	0	0	0.038	0	0	0	0.014	0
BaO	0.192	0.199	0.288	0.219	0.968	0.835	0.824	1.016	0.271	0.28	0.273	0.309
Total	97.028	96.913	97.5	97.935	96.081	95.62	97.166	95.496	96.324	96.195	96.809	96.41
Mg	46	46	45	46	41.2	41	43	41	37	36.5	37	37
Fe	54	54	55	54	58.8	59	57	59	63	63.5	63	62
Fe/(Fe+Mg)	0.54	0.54	0.55	0.54	0.588	0.59	0.57	0.59	0.63	0.635	0.63	0.626262626

	DS04039 (1)	DS04039 (2)	DS04039 (5)	DS04039 (8)	DS04041(2)	DS04041(7)	DS04041(10)	DS05037(2)	DS05037(5)	DS05037(9)	DS05037(13)	DS05037(14)
SiO2	37.507	35.739	36.721	36.672	37.409	37.281	37.634	37.164	37.228	37.749	37.488	37.482
TiO2	2.301	2.213	2.245	2.394	2.053	2.183	2.166	1.945	2.006	1.981	2.02	1.905
Al2O3	15.769	15.421	15.563	15.523	16.324	16.102	16.063	16.459	16.418	16.952	16.632	16.272
Cr2O3	0.008	0	0.006	0	0.017	0.008	0.024	0.016	0.017	0.041	0.036	0.023
FeO	14.97	14.361	14.688	14.543	14.071	14.028	14.272	12.274	12.491	12.549	12.726	12.478
MnO	0.455	0.445	0.453	0.451	0.341	0.353	0.355	0.401	0.433	0.418	0.466	0.429
MgO	14.348	13.485	14.214	14.309	14.788	14.644	14.481	15.09	14.875	15.297	14.922	15.078
CaO	0.006	0.063	0	0.017	0.005	0.011	0	0.016	0	0	0.007	0.003
Na2O	0.148	0.176	0.133	0.137	0.176	0.202	0.196	0.063	0.086	0.06	0.083	0.063
K2O	9.415	8.301	8.781	9.64	9.583	9.58	9.327	10.054	10.149	9.944	10.356	10.118
P2O5	0	0	0	0	0	0	0	0	0	0	0	0
BaO	0.345	0.338	0.309	0.251	0.224	0.21	0.241	0.181	0.194	0.189	0.222	0.174
Total	95.272	90.542	93.113	93.937	94.991	94.602	94.759	93.663	93.897	95.18	94.958	94.025
Mg	63	63	63	64	65.2	65	64.4	68.6	68	68.5	67.6	68.3
Fe	37	37	37	36	34.8	35	35.6	31.3	32	31.5	32.3	31.7
Fe/(Fe+Mg)	0.37	0.37	0.37	0.36	0.348	0.35	0.356	0.31331331	0.32	0.315	0.323323323	0.317

Table A2. Mineral microprobe data; biotite. All Fe is assumed to be Fe2+.

	MR01Cps(2)	MR01Cps(7)	MR01Cps(8)	MR01Cps(9)	MR01Cps(10)	MR01Cps(13)	MR01Gps(2)	MR01Gps(5)	MR01Gps(8)	MR01Gps(10)	MR01Gps(11)	MR01Gps(14)
SiO2	65.04	63.384	64.49	64.224	63.068	64.163	60.562	60.371	59.458	60.649	59.884	60.338
TiO2	0.029	0	0.047	0.023	0	0	0	0	0	0	0	0
Al2O3	18.571	22.737	18.325	18.369	22.72	23.021	24.695	24.839	24.406	24.66	24.203	24.577
Cr2O3	0	0	0.002	0.001	0	0.004	0	0	0	0	0	0
FeO	0.016	0.02	0.029	0.013	0.012	0.046	0	0	0	0	0	0
MnO	0	0	0	0	0	0	0	0	0	0	0	0
MgO	0.004	0.004	0.012	0	0	0	0	0	0	0	0	0
CaO	0.005	4.376	0.014	0.026	4.344	4.319	6.736	6.862	6.78	6.693	6.609	6.748
Na2O	1.015	9.422	0.975	1.037	9.268	9.415	8.042	7.893	7.753	7.903	8.035	7.952
K2O	16.173	0.249	16.178	15.949	0.305	0.29	0.131	0.203	0.193	0.32	0.158	0.183
P2O5	0.043	0	0	0	0	0	0	0	0	0	0	0
BaO	0.564	0	0.608	0.565	0	0	0	0	0	0	0	0
Total	101.46	100.192	100.68	100.207	99.717	101.258	100.166	100.168	98.59	100.225	98.889	99.798
An	0.002	0.2014	0.007	0.0012	0.2022	0.199	0.314	0.3208	0.3222	0.313	0.3097	0.3159
Ab	0.0871	0.785	0.839	0.0898	0.7809	0.7851	0.6787	0.6679	0.6669	0.6691	0.6815	0.6739
Or	0.9127	0.0136	0.9155	0.9089	0.0169	0.0159	0.0073	0.0113	0.0109	0.0178	0.0088	0.0102

	MRO1Dps(2)	MRO1Dps(4)	MRO1Dps(10)	MRO1Dps(11)	MR01Dps(1)	MRO1Dps(12)
SiO2	62.88	61.439	62.1	61.087	63.579	62.76
TiO2	0	0	0	0	0	0
Al2O3	22.853	22.604	22.536	22.482	24.113	23.033
Cr2O3	0	0	0	0	0	0
FeO	0	0	0	0	0.015	0
MnO	0	0	0	0	0	0
MgO	0	0	0	0	0	0
CaO	4.705	4.71	4.654	4.801	4.68	4.712
Na2O	9.017	9.036	9.164	9.004	9.316	9.022
K2O	0.225	0.288	0.277	0.288	0.342	0.286
P2O5	0	0	0	0	0	0
BaO	0	0	0	0	0	0
Total	99.68	98.077	98.731	97.662	102.45	99.813
An	0.2209	0.22	0.2157	0.2239	0.2132	0.2204
Ab	0.7765	0.764	0.769	0.7601	0.7682	0.7637
Or	0.0126	0.016	0.0153	0.016	0.018	0.0159

Table A3. Mineral microprobe data; feldspar

	DS04039(3)	DS04039(6)	DS04039(7)	DS04039(9)	DS04041(3)	DS04041(5)	DS04041(9)	DS04041(11)	DS04041(12)	DS05037(1)	DS05037(4)	DS05037(7)
SiO2	64.957	64.546	64.915	64.838	64.961	65.122	65.35	65.254	64.475	65.106	64.967	64.919
TiO2	0	0	0	0	0	0	0	0	0	0	0	0
Al2O3	20.504	20.863	20.756	20.67	21.339	21.396	21.634	21.325	21.214	21	20.898	20.999
Cr2O3	0	0	0	0	0	0	0	0	0	0	0	0
FeO	0	0.052	0	0	0.021	0	0.029	0.018	0.011	0.007	0.006	0.022
MnO	0	0	0	0	0	0	0	0	0	0	0	0
MgO	0	0	0	0	0	0	0	0	0	0	0	0
CaO	2.69	2.675	2.729	2.69	2.736	2.765	2.677	2.757	2.739	2.43	2.399	2.508
Na2O	8.964	8.602	8.683	8.786	10.354	10.281	10.136	10.028	10.481	10.187	10.361	10.257
K2O	0.071	0.024	0.083	0.086	0.107	0.125	0.076	0.091	0.053	0.267	0.234	0.294
P2O5	0	0	0.134	0	0	0	0	0	0.354	0	0	0
BaO	0	0	0	0	0	0	0	0	0	0	0	0
Total	97.186	96.762	97.3	97.07	99.518	99.689	99.902	99.473	99.327	98.997	98.865	98.999
An	0.1414	0.1466	0.1472	0.144	0.1266	0.1285	0.1264	0.1312	0.1255	0.1147	0.1119	0.1171
Ab	0.854	0.8518	0.8474	0.85	0.8765	0.8646	0.8693	0.8637	0.8693	0.8703	0.8751	0.8666
Or	0.005	0.0016	0.0053	0.0055	0.0059	0.0069	0.0043	0.0059	0.0052	0.015	0.013	0.0163

	DS029.2	29.5	29.8	29.11	DS025.1	25.5	25.9
SiO2	59.0121	59.3001	58.9874	58.936	61.3071	61.7476	61.6876
TiO2	0	0	0	0	0	0	0
Al2O3	24.2755	24.2232	24.375	24.2887	23.3443	22.9069	22.9391
Cr2O3	0	0	0	0	0	0	0
FeO	0	0.0331	0.046	0.0032	0.0427	0.0134	0.0118
MnO	0	0	0	0	0	0	0
MgO	0	0	0	0	0	0	0
CaO	6.96	5.641	7.2636	7.0728	5.5094	5.2483	5.1291
Na2O	8.1355	7.6859	7.9911	8.0068	9.0458	9.2408	9.225
K2O	0.3233	1.196	0.3129	0.3084	0.1277	0.1875	0.1688
P2O5	0	0	0	0.0072	0	0	0
BaO	0	0	0	0	0	0	0
Total	98.7065	98.0793	98.976	98.6232	99.3771	99.3446	99.1615
An	0.3153	0.2688	0.3287	0.3223	0.2499	0.2365	0.2328
Ab	0.6675	0.6634	0.6545	0.6609	0.7431	0.7535	0.758
Or	0.0173	0.0679	0.0169	0.168	0.007	0.0101	0.0091

Table A3. continued Mineral microprobe data; feldspar

	95LH14.10	14.8.12	14.8.14	13.22	13.24	13.28	13.42	13.45	13.5	13.72	13.75	13.78
SiO2	65.885	65.3961	65.6913	56.0228	55.8786	56.3405	58.3902	59.4084	59.6745	57.1437	57.3929	57.0876
TiO2	0	0	0	0	0	0	0	0	0	0	0	0
Al2O3	19.9187	20.5319	19.2704	26.1523	26.4973	26.0086	24.2259	24.25	23.8807	25.445	25.567	25.6475
Cr2O3	0	0	0	0	0	0	0	0	0	0	0	0
FeO	0	0.0549	0.1015	0	0.027	0	0.0122	0	0	0	0	0
MnO	0	0	0	0	0	0	0	0	0	0	0	0
MgO	0	0.0038	0.065	0.0008	0.002	0	0	0	0	0	0	0.0081
CaO	1.4104	0.8795	0.7063	9.2186	9.2946	9.018	7.0043	6.7655	6.5018	8.3103	8.4454	8.5896
Na2O	11.7097	9.8318	11.1258	6.9045	6.6172	6.9221	8.3254	8.445	8.5752	7.0984	7.4281	7.1337
K2O	0	0.6773	0.4485	0.0673	0.2258	0.0534	0.0183	0.0268	0.0206	0.1861	0.0469	0.0542
P2O5	0	0	0	0	0	0	0	0	0	0	0	0
BaO	0	0	0	0	0	0	0	0	0	0	0	0
Total	98.9239	97.3754	97.4089	98.3664	98.5426	98.3427	97.9764	98.8958	98.6529	98.1836	98.8804	98.5208
An	0.062	0.0451	0.033	0.4094	0.4314	0.4173	0.3174	0.3063	0.2948	0.3886	0.3847	0.3983
Ab	0.938	0.9133	0.9419	0.55	0.5561	0.5797	0.6816	0.6923	0.7041	0.601	0.6127	0.5987
Or	0	0.416	0.0251	0.0356	0.0125	0.003	0.001	0.0014	0.0011	0.0104	0.0025	0.003

	13.8	13.83	13.86	13.9	14.2	14.6	14.9	14.12
SiO2	57.0986	57.683	57.6413	57.7678	60.5653	60.2338	60.4347	60.4076
TiO2	0	0	0	0	0	0	0	0
Al2O3	25.6606	24.9171	25.3306	25.1653	23.5474	23.6247	23.7111	23.7122
Cr2O3	0	0	0	0	0	0	0	0
FeO	0.0016	0.0585	0	0	0.0069	0.0059	0.0064	0.0037
MnO	0	0	0	0	0	0	0	0
MgO	0.002	0.038	0	0	0	0	0	0
CaO	8.5964	7.2625	8.1387	8.0303	6.1005	6.1568	6.0649	6.0836
Na2O	7.2805	7.2568	7.6231	7.6788	8.6656	8.7124	8.6787	8.7361
K2O	0.0615	0.7683	0.0212	0.042	0.2014	0.2143	0.236	0.2354
P2O5	0	0	0	0.0024	0	0.0097	0	0
BaO	0	0	0	0	0	0	0	0
Total	98.7013	97.9843	98.755	98.6867	99.0872	98.9576	99.1319	99.1786
An	0.392	0.3415	0.3707	0.3653	0.2768	0.2777	0.2748	0.2741
Ab	0.605	0.6154	0.6282	0.6324	0.7122	0.7108	0.7125	0.7133
Or	0.003	0.0431	0.0011	0.0025	0.011	0.0115	0.0126	0.0126

Table A3.continued Mineral microprobe data; feldspar

	2E.1	2E.5	2E.6	2E.10	4A.2	4A.4	4A.9	4A.12	4C.1	4C.5	4C.6	4C.9
SiO2	57.9951	58.1472	59.914	58.4538	56.6671	56.5264	56.4507	57.0315	55.9093	56.4773	56.674	56.688
TiO2	0	0	0	0	0	0	0	0	0	0	0	0
Al2O3	25.315	25.3297	24.3637	25.0937	25.7131	25.894	26.156	25.8141	26.7001	26.2963	26.2486	25.9477
Cr2O3	0	0	0	0	0	0	0	0	0	0	0	0
FeO	0.0453	0.2458	0.0938	0.1243	0.1115	0.0288	0.0059	0	0	0.064	0.0149	0
MnO	0.0088	0	0	0	0	0	0	0	0	0	0	0
MgO	0	0	0.0386	0	0.1558	0	0	0	0	0	0	0
CaO	8.134	7.9789	6.0708	7.8181	8.631	9.0603	9.351	9.0192	9.8384	9.3892	9.2245	8.9731
Na2O	7.5821	7.721	8.4905	7.7525	6.9991	6.903	6.7908	7.1074	6.3804	6.6674	6.8691	7.0497
K2O	0.1114	0.1278	0.9396	0.1211	0.1018	0.073	0.0841	0.0927	0.025	0.0408	0.0369	0.0251
P2O5	0.0481	0	0	0.0193	0.024	0.0048	0	0.0048	0.0048	0	0	0.0072
BaO	0	0	0	0	0	0	0	0	0	0	0	0
Total	99.2399	99.5504	99.9111	99.3829	98.4035	98.4904	98.8385	99.0698	98.8581	98.9351	99.0681	98.6908
An	0.3699	0.3609	0.2698	0.3621	0.4029	0.4186	0.43	0.4103	0.4594	0.4357	0.4249	0.4357
Ab	0.6441	0.6322	0.6806	0.6312	0.2915	0.5771	0.5653	0.5847	0.5392	0.5621	0.5392	0.5621
Or	0.006	0.0069	0.0495	0.0067	0.0057	0.0043	0.004	0.005	0.0014	0.0022	0.0014	0.0022

	4D.2	4D.6	4D.8	4D.10	4D.11	4D.13	4D.14	4D.14
SiO2	56.2521	55.3346	56.3641	55.8456	57.1196	55.9277	56.1008	56.0708
TiO2	0	0	0	0.0774	0	0	0	0
Al2O3	26.4412	26.9699	26.3817	26.8666	25.8325	26.4792	26.4351	26.5135
Cr2O3	0	0	0	0	0	0	0	0
FeO	0.0903	0.0278	0.0203	0.2526	0.008	0.0016	0.1069	0.1085
MnO	0	0	0	0	0	0	0	0
MgO	0.0083	0.003	0	0.0059	0	0.0006	0	0
CaO	9.3959	10.3848	9.4208	9.9308	8.7293	9.5644	9.4993	9.6675
Na2O	6.7673	6.1805	6.8315	6.4716	6.1958	6.6076	6.6637	6.6187
K2O	0.0776	0.0854	0.0624	0.0297	1.8662	0.0715	0.0624	0.0647
P2O5	0.0048	0	0	0.0096	0	0	0.0168	0
BaO	0	0	0	0	0	0	0	0
Total	99.0376	98.986	99.0809	99.4899	99.7515	98.6527	98.8851	99.0438
An	0.4249	0.4122	0.4321	0.479	0.431	0.4581	0.3936	0.4424
Ab	0.5731	0.5864	0.5636	0.5163	0.5656	0.5403	0.506	0.5537
Or	0.002	0.0014	0.0043	0.0047	0.0034	0.001	0.1004	0.004

Table A3.continued Mineral microprobe data; feldspar

	LH14.8	14.9	14.15	14.17	14.1	14.7	14.1	13.21	13.25	13.3	13.41	13.44	13.47
SiO2	41.8708	41.8994	41.9916	42.7666	40.5876	40.8609	40.9456	43.5095	43.7783	43.3472	42.8971	43.2946	42.6123
TiO2	1.0045	1.0526	0.9647	0.8499	1.3352	1.3027	1.3047	0.706	0.7609	0.6925	1.0833	0.9868	1.0622
Al2O3	12.3762	11.802	12.3091	11.2791	12.1761	11.9935	12.3063	11.8795	11.5726	11.6035	12.2394	11.6477	12.1124
Cr2O3	0	0	0	0	0	0	0	0	0	0	0	0	0
FeO	17.2667	17.4341	17.4398	16.7879	19.6656	19.695	19.7134	16.4724	15.7942	16.2765	17.0465	16.5998	16.5875
MnO	0.2912	0.2925	0.3123	0.2837	0.3329	0.3214	0.3399	0.2983	0.3057	0.2747	0.3032	0.3087	0.3145
MgO	9.4582	9.7563	9.6486	10.2134	8.3748	8.3034	8.4586	10.2248	10.4451	10.3054	9.9792	10.2658	9.9609
CaO	11.6314	11.6675	11.7098	11.6322	11.4356	11.5526	11.5558	12.2356	12.4151	12.2513	11.6227	11.6352	11.7749
Na2O	1.7903	1.8406	1.8326	1.7807	2.104	2.0297	2.0517	1.4651	1.4401	1.4621	1.8869	1.7661	1.9399
K2O	0.9953	1.0253	1.0378	0.8733	1.3342	1.4111	1.3939	0.8928	0.8754	0.8554	0.6337	0.6529	0.68
P2O5	0	0	0	0	0.0138	0	0.0207	0	0	0	0	0	0
BaO	0.0849	0.0221	0.0233	0	0.0551	0.0352	0.0129	0.0187	0.027	0.0082	0.0269	0.0597	0.0269
Total	96.7696	96.7925	97.2697	96.4669	97.4149	97.5056	98.1035	97.7028	97.4145	97.0768	97.719	97.2174	97.0716
mineral	hornblende	hornblende	hornblende	hornblende	hornblende	hornblende	hornblende	hornblende	hornblende	hornblende	hornblende	hornblende	hornblende
Si	40.57318	40.54274	40.42447	41.42822	39.33492	39.59155	39.39065	41.67661	41.99941	41.76038	41.07265	41.65678	41.00688
Ti	0.731915	0.765864	0.698325	0.619074	0.973003	0.949122	0.943799	0.508506	0.548902	0.501656	0.779932	0.713944	0.768619
Al	14.13335	13.45833	13.96492	12.87645	13.90667	13.69527	13.95223	13.41024	13.08415	13.17415	13.81068	13.20755	13.73669
Cr													
Fe	13.99073	14.10613	14.03869	13.5985	15.93659	15.95709	15.85808	13.19375	12.67025	13.11196	13.64782	13.35543	13.34768
Mn	0.238978	0.239701	0.25462	0.23275	0.273236	0.263742	0.276934	0.241992	0.248381	0.22413	0.245863	0.251552	0.256319
Mg	13.66348	14.07393	13.84749	14.74982	12.09997	11.99431	12.13135	14.60118	14.93901	14.80107	14.24444	14.72548	14.29043
Ca	12.07485	12.09498	12.07684	12.07189	11.87315	11.99213	11.90989	12.55612	12.76017	12.64467	11.92213	11.99355	12.1395
Na	3.363272	3.452813	3.420251	3.344188	3.953111	3.812719	3.826556	2.720721	2.678461	2.730793	3.502531	3.294394	3.619173
K	1.230243	1.265509	1.274397	1.079106	1.649358	1.74406	1.710514	1.090866	1.071272	1.051191	0.773958	0.801323	0.834718

Table A4. Mineral microprobe data; amphibole

	LH13.71	13.74	13.77	13.82	13.87	13.92	13.93	2E.2	2E.4	2E.11	4A.1	4A.8	4A.11
SiO2	43.0028	43.4989	43.5518	42.2531	43.1694	43.7465	43.8145	42.6519	42.2634	42.4929	42.7246	43.0032	42.9899
TiO2	0.8427	0.8528	0.8579	0.7532	0.7415	0.6794	0.6854	1.1639	1.0896	1.108	1.1835	0.9418	0.9905
Al2O3	12.0046	11.8689	11.9461	11.7854	11.4287	10.8402	10.9012	12.4373	12.3848	12.2874	13.3002	13.1393	13.1718
Cr2O3	0	0	0	0	0	0	0	0	0	0	0	0	0
FeO	16.0423	15.9964	15.9621	17.7943	17.7524	17.4503	17.2893	17.5062	17.69	17.7598	15.3294	15.0117	15.3821
MnO	0.2855	0.2637	0.2685	0.3291	0.3106	0.3084	0.338	0.259	0.2607	0.2417	0.2283	0.2155	0.2178
MgO	10.2354	10.3816	10.3408	9.2296	9.6072	9.9656	9.8139	9.3755	9.2585	9.275	10.6603	10.7265	10.5651
CaO	11.8603	12.0541	12.0911	12.2412	12.2199	12.3406	12.3138	11.6677	11.7522	11.7384	11.3719	11.5479	11.3896
Na2O	1.6227	1.6366	1.6387	1.6862	1.539	1.5178	1.5644	1.68	1.713	1.7501	1.7877	1.7096	1.7561
K2O	0.6836	0.613	0.6477	0.6775	0.6239	0.5592	0.5669	0.9642	0.9172	0.921	0.5232	0.5273	0.5692
P2O5	0	0	0	0	0	0.0046	0	0	0.0023	0.0069	0.0093	0.0139	0.0255
BaO	0.0657	0.0047	0.0305	0.089	0.0047	0.0047	0.0294	0.0682	0.0493	0.0529	0.0825	0.02	0.0684
Total	96.6457	97.1708	97.3353	96.8387	97.3974	97.4174	97.3169	97.774	97.381	97.6342	97.201	96.8568	97.1261
mineral	hornblende	hornblende	hornblende	hornblende	hornblende	hornblende	hornblende	hornblende	hornblende	hornblende	hornblende	hornblende	hornblende
Si	41.5794	41.79664	41.78714	41.07273	41.71091	42.2186	42.33319	41.00897	40.80452	40.92439	40.88119	41.23781	41.18293
Ti	0.612686	0.61616	0.618951	0.550539	0.538726	0.493025	0.497955	0.841471	0.791032	0.802396	0.851524	0.679105	0.713491
Al	13.67915	13.44013	13.50805	13.50111	13.0137	12.329	12.41274	14.09278	14.09169	13.9462	14.99801	14.849	14.87052
Cr													
Fe	12.97034	12.85252	12.80648	14.46369	14.3428	14.08207	13.96831	14.07458	14.28153	14.30234	12.26518	12.03727	12.32167
Mn	0.23379	0.214591	0.218182	0.270933	0.254164	0.252066	0.276579	0.210901	0.213169	0.197143	0.185008	0.175017	0.176704
Mg	14.75405	14.87141	14.79161	13.37528	13.8387	14.33801	14.1361	13.43878	13.32629	13.31695	15.20687	15.33479	15.08861
Ca	12.28568	12.40851	12.42866	12.74797	12.64921	12.75906	12.7461	12.01843	12.15584	12.11147	11.65737	11.86369	11.6891
Na	3.041782	3.048695	3.048206	3.177696	2.882841	2.839772	2.930349	3.131541	3.20634	3.267662	3.316259	3.178321	3.261432
K	0.843126	0.751333	0.792719	0.840066	0.768949	0.688393	0.698681	1.182542	1.12958	1.131448	0.63859	0.645003	0.695544

Table A4. continued Mineral microprobe data; amphibole

	4C.2	4C.4	4C.8	4C.11	4D.1	4D.5	4D.7	4D.12	DS029.1	29.4	29.9	25.4	25.6	25.8
SiO2	43.5026	43.6748	43.181	43.9146	41.5066	42.2062	42.2304	42.0194	41.77	42.2576	41.9371	41.6113	41.7906	41.5506
TiO2	1.0088	1.0619	1.1494	1.0203	1.0554	1.1876	1.0709	1.114	1.0238	0.8224	0.7942	1.3924	1.4641	1.128
Al2O3	12.7073	12.4366	12.8718	12.2104	13.8409	13.8093	13.5419	13.3542	11.7445	11.5015	11.7461	11.6898	11.6119	11.6557
Cr2O3	0	0	0	0	0	0	0	0	0	0	0	0	0	0
FeO	15.0124	14.9647	14.8024	14.6976	16.2069	16.1405	16.2443	16.0334	15.0914	14.8444	14.8841	18.2625	18.0214	18.371
MnO	0.2522	0.2325	0.233	0.246	0.2603	0.297	0.2958	0.2692	0.3207	0.2968	0.3149	0.3329	0.3226	0.3433
MgO	10.7701	11.0424	10.8023	11.1973	9.7037	9.7889	9.8735	9.8838	11.3432	11.6033	11.9245	9.6332	9.5736	9.6684
CaO	11.825	11.7878	11.7279	11.7044	11.8069	11.9365	11.9489	11.8373	12.1472	12.1923	11.4728	11.5205	11.5028	11.5443
Na2O	1.7472	1.6712	1.7602	1.6942	1.622	1.6492	1.6011	1.6416	1.7135	1.6551	1.6534	2.1097	2.154	2.0952
K2O	0.4598	0.4423	0.4779	0.4059	0.9916	0.966	1.0131	0.9139	1.8121	1.6819	1.6442	1.4273	1.4105	1.2628
P2O5	0.0347	0.0069	0.0232	0.0278	0.0416	0.0069	0.0185	0	0.0115	0	0	0.0069	0.0046	0.0092
BaO	0.0637	0.0283	0.0838	0.1016	0.0472	0	0	0.0071	0	0.032	0	0.0212	0.0706	0.0294
Total	97.3839	97.3494	97.113	97.2202	97.0832	97.9882	97.8384	97.074	96.978	96.8873	96.3714	98.0078	97.9268	97.658
mineral	hornblende	hornblende	hornblende	hornblende	hornblende	hornblende	hornblende	hornblende	hornblende	hornblende	hornblende	hornblende	hornblende	hornblende
Si	41.54897	41.70031	41.32929	41.98147	39.94511	40.22229	40.88119	41.23781	39.84574	40.31865	40.14626	39.78067	39.99501	39.85987
Ti	0.724492	0.762386	0.827217	0.733432	0.763742	0.851028	0.851524	0.679105	0.734371	0.590021	0.571689	1.00094	1.053613	0.813675
Al	14.30304	13.99394	14.51893	13.75652	15.69788	15.50931	14.99801	14.849	13.20329	12.9326	13.25167	13.17037	13.09666	13.17732
Cr														
Fe	11.98943	11.94757	11.84679	11.74893	13.04216	12.86207	12.26518	12.03727	12.03788	11.84314	11.91441	14.59904	14.42178	14.73651
Mn	0.203999	0.188005	0.188869	0.199169	0.212158	0.23971	0.185008	0.175017	0.259093	0.23983	0.255304	0.269534	0.261475	0.278915
Mg	15.33521	15.71798	15.41368	15.95831	13.92223	13.90751	15.20687	15.33479	16.13162	16.5047	17.01813	13.72955	13.65927	13.82732
Ca	12.09952	12.05766	12.02562	11.98726	12.17319	12.1868	11.65737	11.86369	12.41411	12.4626	11.76625	11.79924	11.79377	11.86446
Na	3.235162	3.093464	3.266146	3.139943	3.026256	3.046999	3.316259	3.178321	3.16891	3.061496	3.068548	3.910118	3.996513	3.896659
K	0.560174	0.538684	0.58346	0.494968	1.217284	1.174294	0.63859	0.645003	2.205	2.046965	2.007753	1.740544	1.721906	1.545262

Table A4. continued Mineral microprobe data; amphibole

	MR01Cps(3)	MR01Cps(4)	MR01Cps(6)	MR01Cps(12)	MR01Cps(5)	MR01Gps(7)	MR01Gps(12)	MR01Gps(2core)	MR01Gps(3)	MR01Gps(2 rim)	MR01Gps(5)
SiO2	0.301	0.289	0.273	0.285	0.065	30.742	0.04	37.028	36.328	26.328	33.766
TiO2	0.286	0.309	0.31	0.31	0	35.726	0.004	0.252	0.258	0.258	0.024
Al2O3	0.177	0.183	0.177	0.184	0	1.974	0	23.262	22.999	22.999	0.001
Cr2O3	0.175	0.173	0.176	0.15	0	0.011	0	0.03	0.052	0.052	0
FeO	0.334	0.278	0.297	0.287	0	0.594	0.01	10.2	10.125	10.125	0.043
MnO	0.261	0.251	0.246	0.243	0	0.07	0.038	0.315	0.34	0.34	0
MgO	0.143	0.136	0.143	0.132	0	0	0.002	0.226	0.274	0.274	0
CaO	57.511	57.773	56.674	56.607	54.41	29.343	56.937	20.08	19.632	19.632	0
Na2O	0.172	0.156	0.157	0.184	0.055	0.007	0.016	0.017	0.004	0.004	0.03
K2O	0.127	0.125	0.097	0.093	0.012	0	0	0	0.016	0.016	0
P2O5	41.188	41.525	41.638	41.895	29.974	0.074	42.238	0.027	0.043	0.043	0
BaO	0.577	0.576	0.582	0.61	0.005	0.722	0.005	0.085	0.152	0.152	0
ZrO2 (est.)											66
Total	101.252	101.774	100.77	100.98	84.8	99.263	99.29	91.522	90.223	90.223	99.864
Phase	apatite	apatite	apatite	apatite	apatite	sphene	apatite	epidote	epidote	epidote	zircon

	MR01Dps(3)	MR01Dps(5)	MR01Dps(7)	MR01Dps(9)	MR01Dps(2)	MR01Dps(2)	MR01Dps(13)
SiO2	0.034	37.191	37.737	0	0	33.507	0.003
TiO2	0	0.07	0.022	0	0	0.01	0
Al2O3	0	20.124	20.639	0	0	0	0
Cr2O3	0.023	0.03	0.018	0.019	0	0.013	0.004
FeO	0.018	31.173	31.875	0.057	0.049	0.119	0.027
MnO	0.08	6.313	6.635	0.071	0	0.034	0.087
MgO	0.002	2.358	2.385	0.015	0	0	0.013
CaO	56.679	2.22	1.483	56.315	54.093	0.002	56.266
Na2O	0.097	0.025	0.016	0.09	0.033	0.012	0.092
K2O	0	0	0	0	0	0	0
P2O5	41.875	0	0.019	42.198	42.182	0.119	42.027
BaO	0.008	0.067	0.044	0	0	0	0
ZrO2 (est.)						66	
Total	98.816	99.571	100.873	98.765	96.357	99.507	98.519
Phase	apatite	almandine	almandine	apatite	apatite	zircon	apatite
Alm		0.698706735	0.712333407				
Sps		0.1433137	0.150179147				
Prp		0.094228409	0.095026171				
Grs		0.063751157	0.042461276				

Table A5. Mineral microprobe data; accessories

	DS04039(4)	DS04039(10)	DS04039(11)	DS04039(12)	DS04039(13)	DS04041(1)	DS04041(4)	DS04041(6)	DS05037(3)	DS05037(6)	DS05037(11)
SiO2	0	0	0	0	0	0	0	0	0	0	0
TiO2	0.216	0.198	0.173	13.297	12.934	9.644	9.022	0.172	9.511	6.752	7.442
Al2O3	0.046	0.056	0.058	0.03	0.027	0.073	0.077	0.117	0.062	0.09	0.047
Cr2O3	0.122	0.151	0.186	0.095	0.103	0.137	0.143	0.153	0.147	0.13	0.147
FeO	91.621	92.458	91.538	77.645	77.524	81.658	80.85	92.208	80.843	83.57	81.895
MnO	0.285	0.282	0.337	0.399	0.386	0.276	0.149	0.273	0.204	0.311	0.322
MgO	0	0	0	0.002	0.027	0.041	0.017	0.025	0.045	0.101	0.04
CaO	0.061	0.051	0.06	0.073	0.065	0.093	0.057	0.083	0.064	0.075	0.081
Na2O	0	0.009	0	0	0.014	0	0	0	0	0	0
K2O	0.025	0	0.018	0.003	0.012	0.019	0.028	0.03	0.029	0.024	0.038
P2O5	0.346	0.385	0.423	0.985	0.72	0.983	0.606	0.612	0.906	0.72	0.151
BaO	0.327	0.303	0.316	0.541	0.532	0.45	0.454	0.257	0.424	0.37	0.376
Total	93.049	93.893	93.109	93.07	92.344	93.374	91.403	93.93	92.235	92.143	90.539
Phase	magnetite	magnetite	magnetite	ilmenite	ilmenite	ilmenite	ilmenite	magnetite	ilmenite	ilmenite	ilmenite

	LH14.11	14.13	14.16	13.23	13.26	13.27	13.29	13.43	13.46	13.48	13.49
SiO2	29.8387	30.229	30.1609	98.1535	30.2206	97.2936	30.0932	30.2358	30.1632	98.1642	30.1919
TiO2	38.8272	38.1543	38.2888	0	38.5954	0	37.8783	38.2348	38.7345	0	38.8311
Al2O3	1.0691	1.2045	0.9506	0	1.2781	0	1.2247	1.264	0.842	0	0.913
Cr2O3	0	0	0	0	0	0	0	0	0	0	0
FeO	0.3819	0.3439	0.477	0	0.2884	0	0.47	0.5111	0.4138	0.0021	0.4151
MnO	0.0892	0.0892	0.0963	0	0.0689	0	0.0578	0.0807	0.1147	0	0.0919
MgO	0.0142	0.0065	0.016	0	0.0153	0	0.0065	0.0173	0.025	0	0.0102
CaO	29.4088	29.2189	29.2576	0	29.3576	0	29.3329	28.951	28.9986	0	29.1967
Na2O	0.0088	0.0018	0.0202	0	0.0004	0	0	0.0051	0.0074	0	0.0063
K2O	0	0	0	0	0	0	0	0	0	0	0
P2O5	0.0834	0.0102	0.1306	0	0.049	0	0.1083	0.0983	0.0695	0	0.1002
BaO	0.7756	0.7634	0.7784	0	0.6537	0	0.7049	0.7255	0.7961	0	0.7706
Total	100.4968	100.0217	100.1763	98.1536	100.5273	97.2937	99.8767	100.1236	100.1648	98.1664	100.527
mineral	titanite	titanite	titanite	quartz	titanite	quartz	titanite	titanite	titanite	quartz	titanite

Table A5. continued Mineral microprobe data;accessories

	13.73	13.76	13.79	13.81	13.84	13.85	13.89	13.91	2E.7	2E.8	2E.9	
SiO2	30.1506	30.2425	98.0413	30.0925	30.0729	97.8411	30.2224	98.058	0	30.2317	97.9496	
TiO2	38.4766	38.8703	0	38.3912	37.5127	0	39.0918	0	0	38.2166	0	
Al2O3	1.0744	0.908	0	0.8815	1.2753	0	0.7206	0	0	1.1773	0.0006	
Cr2O3	0	0	0	0	0	0	0	0	0	0	0	
FeO	0.3591	0.3647	0.2077	0.3158	0.3643	0	0.4095	0.022	0.0534	0.4888	0.0919	
MnO	0.0691	0.1014	0	0.0698	0.0487	0	0.0611	0	0.0469	0.0777	0	
MgO	0.011	0.007	0	0.0041	0.0016	0.0025	0.0079	0	0.0061	0	0	
CaO	29.1272	29.1771	0	29.2278	29.363	0	29.2045	0	57.0543	29.2517	0	
Na2O	0.0184	0.0103	0	0.0011	0	0	0	0.0076	0.0164	0.0185	0.0123	
K2O	0	0	0	0	0	0	0	0	0	0	0	
P2O5	0.0962	0.0696	0	0.0061	0.0882	0	0.0349	0	29.9488	0.14	0	
BaO	0.7122	0.7327	0	0.7154	0.6804	0	0.7254	0	0.0582	0.7241	0	
Total	100.0947	100.4836	98.2491	99.7054	99.4072	97.8437	100.478	98.0877	87.1842	100.3263	98.086	
mineral	titanite	titanite	quartz	titanite	titanite	quartz	titanite	quartz	apatite	titanite	quartz	

	2E.12	2E.51	2E.53	4A.3	4A.5	4A.6	4A.7	4A.10	4C.7	4C.10	4C.12	
SiO2	30.3872	39.1217	38.7925	0	0	0	0	98.4818	30.219	0	30.4243	
TiO2	37.8385	0.0823	0.0723	0	52.173	52.0126	0.0021	0	38.4028	52.3343	38.7734	
Al2O3	1.2119	20.1776	20.4361	0	0.0084	0	0	0	1.0694	0	1.0144	
Cr2O3	0	0	0	0	0	0	0	0	0	0	0	
FeO	0.483	24.8052	24.4932	0.1756	46.2219	46.3317	0.2096	0.043	0.4008	46.2055	0.3445	
MnO	0.0859	3.0363	3.6159	0.0547	0.9164	0.8742	0.0725	0	0.1306	1.4035	0.0836	
MgO	0.0039	2.5516	2.2639	0.0175	0.8364	0.619	0.009	0	0.0138	0	0	
CaO	29.3939	11.3121	11.3567	56.4657	0.0437	0.1219	56.3775	0	29.3219	0.1893	29.6267	
Na2O	0.0048	0	0.0036	0.0179	0	0	0.0249	0.0018	0.0093	0	0.0056	
K2O	0	0	0	0	0.0028	0.0285	0	0	0	0.0116	0	
P2O5	0.0618	0	0	28.7879	0.0398	0.0438	28.9061	0	0.2118	0.0358	0.1378	
BaO	0.8112	0.0496	0.0436	0.0633	1.3239	1.189	0.1189	0.0145	0.7937	1.2426	0.8038	
Total	100.282	101.1361	101.0778	85.5826	101.5663	101.2207	85.7206	98.5412	100.5731	101.4225	101.2141	
mineral	titanite	garnet	garnet	apatite	ilmenite	ilmenite	apatite	quartz	titanite	ilmenite	titanite	
Alm		0.528638921	0.524008298									
Sps		0.065538526	0.078351017									
Prp		0.096950649	0.086351841									
Grs		0.308871904	0.311288844									

Table A5. continued Mineral microprobe data;accessories

	4D.3	4D.4	4D.9
SiO2	98.5864	0	0
TiO2	0.3183	51.6813	0.0157
Al2O3	0.0154	0	0
Cr2O3	0	0	0
FeO	0.4361	47.0791	0.0647
MnO	0	1.5201	0.0988
MgO	0.0246	0.1052	0.0164
CaO	0.0052	0.1333	56.6146
Na2O	0	0	0.0067
K2O	0	0.0019	0
P2O5	0	0.0379	27.4373
BaO	0	1.1723	0
Total	99.3861	101.7311	84.2542
mineral	quartz	ilmenite	apatite

	DS02029.3	29.6	29.7	29.1	25.2	25.3	25.7	25.1	25.11
SiO2	29.9413	0	36.8887	30.0511	0	36.1227	30.288	30.1131	36.1503
TiO2	38.3004	0.0135	2.325	37.4568	46.0205	3.6094	37.2449	37.3069	3.5726
Al2O3	1.2088	0	15.0547	1.3817	0.0449	14.5431	1.2078	1.2968	14.4672
Cr2O3	0	0	0	0	0	0	0	0	0
FeO	0.354	0.1662	15.0631	0.6495	50.1125	18.8699	0.7598	0.6564	18.9743
MnO	0.1291	0.0339	0.1989	0.1155	1.5629	0.1761	0.1261	0.1343	0.1893
MgO	0.0023	0.0164	14.3591	0.0132	0.1726	11.9624	0.0132	0.0073	11.9267
CaO	29.2727	57.4565	0	29.1048	0.1265	0	28.7293	28.6535	0
Na2O	0.0063	0.007	0.0149	0.0015	0	0.1814	0.0174	0.0096	0.1937
K2O	0	0	11.756	0	0.0123	11.4826	0	0	11.4904
P2O5	0.0659	28.0294	0.0046	0.0742	0.0481	0.0114	0.095	0.0784	0.0182
BaO	0.699	0.0203	0.2351	0.6928	1.0431	0.393	0.7381	0.6783	0.45
Total	99.9798	85.7433	95.9001	99.5412	99.1435	97.352	99.2197	98.9347	97.4328
mineral	titanite	apatite	biotite	titanite	ilmenite	biotite	titanite	titanite	biotite

Table A5. continued Mineral microprobe data;accessories

	Lighthouse gneiss association-upper unit								lower unit								metasediments			
Sample	2D	2E	3B	4A	4C	4D	4E	4G	13.2	13.4	13.7	13.1a	13.1b	13.8	14.8	14.9	MROID	MR01G	MR01C	DS-3-46
SiO2	45.79	50.23	45.84	46.02	46.2	46.9	45.41	45.85	48.37	47.45	46.54	47.77	47.95	48.4	47.45	47.25	64.78	57.54	60.51	52.9
TiO2	2.16	1.77	1.27	0.96	1.21	1.84	1.94	1.23	1.54	1.45	1.55	2.18	1.96	1.58	1.65	1.38	1.132	0.953	0.916	1.2
Al2O3	13.87	14.12	16.96	17.52	15.8	14.78	14.61	16.59	13.81	13.39	14.13	12.62	13.26	13.71	13.39	13.93	14.74	20.3	16.25	17.23
Fe2O3	15.02	13.46	12.42	11.5	12.55	14.83	14.96	12.27	13.56	14.03	13.3	15.76	15.52	13.65	14.17	13.48	7.55	4.93	7.7	9.27
MnO	0.21	0.24	0.2	0.17	0.2	0.23	0.22	0.18	0.22	0.24	0.21	0.25	0.24	0.21	0.21	0.23	0.123	0.06	0.092	0.17
MgO	6.97	5.61	7.42	8.63	7.97	7.23	7.28	8.35	7.2	8.17	7.61	6.09	6.25	6.94	7.01	7.77	0.123	0.06	0.092	4.64
CaO	11.04	9.91	10.86	10.42	10.93	10.34	10.66	10.98	11.15	10.57	10.88	10.22	10.37	10.86	9.69	11.11	2.07	1.74	3.15	7.54
Na2O	2.03	2.39	2.77	2.58	2.49	2.84	2.69	2.24	1.92	2.39	2.38	2.11	1.86	2.3	2.52	2.75	2.12	5.68	1.89	3.33
K2O	0.63	0.59	0.45	0.33	0.37	0.43	0.48	0.4	0.64	0.49	0.5	0.84	0.52	0.5	1.09	0.82	3.64	5.02	3.72	1.49
P2O5	0.28	0.25	0.12	0.09	0.11	0.23	0.2	0.1	0.13	0.13	0.15	0.23	0.18	0.15	0.17	0.13	2.89	1.91	4.87	0.23
Total	98.31	98.76	98.87	98.78	98.24	100	98.79	98.79	98.95	98.8	98.06	98.56	98.6	98.92	98.33	99.67	99.65	99.06	94.32	98
Cr (ppm)	109	79	86	83	146	84	88	121	253	276	260	87	146	252	181	325	146	104	119	62
Ni	50	12	67	88	70	54	51	103	54	93	82	16	28	49	51	69	41	10	51	27
Co	46	37	54	57	56	47	53	54	51	51	52	49	50	46	46	46	73	44	61	0
V	347	361	264	220	273	330	337	239	379	336	312	427	424	396	380	345	278	587	240	167
Cu	67	31	18	43	72	79	11	72	88	41	95	90	111	87	56	34	581	1321	972	13
Zn	112	106	91	72	92	78	62	84	121	128	158	110	117	154	100	115	28	25	45	116
Rb	6	3	4	4	6	7	6	8	6	9	8	11	5	8	20	3	30	25	37	
Ba	290	135	14	327	334	588	534	435	29	349	368	61	169	318	275	349	21	0	35	
Sr	161	347	327	273	261	321	293	253	142	162	158	168	154	174	130	159	4	33	5	
Ga	13	14	14	16	14	14	14	15	14	13	14	12	13	14	13	14	125	64	143	18
Nb	5.9	6	3.6	3.5	3.2	6	7.4	3.6	2.3	2.3	2.7	4	5.4	2.7	4.2	2.1	20	24	23	3
Hf	3.38	3.78	2.17	1.81	1.91	2.84	3.12	1.86	2.42	2.32	2.57	3.81	3.3	2.59	2.72	2.08	89	43	120	
Zr	118	136	76	63	70	108	117	69	87	83	92	137	118	92	100	79	203	768	232	116
Y	36	37	21	16	20	32	33	21	33	31	32	44	43	35	34	29	50	26	32	25
Th	0.53	0.55	0.34	0.26	0.37	0.67	0.81	0.26	0.46	0.53	0.47	0.88	1.15	0.62	0.91	0.49	17	10	14	
La	8.79	11.7	4.4	3.64	4.7	7.98	9.26	4.29	6.3	5.56	5.59	9.1	7.73	6.37	6.85	4.9	11	9	7	
Ce	22.87	28.74	11.92	9.92	11.79	21.38	23.95	11.05	15.79	14.11	14.99	23.72	20.5	16.09	17.68	12.93	7	0	7	
Pr	3.62	4.3	1.88	1.58	1.87	3.36	3.84	1.85	2.58	2.27	2.47	3.83	3.29	2.61	2.78	2.09	2	1	2	
Sm	5.16	5.3	2.82	2.29	2.7	4.67	5.16	2.72	3.79	3.57	3.79	5.77	4.9	3.94	4.1	3.27				
Eu	1.78	1.69	1.14	0.9	1.02	1.61	1.72	1.06	1.36	1.27	1.34	1.94	1.64	1.4	1.35	1.17				
Tb	0.94	0.94	0.55	0.41	0.52	0.84	0.97	0.56	0.85	0.78	0.83	1.23	1.08	0.9	0.87	0.72				
Dy	6.26	6.32	3.64	2.73	3.54	5.41	6.04	3.63	5.64	5.25	5.5	8.04	6.82	5.76	5.63	4.86				
Ho	1.3	1.33	0.76	0.57	0.69	1.12	1.28	0.77	1.23	1.15	1.21	1.75	1.51	1.24	1.22	1.06				
Er	3.79	3.81	2.14	1.62	2.03	3.21	3.6	2.2	3.47	3.26	3.4	4.96	4.4	3.58	3.52	3.08				
Tm	0.52	0.53	0.29	0.21	0.29	0.45	0.51	0.31	0.49	0.47	0.49	0.72	0.63	0.52	0.51	0.44				
Yb	3.46	3.64	1.9	1.51	1.82	2.96	3.22	1.9	3.13	3.04	3.11	4.57	4.13	3.3	3.4	2.88				
Lu	0.53	0.55	0.3	0.22	0.28	0.46	0.51	0.3	0.49	0.48	0.49	0.71	0.64	0.53	0.53	0.46				

Table A6. Major element data, Lighthouse and Sand Bay gneiss associations

	Sand Bay gneiss associaiton (Dillon schist)																						
Sample	-62	-67	-39	-41	-45	-36	-37	-90	-92	-93	-61	-67	-70	-71	4-75	-76	-78	-79	-80	-88	5-91	-92	-93
SiO2	61.21	59.94	59.11	60.87	60.25	55.28	59.08	57.28	58.3	53.92	64.3	57.97	56.26	54.99	55.18	59.03	60.38	56.66	57.48	50.06	59.02	58.3	56.38
TiO2	0.85	1.24	0.93	0.81	0.9	0.93	1.14	1.1	0.94	0.91	0.74	1.25	1.33	1.3	0.85	0.98	0.88	1.08	1.01	1.57	0.95	0.94	0.92
Al2O3	16.31	16.03	15.91	16.46	16.01	16.01	15.32	16.16	16.81	16.17	15.18	16.23	15.83	16.77	17.11	16.28	16.12	16.46	16.92	15.78	16.09	16.81	15.19
Fe2O3	6	7.42	8.3	6.17	7.35	7.83	7.98	7.77	6.78	7.71	5.12	8.13	9.35	7.57	7.67	7.35	7.18	7.29	7.03	10.3	6.52	6.78	7.16
MnO	0.14	0.07	0.15	0.11	0.11	0.22	0.13	0.22	0.15	0.23	0.05	0.09	0.1	0.11	0.22	0.14	0.11	0.19	0.14	0.39	0.17	0.15	0.24
MgO	3.79	2.75	4.13	4.1	2.85	4.73	4.3	5.07	4.46	5.56	2.82	3.49	3.6	4	4.4	2.82	2.79	3.3	3.44	5.7	4.86	4.46	4.05
CaO	2.15	2.4	1.72	1.61	1.93	4.53	1.38	1.89	2	4.9	2.03	2.93	3.15	4.55	3.14	2.29	1.8	3.45	2.68	4.4	1.97	2	5.79
Na2O	4.57	5.1	5.11	5.2	5.58	3.4	4.65	4.27	5.14	4.04	4.89	5.56	4.82	5.83	5.57	5.11	5.39	5	4.86	3.45	4.64	5.14	4.02
K2O	3.07	2.91	2.7	2.53	2.77	3.68	3.15	3.7	3	3.29	2.44	2.4	3.23	1.68	2.88	2.74	2.78	2.67	3.53	3.06	3.05	3	2.27
P2O5	0.16	0.48	0.19	0.18	0.21	0.24	0.19	0.25	0.18	0.26	0.13	0.4	0.76	0.38	0.15	0.19	0.16	0.18	0.21	0.29	0.17	0.18	0.25
Total	98.25	98.34	98.25	98.04	97.96	96.85	97.32	97.71	97.76	96.99	97.7	98.45	98.43	97.18	97.17	96.93	97.59	96.28	97.3	95	97.44	97.76	96.27
Mg#																							
Cr (ppm)	59	21	57	53	61	138	64	55	77	171	32	13	13	15	73	49	41	53	46	22	65	77	125
Ni	27	0	23	25	21	46	27	21	32	49	17	1	0	8	24	9	9	18	15	2	26	32	38
Co	21	0	0	0	0	0	0	25	17	25	14	12	23	12	28	20	15	23	23	37	18	17	18
V	115	93	142	115	106	146	170	160	124	153	78	137	240	152	142	143	114	170	152	264	138	124	183
Cu	0	0	32	53	7	10	12	0	0	0	2	6	13	4	7	31	4	4	4	10	4	0	23
Zn	71	69	75	51	98	248	94	141	115	182	31	71	104	67	156	89	80	125	115	347	130	115	190
Rb																							
Ba																							
Sr																							
Ga	16	20	21	18	19	21	20	20	20	20	19	16	15	18	17	18	19	18	18	16	19	20	18
Nb	0	11	3	3	6	5	3	8	9	8	7	8	10	8	6	7	9	6	7	8	7	9	7
Hf																							
Zr	156	192	127	145	178	146	129	152	170	173	142	175	188	168	117	155	206	161	146	165	141	191	174
Y	25	38	25	21	33	24	26	25	25	24	23	38	29	31	16	27	29	26	23	20	27	33	28

Table A6. Major element data, Lighthouse and Sand Bay gneiss associations

Appendix B.

U-Pb data Age errors, discordance and regression lines.

U-Pb age errors

With over 20 years as one of the foremost U-Pb geochronology laboratories in the world, the Jack Satterley Geochronology Laboratory of the Royal Ontario Museum (ROM) produces extremely high precision data. Analytical uncertainties that contribute to U-Pb age errors that in this study vary from 1.8 - 41.8 my include:

1) Ion-beam instability; variations in the flux of ions from the sample as a result of variations in the efficiency and intensity of sample fusion.
2) In-run variability; systematic mass-discrimination errors during ion counting using the Daly and Faraday-cup detectors.
3) Uncertainties in the isotopic composition and amount of initial Pb and Pb-blank.

See Davis (1982) for a complete discussion of R.O.M. U-Pb mass spectrometry uncertainties.

Discordance

The U – Pb concordia method derives an age from $^{206}Pb/^{238}U$ to $^{207}Pb/^{235}U$; these ratios are calculated from the following equations using measurements of U and Pb:

$$^{206}Pb/^{238}U = [(^{206}Pb/^{204}Pb)_{measured} - (^{206}Pb/^{204}Pb)_{initial}]/ (^{238}U/^{204}Pb)_{measured}$$

and

$$^{207}Pb/^{235}U = [(^{207}Pb/^{204}Pb)_{measured} - (^{207}Pb/^{204}Pb)_{initial}]/ (^{235}U/^{204}Pb)_{measured}$$

Figure B1 shows the changes in $^{206}Pb/^{238}U$ to $^{207}Pb/^{235}U$, from a starting point (at time = 0) of x=0 and y=0, when no radiogenic Pb was present, with a gradual ^{206}Pb and ^{207}Pb increase, and ^{238}U and ^{235}U decrease, as the latter decay. The position of a sample on the concordia line (produced by the above equations; Figure B1) gives the time that has passed since radiogenic Pb started accumulating. Five assumptions that need to be met for a valid age to be derived from the U-Pb concordia method are:

1) The mineral has been closed to the redistribution of U and Pb and all intermediate daughters throughout its history
2) Correct initial $^{206}Pb/^{204}Pb$ and $^{207}Pb/^{204}Pb$ were chosen
3) ^{238}U and ^{235}U decay constants are known accurately
4) U isotopic composition is 'normal', there has been no natural fission reactions in the history of the U in the sample (e.g. the Oklo event; Faure 1986)
5) The results are not affected by an major analytical inaccuracy, imprecision and there are no systematic errors.

Of the assumptions listed in table B1 assumption (1) is not normally fulfilled, as a result of Pb-loss most samples analysed are discordant, i.e. they do not lie on a concordia

line. For discussion of the other assumptions see Dickin (1995), or Faure (1986). The two main causes of discordance are disturbance and diffusion.
Discordia caused by geological disturbance is usually in the form of thermal events that remove some Pb. In simple, single-event disturbance scenarios, the intersection of a straight line (discordia) with the final (measured) isotopic composition and the original concordia gives both the time since the Pb-loss event; the lower intercept, and the time since original crystallisation; the upper intercept. Figure B1 shows an example of an ancient geological event (0') that has removed some Pb; following Pb loss the sample continues to evolve its Pb/U, producing another concordia line (X–X'), which fixes a discordia line that intersects the original concordia at T'; the initial crystallisation event, and the disturbance event; 0'.

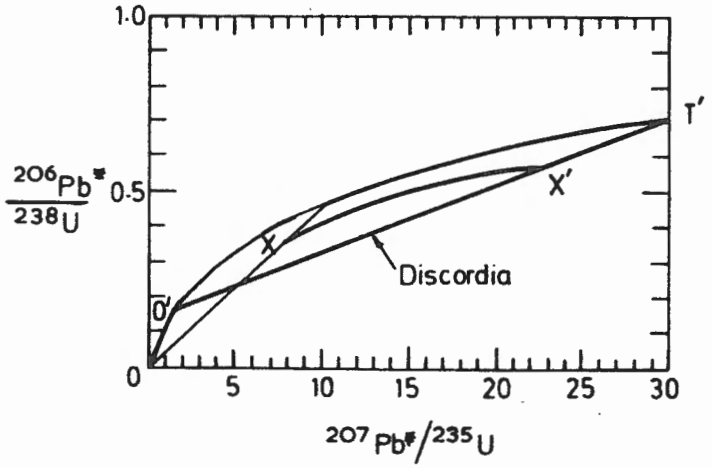

Figure B1. The production and evolution of a discordant U-Pb sample, from Nisbet (1987). T'- initial crystallization, 0'- disturbance event, X-X' – post-disturbance sample evolution.

Some discordia may have ambiguous geological meaning. Tilton (1960) noted that the lower intercept of a discordia line at 600Ma from many worldwide U-Pb samples did not correlate with any known geological event, and reasoned that the Pb-loss that appeared to have taken place was the result of gradual Pb diffusion.

Calculating discordia or regression lines from data arrays

Regression or discordia lines calculated from linear or quasi-linear arrays of related discordant data points can yield geologically meaningful ages (e.g. Fig. 3.2). Techniques for regressing data arrays include the least squares method (York 1967), the least squares cubic method (Ludwig 1980), and the maximum likelihood function method (Davis 1982), the latter being the preferred technique at the R.O.M.. The maximum likelihood function calculates a probability density that a given data set is derived from a particular regression line (Davis 1982). Upper and lower intercepts of regression lines

with concordia are calculated by iterative solutions of the equations of the concordia and regression lines (Davis 1982). All calculations use the R.O.M. in-house software ROMAGE. Uncertainties in plotting regression lines as a result of the co-variance of errors on $^{206}Pb/^{238}U - ^{207}Pb/^{235}U$ plots, and the combination of geological and analytical scatter, are accounted for by employing error expansion routine of Davis (1982). The error expansion technique involves enlargement of the error ellipse of a particular sample in a direction normal to the regression line by an amount proportional to sample discordance. Error ellipses are enlarged until they all intersect the regression line. Errors on upper and lower intercept ages are therefore a combination of the weighted errors of the samples, and the additional error introduced by the error expansion routine (Davis 1982).

Igneous rocks	207Pb/206Pb (Ma)	2 sigma
Shawanaga domain		
Shawanaga pluton	1460 +12/-8 Ma	
Ojibway	1466±11	
Britt domain		
Tonalitic gneiss	2680	
Granitic gneiss	1800-1600	
Megacrystic granitoid	1460-1430	
Mid continent		
Central Plains Orogen	1800-1600	
Northwestern granite-rhyolite province	1470 - 1550	
Southern and eastern granite-rhyolite province	ca. 1370 and ca. 1470	
Parry Sound domain		
Basal Parry Sound domain		
Granodiorite	1353	9.3
	1352	4.8
	1346.8	3.9
	1330.4	10
	1362.5	7.8
	1352.1	1.6
	1343.2	1.8
	1364-1394	18
Whitestone anorthosite	1350	50

	207Pb/206Pb (Ma)	2 sigma
Parry Sound domain		
Basal Parry Sound domain		
Isabella Island granitic gneiss	1257	5.3
	1285	5.7
	1287	4.9
	1301	2.1
	1279.1	1.7
	1295	3
	1383	14
Tonalitic gneiss	1368.2	12.1
	1331.9	2.6
	1344.4	2.7
	1382	1.6
	1437	1.4
	1332-1383	+/-14
Parry Island anorthosite	1160	
Parry Island mafic dyke	1151	1
Interior Parry Sound domain		
Tonalitic gneiss		
	1250	7.8
	1267.6	7.2
	1297.2	10.6
	1300.3	3.1
	1277.7	11.5
	1314	+12/-9

Table B1. Age data and errors where available for (meta)igneous rocks on figure 3.6

LH lower unti psammite MR01C		LH upper unit psammites MR01G, MR01D			SB Dillon Schist		SB quartzite	
207Pb/206Pb (2 sigma	discord.%	207Pb/206Pb (2 sigma		discord.%	discord.%	207Pb/206Pb (2 sigma		207Pb/206Pb (2 sigma
1379.1	13.1	0.9	1847	2.4	2.6	0.6	1914 23	2466 12
1361.6	5.2	1.3	1328	2.3	2.7	1.8	1708 28	2359 10
1381.5	4.9	1.1	1435.1	7	0.1	1.4	1394 16	1917 14
1384.2	3.7	1.4	1337.8	1.8	0.5	-1	1383 48	1885 14
1379.6	3.1	2.8	1458	4.2	0.6	1.6	1368 36	1754 17
1357.8	5.6	0.9	1354.1	3.1	0.8	4.2	1362 35	1417 5
1342.5	6.4	1.2	1325.1	4.4	0.3	4.3		
1383.3	4.9	0.2	1331.3	10	0.1	7.8		
1382.5	7	0	1327.7	41.8	-0.3	2.2		

Parry Sound domain				Frontenac Adirondack belt			
PSD basal quartzite		PSD TMB		Frontenac quartzite		Frontenac quartzite	
207Pb/206Pb (2 sigma		207Pb/206I	2 sigma	207Pb/206I	2 sigma	207Pb/206I	2 sigma
2673	3.5	1915	15.7	1416	1.9	1606 1.5	1801 1.3
2572	1.2	1334	5.3	1958	1.2	1684 1.3	2190 1.8
2466	1.7	1181	20.8	1745	1	2123 1.2	1852 1
2026	6.2	1155	9.4	2064	1	2345 1	2405 1.5
1867	8.3	1154	9	1826	1	2580 1	1786 2
1748	1.8	1150	22	1817	1	1511 2.1	2533 1
1562	2.3	1139	5.4	1832	1	1795 1	1911 2.4
1420	1.5	1136	11	1493	1	1306 16	1652 2
1417	3.6	1135	22	1891	1	3184 3	2026 2.5
1384	3.7	1134	5	1823	5		1843 1.8
		1110	24				

Notes and sources for table B1 and B2 :

abbreviations PSD - Parry Sound domain (Wodicka et al. 1996),

LH and SB: Lighthouse and Sand Bay gneiss associaitons (Culshaw and Dostal 1997, 2002, and T.Krogh pers. comm.)

Britt - Ketchum and Davidson (2000), mid-continent U-Pb and Nd model ages Van Schmus et al. (1996).

Table B2. Detrital age data and errors for metasedimentary rocks used for figure 3.6

Appendix C - ε_{Nd}, mixing models, contaminant detection limits

ε_{Nd} values are calculated using:

$$\varepsilon_{Nd}(t) = ([(^{143}Nd/^{144}Nd)_{sample}^{(t)} / (^{143}Nd/^{144}Nd)_{CHUR}^{(t)}]-1) * 10^4$$

t - estimated from likely deposition age of interlayered metasediment protoliths
λ - decay rate $t^{1/2}=1.06X10^{11}$years.

$$^{143}Nd/^{144}Nd\ sample^{(t)} = [^{147}Sm/^{144}Nd\ sample^{(t=0)} * (e\lambda t - 1)] - ^{143}Nd/^{144}Nd\ sample^{(t=0)}$$

$$^{143}Nd/^{144}Nd\ CHUR^{(t)} = [^{147}Sm/^{144}Nd\ CHUR^{(t=0)} * (e\lambda t - 1)] - ^{143}Nd/^{144}Nd\ CHUR^{(t=0)}$$

$^{143}Nd/^{144}Nd_{sample}^{(t=0)}$ and $^{147}Sm/^{144}Nd^{(t=0)}$ are calculated using measured ^{147}Sm, ^{144}Nd and ^{143}Nd

CHUR (Chondritic Uniform Reservoir) values [$^{147}Sm/^{144}Nd\ CHUR^{(t=0)}$ and $^{143}Nd/^{144}Nd\ CHUR^{(t=0)}$] are calculated from planetary evolution models using measured chondrite compositions (Zindler and Hart 1986).

Mixing and contamination
Simple binary mixing models following Patchett and Bridgewater (1984), Kerr and Fryer (1990) Chauvel et al. (1987) are used. The proportion X, of a contaminant, as expressed in ε_{Nd}, is found from the concentrations of Nd in the sources and their ε_{Nd} values, such that:

$$X = \frac{(C_{Nd}(DM)[\varepsilon_{Nd}(NC) - \varepsilon_{Nd}(DM)])}{(C_{Nd}(CC)\ [\varepsilon_{Nd}(CC) - \varepsilon_{Nd}(NC)])} \quad (1)$$

Where CC is the contaminant; DM the depleted mantle; NC the final product of mixing; C_{Nd} Nd concentration in ppm; ε_{Nd} the sources $^{143}Nd/^{144}Nd$ normalized to CHUR (after De Paolo and Wasserburg).

source► parameter▼	CC Archean	CC SCLM	CC Britt	CC Penokean	CC Muskoka	CC juvenile felsic	DM
C_{Nd}	25	40	41	30	40	40	5
$\varepsilon_{Nd\ 1.37\ Ga}$	-18	-4	- 8	-2	+1.5	+5	+5.5
C_{SIO2}	70	45	73	65	60	50	42
age (Ga.)	2.75	2.5	2.25	1.9	1.45	1.37	1.37

Table C1. Contaminants, their age, Nd content, isotopic composition and SiO_2 content. Data sources: Kerr and Fryer (1990), Wilson 1989, R. North pers comm., Slagstad et al. *in press*.

The sources were chosen to best resemble possible contaminants to Lighthouse gneiss association precursor magmas at a formation age of ca. 1.4 Ga, at potential environments of magma genesis, using the tectonic reconstructions of Culshaw and Dostal (1997, 2002), Slagstad et al. *in press* and Carr et al. (2000). More than 10% binary contamination is unlikely as it would to alter the major element characteristics of the magma producing more felsic magmas than the Lighthouse amphibolite protoliths.

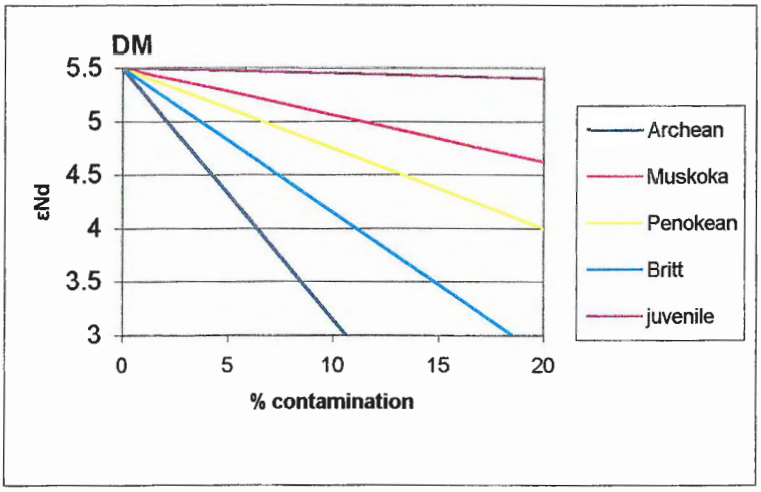

Figure C1. DM-contaminant mixing lines, error - ±0.5 units

REFERENCES

Åhäll, K., -I., and Connelly, J. 1998. Intermittent 1.53-1.13 Ga magmatism in western Baltica; age constraints and correlations within a postulated supercontinent. Precambrian Research 92, 1-20.

Åhäll, K., -I., Connelly, J., and Brewer, T.S. 2000. Episodic rapakivi magmatism due to distal orogenesis? Correlation of 1.69-1.50 Ga orogenic and inboard "anorogenic" events in the Baltic shield. Geology 28, 823-826.

Arndt, N.T., and Goldstein, S.L. 1987. Use and abuse of Nd model ages. Geology 15, 893-895.

Barr, S.M., White, C.E., Culshaw, N.G., and Ketchum, J.W.F. 1997. Petrology, age, and tectonic setting of the Island Habour Bay plutonic suite, Makkovik Province, Labrador: preliminary results. In Wardie, R.J., Hall, J. (Eds), Eastern Canadian Shield Onshore- Offshore Transect (ECSOOT) Report of 1997 Transect Meeting, The University of British Columbia, Lithoprobe Secretariat, Report No. 61, 12-24.

Barr, S.M., White, C.E., Culshaw, N.G., and Ketchum, J.W.F. 2001. Geology and tectonic setting of Palaeoproterozoic granitoid suites in the Island Harbour Bay area, Makkovik Province, Labrador. Canadian Journal of Earth Sciences 38, 441-463.

Bickford, M.E. 1988. The formation of continental crust: Part 1. A review of some principles; Part 2. An application to the Proterozoic evolution of southern North America. Geological Society of America Bulletin 100, 1375-1391.

Bingen, B., Birkeland, A., Nordgulen, Ø, and Sigmond, E.M.O. 2001. Correlation of supercrustal sequences and origin of terranes in the Sveconorwegian orogen of Scandinavia: SIMS data on zircon in clastic metasediments. Precambrian Research 108, 293-318.

Brewer, T.S., Åhäll, K.-I., Darbyshire, D.P.F., and Menuge, J.F. 2002. Geochemistry of Late Mesoproterozoic volcanism in southwestern Scandinavia: implications for Sveconorwegian/Grenvillian plate tectonic models. Journal of the Geological Society of London 159, 129-144.

Buchan, K.L., Mertanen, S., Park, R.G., Pesonen, L.J., Elming, S.Å., Abrahamsen, N., and Bylund, G. 2000. Comparing the drift of Laurentia and Baltica in the Proterozoic: the importance of key palaeomagnetic poles. Tectonophysics 319, 167-198.

Bussy, F., Krogh, T.E., Klemens, W.P., and Schweidtner, W.M. 1995. Tectonic and metamorphic events in the westernmost Grenville Province, central Ontario: new results from high-precision U-Pb zircon geochronology. Canadian Journal of Earth Sciences 32, 660-671.

Carr, S. D., Easton, R. M, Jamieson, R. A., and Culshaw, N. G. 2000. Geological transect across the Grenville orogen of Ontario and New York. Canadian Journal of Earth Sciences 37, 193-216.

Cas, R.A.F. and Wright, J.V. 1987. Volcanic Successions. Allen and Unwin.

Chauvel, C., Arndt, N.T., Keilinzcuk, S., and Thom, A. 1987. Formation of Canadian 1.9 Ga old continental crust. 1: Nd isotopic data. Canadian Journal of Earth Sciences 24, 396-406.

Chen, Y.D., Krogh, T.E., and Lumbers, S.B. 1995. Neoarchean trondhjemitic and tonalitic orthogneiss identified within the northern Grenville Province in Ontario by precise U-Pb dating and petrologic studies. Precambrian Research 72, 263-281.

Corrigan, D. 1995. Mesoproterozoic evolution of the south-central Grenville orogen: structural, metamorphic and geochronologic constraints from the Mauricie transect. Ph.D. thesis, Carlton, University, Ottawa, Ontario.

Corrigan, D. and Van Breemen, O. 1997. U-Pb age for the lithotectonic evolution of the Grenville Province along the Mauricie transect, Quebec. Canadian Journal of Earth Sciences 34, 299-316.

Corriveau, L. and van Breemen, O. 2000. Polyphased record of Grenvillian orogenesis in the Central Metasedimentary Belt, Quebec: the role of intrusive suites in unraveling strongly partitioned tectono-metamorphic events. Canadian Journal of Earth Sciences 37, 253-269.

Culshaw, N.G. and Dostal, J. 1997. Sand Bay gneiss association, Grenville Province, Ontario: a Grenvillian rift- (and –drift) assemblage stranded in the Central Gneiss Belt. Precambrian Research 85, 97–113.

Culshaw, N.G. and Dostal, J. 2002. Amphibolites of the Shawanaga domain, Central Gneiss Belt, Grenville Province, Ontario: tectonic setting and implications for relations between the Central Gneiss Belt and Midcontinental USA. Precambrian Research 113, 65 -85.

Culshaw, N.G., Check, G., Corrigan, D., Drage, J., Gower, R., Haggart, M.J., Wallace, P., and Wodicka, N. 1989. Georgian Bay geological synthesis: Dillon to Twelve Mile Bay, Grenville Province of Ontario. In: Current research, Part C, Geological Survey of Canada Paper 89-1C, 157-163.

Culshaw, N.G., Ketchum, J.W.F., Wodicka, N., and Wallace, P. 1994. Ductile extension following thrusting in the deep crust: evidence form the southern Britt domain, southwest Grenville Province, Georgian Bay, Ontario. Canadian Journal of Earth Sciences 31, 160-175.

Culshaw, N.G., Jamieson, R.A.J., Ketchum, J.W.F., Wodicka, N., Corrigan, D., and Reynolds, P.H. 1997. Transect across the northwestern Grenville orogen, Georgian Bay, Ontario: Polystage convergence and extension in the lower orogenic crust. Tectonics 16, 6, 966-982.

Culshaw, N.G., Ketchum, J.W.F., and Barr, S. 2000. Structural evolution of the Makkovik Province Labrador, Canada: tectonic processes during 200 My at a Palaeoproterozoic active margin. Tectonics 19, 961-977.

Dalziel, I.W.D. 1991. Pacific margins of Laurentian and East Antarctica-Australia as a conjugate rift pair: Evidence and implications for an Eocambrian supercontinent. Geology 19, 598-601.

Dalziel, I.W.D. 1992. On the organization of American plates in the Neoproterozoic and the breakout of Laurentia. GSA today 2 (11), 237-241.

Davidson, A. 1984. Identification of ductile shear zones in the southwestern Grenville Province of the Canadian Shield. in Precambrian Tectonics Illustrated, editors Kröner, A. and Greiling, R. E.Scweizerbart'sche Verlagbuchhandlung Stuttgart 263-279.

Davidson, J. 1985. Mechanisms of contamination in Lesser Antilles island arc magmas from radiogenic and oxygen isotope relationships. Earth and Planetary Science Letters 72, 163-174.

Davis, D.W. 1982. Optimum linear regression and error estimation applied to U-Pb data. Canadian Journal of Earth Sciences 19, 2141-2149.

De Paolo, D.J. and Wasserburg, G.J. 1976. Inferences about magma sources and mantle structure from $^{143}Nd/^{144}Nd$ variations. Geophysical Research Letters 3, 249–252.

De Paolo, D.J. 1981. Neodynium isotopes in the Colorado Front Range and crust-mantle evolution in the Proterozoic. Nature 291, 193-196.

Dickin, A.P. and McNutt, R.H. 1989. Nd model age mapping of the southeast margin of the Archean foreland in the Grenville province of Ontario. Geology 17, 299-302.

Dickin, A.P. and McNutt, R.H. 1990. Nd model age mapping of Grenville lithotectonic domains: Mid-Proterozoic crustal evolution in Ontario. In Gower, C.F., Rivers, T.

and Ryan, A.B. (editors) Mid-Proterozoic Laurentia – Baltica, Geological Association of Canada Special Paper 38, 79-94.

Dickin, A.P. 1995. Radiogenic Isotope Geology. Cambridge University Press, Cambridge.

Dostal, J., Dupuy, C., and Caby, R. 1994. Geochemistry of the Neoproterozoic Tilemsi belt of Iforas (Mali, Sahara): a crustal section of an oceanic island arc. Precambrian Research 65, 55-69.

Dudás, F.Ö., Davidson, A., and Bethune, K.M. 1994. Age of the Sudbury diabase dykes and their metamorphism in the Grenville Province. In: Radiogenic age and isotopic studies: Report 8. Geological Survey of Canada, Current Research 1994-F, 97–106.

Easton, R.M. 1986a. Geochronology of the Grenville Province. In: The Grenville Province, Geological Association of Canada, Special Paper 31, 127-173.

Easton, R.M. 1986b. Paleoenvironment and facies of the Apsley Formation, Peterborough County, in Summary of field work and other activities 1986, Ontario Geological Survey, Miscellaneous Paper 132, 141-151.

Faure, G. 1986. Principles of Isotope Geology, Wiley, 2nd edition.

Fitton, J.G., Saunders, A.D., Norry, M.J., Hardarson, B. and Taylor, R.N. 1997. Thermal and chemical structure of the Iceland plume. Earth and Planetary Science Letters 153, 197-208.

Fitzsimons, I.C.W. 2000. Grenville-age basement provinces in East Antarctica: evidence for three separate collisional orogens. Geology 28, 879-882.

Fralick, P.W. and Kronberg, B.I. 1997. Geochemical discrimination of clastic sedimentary rock sources. Sedimentary Geology 113, 111-124.

Gaál, G. and Gorbatschev, R. 1987. An outline of the Precambrian evolution of the Baltic Shield. Precambrian Research 35, 15-52.

Gamble, J.A., Wright, I.C., Woodhead, J.D., and McCulloch, M.T. 1995. Arc and back-arc geochemistry in the southern Kermadec arc-Ngatoro Basin and offshore Taupo Volcanic Zone, SW Pacific. In: Smellie, J.L. (editor) Volcanism Associated with Extension at Consuming Plate Margins. Geological Society Special Publication 81, 193-212.

Gnibidenko, H. 1979. The tectonics of the Japan Sea. Marine Geology 32, 71-87.

Goldstein, S.L., O'Nions, R.K., and Hamilton, P.J. 1984. A Sm-Nd study of atmospheric dusts and particulates from major river sytems. Earth and Planetary Science Letters 70, 221-236.

Goodge, J.W., Myrow, P., Williams, I.S., and Bowring, S.A. 2002. Age and Provenance of the Beardmore Group, Antarctica: constraints on Rodinia Supercontinent Breakup. Journal of Geology 110, 393-406.

Gower, C.F. and Tucker, R.D. 1994. Distribution of pre-1400 Ma crust in the Grenville Province: implications for rifting in Laurentia-Baltica during geon 14. Geology 22, 827-830.

Gower, C.F. 1996. The evolution of the Grenville Province in eastern Labrador, Canada. In Brewer, T.S. (ed.) Precambrian crustal Evolution in the North Atlantic Regions. Geological Society Special Publications 112, 197-218.

Gower, C.F., Krogh, T.E., and James, D.T. 2002. Correlation chart of the eastern Grenville Province and its northern foreland. Canadian Journal of Earth Sciences 39, 897.

Hanmer, S., Corrigan, D., Pehrsson, S., and Nadeau, L. 2000. SW Grenville Province, Canada: the case against post-1.4 Ga accretionary tectonics. Tectonophysics 319, 33-51.

Hawkesworth, C.J., O'Nions, R.K., and Arculus, R.J. 1977. Nd and Sr isotope geochemistry of island arc volcanics, Grenada, lesser Antilles. Earth and Planetary Science Letters 45, 237-248.

Horte, E.H. and Torsvik, T.H. 2002. Baltica upside down: A new plate tectonic model for Rodinia and the Iapetus Ocean. Geology 30, 255-238.

Isozaki, Y. 1996. Anatomy and genesis of a subduction-related Orogen: A new view of geotectonic subdivision and evolution of the Japanese Islands. The Island Arc 5 289-320.

Jaffey, A.H., Flynn, K.F., Glendenin, L.E., Bentley, W.C. and Essling, A.M. 1971. Precise measurements of half lifes and specific activities of ^{235}U and ^{238}U. Physical Review 4, 1889-1906.

Jolivet, L., Shibuga, H., and Fournier, M. 1995. The Sea of Japan. In Taylor, B., and Natland, J. (eds.) Active Margins and Marginal basins of the Western Pacific. American Geophysical Union Geophysical Monograph 88, 165-182.

Karlstrom, K. E., Ahall, K., Harlan, S.S., Williams, M. L., McLelland, J., and Geissman, J. W., 2001, Long-lived (1.8-1.0 Ga) convergent orogen in southern Laurentia, its extensions to Australia and Baltica, and implications for refining Rodinia. Precambrian Research 111, 5-30.

Kay, S.M., Ramos, V.A., Mpodozis, C., and Sruoga, P. 1989. Late Palaeozoic to Jurassic silicic magmatism at the Gondwana margin: Analogy to the Middle Proterozoic in North America? Geology 17, 324-328.

Ketchum, J.W.F. 1995. Extensional shear zones and lithotectonic domains in the southwest Grenville orogen: Structure, metamorphism, and U-Pb geochronology of the Central Gneiss Belt near Pointe-au-Baril, Ontario, Ph.D. thesis, Dalhousie Univ., Halifax, Nova Scotia, Canada.

Ketchum, J.W.F. and Krogh, T.E. 1998. U-Pb constraints on high-pressure metamorphism in the southwestern Grenville orogen, Canada. Goldshmidt Conference 1998, Abstracts Volume, Mineralogical Magazine 62A, 775-776.

Ketchum, J.W.F. and Davidson, A. 2000. Crustal architecture and tectonic assembly of the Central Gneiss Belt, southwestern Grenville Province, Canada: a new interpretation. Canadian Journal of Earth Sciences 37, 217-234.

Ketchum, J.W.F., Culshaw, N.G., Heaman, L.M., Krogh, T.E., and Jamieson, R.A. 1993. Late orogenic ductile extension in the middle Proterozoic Grenville orogen: an example from Ontario Canada. In Late orogenic extension in Mountain Belts, Abstracts, edited by Serrane, M. and Malavielle, J. Doc. B. R. G. M. 219, 108-109.

Ketchum, J.W.F., Heaman, L.M., Krogh, T.E., Culshaw, N.G., and Jamieson, R.A. 1998. Timing and thermal influence of late orogenic extension in the lower crust: a U-Pb geochronological studyfrom the southwest Grenville Orogen, Canada. Precambrian research 89, 25-45.

Ketchum, J.W.F., Jamieson, R.A., Heaman, L.M., Culshaw, N.G., and Krogh, T.E. 1994. 1.45 Ga granulites in the southwestern Grenville Province: geologic setting, P-T conditions, and U-Pb geochronology. Geology 22, 215–218.

Ketchum, J.W.F., Jackson, S.E., Culshaw, N.G., and Barr, S.M. 2001. Depositional and tectonic setting of the Paleoproterozoic Lower Aillik Group, Makkovik Province, Canada: evolution of a passive margin-foredeep sequence based on petrochemistry and U-Pb (TIMS and LAM-ICP-MS) geochronology. Precambrian Research 105, 331–356.

Ketchum, J., Culshaw, N.G., and Barr, S.M. 2002. Anatomy and orogenic history of a Paleoproterozoic accretionary belt: the Makkovik Province, Labrador, Canada. Canadian Journal of Earth Sciences 39, 711-730.

Krogh, T.E. 1973. A low-contamination method for hydrothermal decomposition of zircon and extraction of U and Pb for isotopic age determinations. Geochimica et Cosmochimica Acta 37, 485-649.

Krogh, T.E. 1982. Improved accuracy of U-Pb zircon ages by the creation of a more concordant system using an air abrasion technique. Geochimica et Cosmochimica Acta 46, 637-649.

Krogh, T.E. and Davis, G.L. 1975. The production and preparation of ^{205}Pb for use as a tracer for isotope dilution analyses. Carnegie Institute of Washington Yearbook 74, 416-417.

Krogh, T.E., Corfu, F., Davis, D., Dunning, G.R., Heaman, L.M., Kamo, S.L., Machado, N., Greendough, J.D., and Nakamura, E. 1987. Precise U-Pb isotopic ages of diabase dykes and mafic to ultramafic rocks using trace amounts of baddeleyite and zircon. In: mafic dyke swarms. Edited by Halls, H.C., and Fahrig, W.F. Geological Association of Canada, Special Paper 34, 147-152.

Ludwig, K.R. 1980. Calculation of uncertainties of U-Pb isotopic data. Earth and Planetary Science Letters. 46, 212-220.

Macdougall, J.D. 1988. Continental flood Basalts, Kluwer Academic Publishers Dordrecht.

McLelland. J. and Chiarenzelli, J. 1990. Isotopic constraints on the emplacement age of anorthositic rocks of the Marcy massif, Adirondack Mountians, New York. Journal of Geology 98, 19-41.

McLelland, J.M., Daly, S., and Chiarenzelli, J 1993. Sm-Nd and U-Pb isotopic evidence of juvenile crust in the Adirondack lowlands and implications for the evolution of the Adirondack Mts. Journal of Geology 101, 97-105.

McLelland, J.M., Daly, S., and McLelland, J 1996. The Grenville orogenic cycle (ca. 1350-1000 Ma): an Adirondack perspective. Tectonophysics 265, 1-28.

McMenamin, M.A.S. and McMenamin, D.L. 1990. The Emergence of Animals; The Cambrian Breakthrough, Columbia University Press New York, N.Y..

McMullen, S.M., Carr, S.D., and Easton, R.M. 1999. Tectonic evolution of the Bark Lake area, eastern Central Gneiss Belt, SW-Ontario Grenville: constraints from geology, geochemistry and U-Pb geochronology. Geological Association of Canada – Mineralogical Association of Canada, Abstracts 24, 82.

Marsaglia, K.M. 1995. Interarc and Backarc Basins. In: Busby, C.J. and Ingersoll, R.V. (editors) Tectonics of Sedimentary Basins. Blackwell Science Massachusetts 119-148.

Martignole, J., Machado, N., Indares, A. 1994. The Wakenham terrane: a Mesoproterozoic terrestrial rift in the eastern part of the Grenville Province. Precambrian Research 68, 291-306.

Menuge, J.F. and Brewer, T.S. 1996. Anorogenic magmatism in southern Norway. In Brewer, T.S. (ed.) Precambrian crustal Evolution in the North Atlantic Regions. Geological Society Special Publications 112, 275-296.

Meert, J.G. and Powell, C.McA 2001 Assembly and break-up of Rodinia: introduction to the special volume. Precambrian Research 110, 1-8.

Moores, E.M. 1991. Southwest U.S. – East Antarctica (SWEAT) connection: a hypothesis. Geology 19, 598-601.

Nance, R.D. and Thompson, M.D. 1996 Avalonian and related peri-Gondwanan Terranes of the Circum-North Atlantic: An introduction In: Nance, R.D. and Thompson, M.D. (editors) Avalonian and related peri-Gondwanan Terranes of the Circum-North Atlantic 1-9.

Nance, R.D. and Murphy, J.B. 1996. Basement Isotopic Signatures and Neoproterozoic Palaeogeography of Avalonian-Cadomian and Related terranes in the Circum-North Atlantic. In: Nance, R.D. and Thompson, M.D. (editors) Avalonian and related peri-Gondwanan Terranes of the Circum-North Atlantic 333-346.

Nadeau, L. and Van Breemen, O. 1994. Do the 1.45 – 1.39 Ga Montauban Group and the La Bostonnais complex constitute a Grenvillian accreted terrane. In: Waterloo'94 Geological Associaiotn of Canada-Mineralogical Association of Canada Program with abstracts 19, A81.

Nelson, B.K. and DePaolo, D.J. 1985. Rapid production of continental crust 1.7 to 1.9 b.y. ago: Nd isotopic evidence from the basement of the North American mid-continent. Geological Society of America Bulletin 96, 746-754.

Nisbet, E.G. 1987. The Young Earth; An Introduction to Archean Geology, Unwin Hyman, Massachusets.

Nishimura, A., Rodolfo, K., Koizumi, A., Gill, J., and Fujioka, K. 1992. Episodic deposition of Pliocene-Pliestocene pumice from the Izu-Bonin Arc. In: Taylor, B. and Fujioka, K. and 14 others. Proceedings of the Ocean Drilling Programme, Scientific Results 126, 3-22.

Nohda, S., and Wasserburg, G.J. 1981. Nd and Sr isotopic study of volcanic rocks from Japan. Earth and Planetary Science Letters 52, 264–276.

Patchett, P.J. 1980. Thermal effects of basalt on continental crust and crustal contamination of magmas. Nature 283, 559-561.

Patchett, P.J. and Bridgewater, D. 1984. Origin of continental crust of 1.9-1.7 Ga age defined by Nd isotopes in the Ketilidian terrain of South Greenland. Contributioins to Mineralogy and Petrology 87, 311-318.

Petford, N. and Atherton, M.P. 1995. Cretaceous-Tertiary volcanism and syn-subduction crustal extensioin in northern central Peru. In: Smellie, J.L. (editor) Volcanism Associated with Extension at Consuming Plate Margins. Geological Society Special Publication 81, 3-28.

Piper, J.D.A. 1982. The Precambrian palaeomagnetic record: the case for the Proterozoic supercontinent. Earth and Planetary Science Letters 59, 61-89.

Powell, R. 1984. Inversion of the assimilation and fractional crystallization (AFC) equations: Characterization of contaminants from isotope and trace element relationships in volcanic suites. Journal of the Geological Society of London 141, 447-452.

Pouclet, A., Lee, J,-S., Vidal, Ph., Cousens, B., and Bellon, H. 1995. Cretaceous to Cenozoic volcanism in South Korea and the Sea of Japan: magmatic constraints on the opening of the back-arc basin. In: Smellie, J.L. (editor) Volcanism Associated with Extension at Consuming Plate Margins. Geological Society Special Publication 81, 169-191.

Reynolds, P.H., Culshaw, N.G., Jamieson, R.A., Grant, S.L., and McKenzie, K. 1995. $^{40}Ar/^{39}Ar$ traverse - Grenville Front Tectonic Zone to Britt domain, Grenville Province, Ontario, Canada. Journal of Metamorphic Geology 13, 209-221.

Rivers, T. 1997. Lithotectonic elements of the Grenville Province: review and tectonic implications. Precambrian Research 86, 11-154.

Rivers, T. and Corrigan, D. 2000. Convergent margin on south-eastern Laurentia during the Mesoproterozoic: tectonic implications. Candian Journal of Earth Sciences 37, 359-383.

Rivers, T., Martignole, J., Gower, C.F. and Davidson, A. 1989. New tectonic subdivisions of the Grenville Province, southeast Canadian Shield. Tectonics 8, 63-84.

Rollinson, H. 1996. Using Geochemical Data: Evaluation, Presentation, Interpretation. Longman Limited Essex, England.

Rudnick, R.L. and Fountain, D.M. 1995. Nature and composition of the continental crust: a lower crustal perspective. Reviews in Geophysics 33, 267-309.

Sadowski, G.R. and Bettencourt, J.S. 1996. Mesoproterozoic tectonic correlations between eastern Laurentia and the western border of the Amazon Craton. Precambrian Research 76, 213–227.

Sager-Kinsman, E.A. and Parrish, R.R. 1993. Geochronology of detrital zircons from the Elzevir and Frontenac terranes, Central Metasedimentary Belt, Grenville Province, Ontario. Canadian Journal of Earth Sciences 30, 465-473.

Shaw, D. 1272. The Origin of the Apsley Gneiss, Ontario. Canadian Journal of Earth Science 9, 18-35.

Sims, P.K. 1993. The Lake Superior region and Trans Hudson Orogen; Precambrian Volume, Decade of North American Geology. Geological Society of America Vol. C-2, 11-120.

Slagstad, T., Culshaw, N.G. and Jamieson, R.A. *in press.* Geochemistry of high-grade gneisses in the Grenville Province, Ontario: Arc magmatism and rifting at 1.48-1.36 Ga. Bulletin of the Geological Society of America.

Smith, T.E., Huang, P.E., Dennison, N.M., and Harris, M.J. 1997. Crustal assimilation in the Burnt Lake metavolcanics, Grenville Province, southeastern Ontario, and its tectonic significance. Canadian Journal of Earth Sciences 34, 1272-1285.

Storey, B.C., Alabaster, T., Hole, M.J., Pankhurst, R.J., and Wever, H.E. 1992. Role of subduction-plate boundary forces during the initial stages of Gondwana break-up: evidence from the proto-Pacific margin of Antarctica. In: Magmatism and the Causes of Continental Break-up, Storey, B.C., Alabaster, T., ad Pankhurst, R.J. (editors) Geological Society Special Publication 68, 149–163.

Sugimura, A. and Uyeda, S. 1973. Island arcs; Japan and its environs. Developments in Geotectonics 3. Elsevier Amsterdam.

Sun, S. –S. and McDonough, W.F. 1989. Chemical and isotopic systematics of oceanic basalts: implications for mantle composition and processes, In: Magmatism in the Ocean Basins, Saunders, A.D. and Norry, M.J. (editors), Geological Society Special Publication 42, 313-345.

Swinden, H.S., Jenner, G.A., Fryer, B.J., and Hertogen, J.C. 1990. Petrogenesis and paleotectonic history of the Wild Bight Group, and Ordovician rifted island arc in central Newfoundland. Contributions to Mineralogy and Petrology 105, 219-241.

Tassinari, C.G., Bettencourt, J.S., Geraldes, M.C., Macambira, M.J.B. and Lafon, J.M. 2000. The Amazonian Craton In: Tectonic Evolution of South America, Cordani, U.G., Milai, E.J., Thomaz Filho, A. and Campos, D.A. (editors). 31st International Geological Congress, Rio de Janeiro 1-19.

Taylor, St.R. and McLennan, S.M., 1985. The Continental Crust: its Composition and Evolution. Blackwell Scientific Publications. Geoscience texts.

Timmerman, H., Parrish, R.R., Jamieson, R.A., and Culshaw, N.G. 1997. Time of metamorphism beneath the Central Metasedimentary Belt Boundary Thrust Zone, Grenville Orogen, Ontario: Accretion at 1080 Ma? Canadian Journal of Earth Sciences 34, 1023-1029.

Tomlinson, K.Y., Davis, D.W., Percival, J.A., Hughes, D.J., and Thurston, P.C. 2002. Mafic to felsic magmatism and crustal recycling in the Obonga Lake greenstone belt, western Superior Province: evidence from geochemistry, Nd isotopes and U-Pb geochronology. Precambrian Research 114, 295-325.

Tuccillo, M.E., Mezger, K., Essene, E.J. and van der Pluijm 1992. Thermobarometry, geochronology and the interpetation of P-T-t data in the Britt domain, Ontario Grenville orogen, Canada. Journal of Petrology 33, 1225-1259.

Uyeda, S. and Miyashiro, A. 1974. Plate tectonics and the Japanese Islands, Geological Society of America Bulletin 85, 1159-1170.

van Breemen, O. and Davidson, A. 1988. Northeast extension of Proterozoic terranes of mid-continental North America. Geological Society of America Bulletin 100, 630-638.

van Breemen, O. and Davidson, A. 1990. U-Pb zircon and baddeleyite ages from the Central Gneiss Belt, Ontario. In: Radiogenic age and isotopic studies: report 3. Geological Survey of Canada, Paper 89-2, 85-92.

Van Schmus, W.R., Bickford, M.E. and Turek, A. 1996. Proterozoic geology of the east-central Midcontinent basement. In: van-der-Pluijm, B.A. and Catacosinos, P.A., Basement and Basins of Eastern North America. Special Paper Geological Society of America 308, 7-32.

Van Schmus, W.R. and Bickford, M.E. 1993. Transcontinental Proterozoic Provinces, Precambrian Volume, Decade of North American Geology. Geological Society of America 172-176.

Weil, A.B., Van der Voo, R., MacNiocall, C. and Meert, J.G. 1988. The Proterozoic supercontinent Rodinia: palaeomagnetically derived reconstructios for 1100 to 800 Ma. Earth and Planetary Science Letters 154, 13-24.

White, D.J., Easton, R.M., Culshaw, N.G., Milkereit, B., Forsyth, D.A., Carr, S., Green, A.G. and Davidson, A. 1994. Seismic images of the Grenville Orogen in Ontario. Canadian Journal of Earth Sciences 31, 293-307.

White, D.J., Forsyth, D.A., Asudeh, I.A., Carr, S.D., Wu, H., Easton, R.M., and Mereu, R.F. 2000. Seismic-Based Cross-Section Across the Grenville Front in Ontario. Canadian Journal of Earth Sciences 37, 183-192.

Winn, R.D.Jr. 1978 Upper Mesozoic Flysch of Tierra del Fuego and South Georgia Island: a sedimentologic approach to lithosphere plate restoration. Geological Society of America Bulletin 89, 533-547.

Wilson, M. 1989 Igneous Petrogenesis A global tectonic approach. London Unwin Hyman.

Wodicka, N. 1994. Middle Proterozoic evolution of the Parry Sound Domain, Southwestern Grenville Orogen Ontario: Structural, metamorphic, U/Pb, and 40Ar/39Ar constraints. PhD thesis, Dalhousie University, Halifax, Nova Scotia, Canada.

Wodicka, N., Parrish, R.R. and Jamieson, R.A. 1996. The Parry Sound domain: a far-travelled allochthon? New evidence from U-Pb zircon geochronology. Canadian Journal of Earth Sciences 33, 1087-1104.

Wodicka, N., Ketchum, J.W.F. and Jamieson, R.A. 2000. Grenvillian metamorphism of monocyclic rocks, Georgian Bay, Onatrio, Canada: implications for convergence history. Canadian Mineralogist 38, 471-510.

Wynne- Edwards, H.R., 1972. The Grenville Province, in Variations in Tectonic Styles in Canada, edited by Price, R.A. and Douglas, R.J.W. Geological Association of Canada Special Paper 11, 263-334.

York, D. 1969. Least squares fitting of a straight line with correlated errors. Earth and Planetary Science Letters 5, 320-324.

Zindler, A. and Hart, S, 1986. Chemical Geodynamics. Annual Reviews in the Earth and Planetary Science 14, 493-571.